Transformation of visual signals at the synaptic terminals of retinal bipolar cells

Sofie-Helene Seibel

Submitted for the degree of Doctor of Philosophy

University of Sussex

February 2021

DECLARATION

Parts of this thesis (chapter 5) have been published:

Johnston, J., Seibel, S.-H., Darnet, L. S. A., Renninger, S., Orger, M., & Lagnado, L. (2019). A Retinal Circuit Generating a Dynamic Predictive Code for Oriented Features. *Neuron*, *102*(6), 1211-1222.e3. https://doi.org/10.1016/j.neuron.2019.04.002

Code written by Leon Lagnado (chapters 3 and 4) and Jamie Johnston (chapter 5)

I hereby declare that this thesis has not been and will not be, submitted in whole or in part to another University for the award of any other degree.

Signature:

Summary

For a long time, the retina has been thought to be a part of the brain that performs only simple computations before more complex processes within higher visual centres disentangle the relevant features of the stimulus from the irrelevant background information. However, since the first electrical recordings from retinal ganglion cells in the 1930s, more recent advances in genetic engineering, electrophysiology, and optics, have made it clear that the retina performs intricate feature-extracting computations. Central to these computations is the inner plexiform layer in which the terminals of bipolar cells make connections to the dendrites of ganglion- and amacrine cells.

In this thesis, we describe two novel circuits within the inner plexiform layer of larval zebrafish.

Chapter 1 comprises a general introduction. Chapter 2 describes the methods we used to study transgenic zebrafish larvae *in vivo* under two-photon illumination. Chapters 3 and 4 give insights into the computational power of individual bipolar cells. Given that most bipolar cells have multiple output synapses begs the question of whether each synapse can signal different properties of a stimulus. We show that the output synapses of many individual bipolar cells release glutamate in a heterogeneous manner in response to changes in light intensity: some terminals give an excitatory response whenever the light increases (ON) or decreases (OFF), whilst others signal both polarities. This finding contradicts the classical view that ON and OFF pathways are separated from each other before they converge at later stages in the visual system.

Chapter 5 comprises an investigation into the emergence of retinal orientation- and direction-selectivity. Previous studies have located these properties to the dendritic trees of retinal ganglion cells. However, we show that ~25% of bipolar cell terminals are tuned to the orientation but not the direction of a stimulus. Orientation selectivity could not be explained by asymmetric receptive fields but was removed by blocking inhibition. Chapter 6 encompasses a general discussion.

Acknowledgements

First and foremost, I would like to thank Leon. Thank you for offering me to do a PhD as a part-time student in addition to my role as a research assistant. Pursuing a PhD without this option would not have been possible otherwise. Despite having faced quite a few, to PhD students common, obstacles, I would not have liked missing out on this opportunity. Thank you for your guidance, support, and often quite amusing but contagious outbursts of excitement about science.

Thank you, Claudio, for stepping in as my second supervisor and for always being approachable when needed.

Thank you to all of the Lagnado lab members, past and present. Your scientific and non-scientific support in the form of banter over a cup of coffee or bunch of pints has enriched my day-to-day life beyond measure. While I cannot mention every single of you, special thanks must go to Paul, who always went an extra mile to help myself and others.

Thank you, Emma and Guy, for helping us getting settled and making us feel welcome at Sussex.

Thank you to all people who support our research: I address special thanks to all Biomedical Research Facility members that have ensured the well-being of our zebrafish. Thank you, Hazel, for always being there and for being incredibly caring. Thank you to all lovely people from stores and technical supports. The Andy's, Steve, Sue, Dan, Barry, Paul, Chris, Scott, Alex and Crispin thank you all for your help and the friendly chats and "hellos" in between doors, you not only ensure that the School operates smoothly but also give this building a warm appearance.

I want to thank all my friends, distant and near, for always checking in on me, for making me laugh and feel loved.

Most importantly, I thank my family for continuous support and love since the day I entered the stage of life. I dedicate this thesis in loving memory to my mother Dagmar Seibel née Kunkel.

Table of Content

Table of Figures

Table of Tables

Chapter 1

General Introduction

1. General Introduction

1.1 The basic design and functions of the retina

The retina transforms patterns of light into neural signals which are sent to visual centres in the brain. The information received by the eye when observing a natural scene contains a vast amount of information, some of which is redundant. The amount of information that neurons are able to transmit is ultimately limited by the specific metabolic rate a given tissue can generate. Evolution has developed systems, including the complex circuitries of the retina, that optimize the use of space, materials, and energy accordingly (Attneave, 1954; Barlow, 2013; Sterling & Laughlin, 2015).

The retina (Fig. 1) extracts an image by separating different features of a stimulus into distinct, spatiotemporally operating channels.

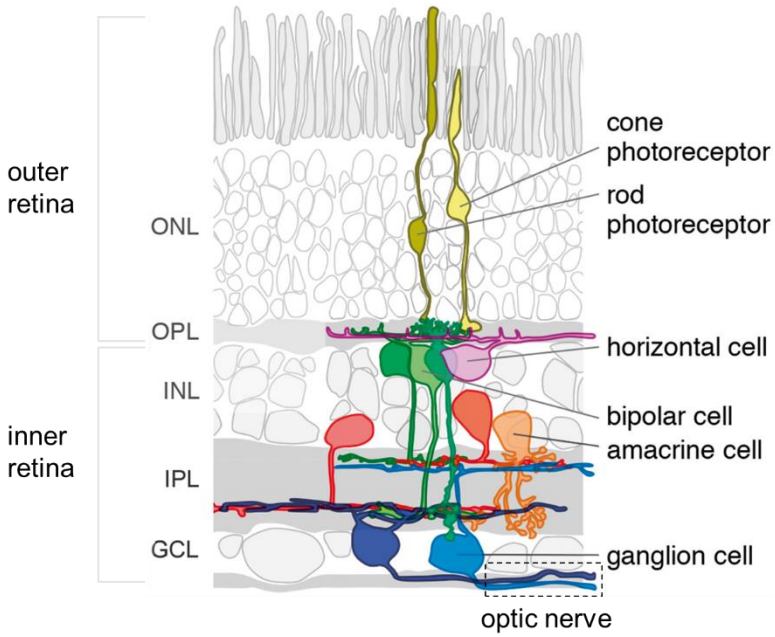

Figure 1.1: Schematic of the retina

Cone and rod photoreceptors (yellow) detect photons and transduce their energy into an electrical signal which feeds into an array of BCs (green) where different features of a stimulus are extracted in parallel and conveyed to ganglion cells (blue). Ganglion cells then send the information to the brain via the axons of the optic nerve. This vertical pathway, mediated by the neurotransmitter glutamate, is modulated by inhibitory inputs provided by horizontal (lilac) and amacrine cells (red) in the outer and inner retina, respectively. Figure adapted from (Berens & Euler, 2017).

In the outer retina photoreceptors (PRs) with different spectral sensitivities decompose the visual information into a broad array of chromatic and achromatic channels which feed onto a functionally diverse pool of bipolar cells (BCs). The task of these interneurons is to relay information from the outer retina onto ganglion cells (GCs) - the output neurons that send the signals to higher visual centres in the brain. The excitatory neurotransmitter glutamate drives this "vertical" pathway, whereas horizontal (HCs) and amacrine cells (ACs) provide inhibition within the two synaptic layers, the outer- (OPL) and the inner plexiform layer (IPL), respectively, with gamma-aminobutyric acid (GABA) and glycine being the inhibitory neurotransmitters of the retina (Masland, 2001, 2012a).

HCs modulate the output of PRs and drive more broad functions in the outer retina by regulating the overall gain and enhancing the contrast (Chapot et al., 2017; Masland, 2001). ACs perform more heterogeneous and complex computations by forming synapses onto BCs, GCs and other ACs in the IPL. With roughly 40 subtypes, they represent the most diverse but least understood class of neurons in the retina (Diamond, 2017; Helmstaedter et al., 2013; Macneil & Masland, 1998; Masland, 2012b).

The work presented in this thesis focuses on the transformation of visual signals at the output of BCs. As described above, BCs comprise the only neuron group that connects the outer with the inner retina. However, their role in signal transmission is far more complex than merely forwarding signals along the visual pathway. The following part of this introduction will highlight the essential intrinsic and extrinsic features of these neurons. The information will provide the reader with basic knowledge to understand the newly discovered circuitries presented in chapters 3,4 and 5.

We will start at the input of BCs - that is their dendritic tree residing within the OPL - and then move to their output in the IPL.

1.2 Bipolar cells

Anatomical and functional census of BCs reveals a multiplicity of subtypes. The adult zebrafish retina contains 17 types (Fig. 1.2A, next page) (Connaughton, 2011), whereas 14 have been described in mice (Fig. 1.2B) (Franke et al., 2017). The increase of BCs types in the zebrafish likely reflects their increased spectral

diversity of cones. Whereas the cones in mice comprise two types that are sensitive to colours with short or medium wavelengths, zebrafish's cones can additionally detect long wavelengths and UV-light (Baden & Osorio, 2019).

BCs differ in the number of cones they contact, their dendritic tree size and their axonal stratification pattern within the different layers of the IPL (Fig. 1.2).

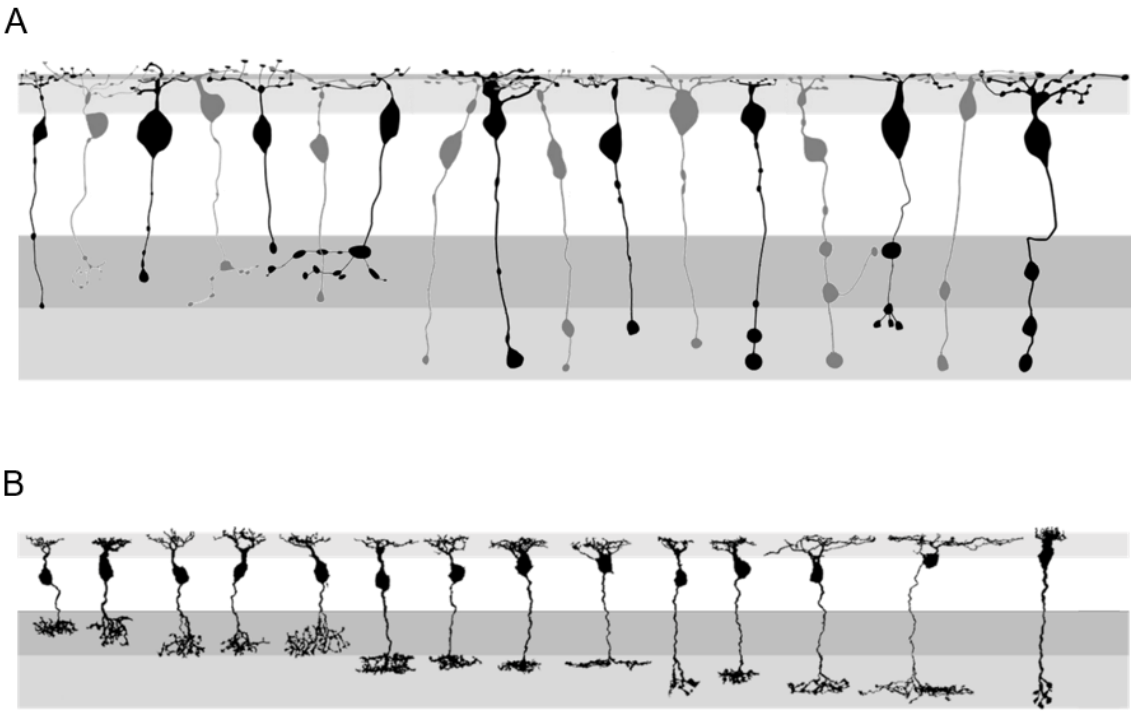

Figure 1.2: Morphological atlas of bipolar cells in zebrafish and mice

A: The zebrafish retina comprises 17 types of BCs out of which seven and six project their terminals to the OFF layer (dark grey) and ON layer (light grey), respectively. Four BCs form synapses in both layers. **B:** Mice possess five ON and eight OFF BCs that contact cones and one rod BC. Note the different spread of dendric trees, projection length and stratification pattern. OFF cells tend to project their axons into the retina's proximal depth (sublamina a), ON cell terminals are in the distal part of the IPL (sublamina b). Figure adapted from (Connaughton, 2011) and (Berens & Euler, 2017).

1.2.1 Intrinsic properties of bipolar cells

1.2.1.1 Dendritic composition and inferred mechanisms

The type and number of connections the dendritic tree of a BC makes to neurons of the OPL establish some cardinal channels such as chromatic and achromatic pathways. Some BCs contact rod PRs or cones only whereas others receive

mixed input. Cone-selective BCs either contact cones of one spectral class or innervate different cones in a non-selective manner. Depending on the contacts a BCs' dendritic tree makes to spectrally different cones, chromatic or achromatic cell types can be distinguished. Many mammalian BC types contact all cones within the spread of their dendritic tree and thus cannot encode colour: they code luminance (Euler et al., 2014).

1.2.1.1.1 ON-OFF Pathways

The ON-OFF channel system accounts for a prominent pathway in vertebrate vision as it allows for the detection in increases or decreases of light against a dark or light background, respectively (Werblin & Dowling, 1969; Westheimer, 2007). Complex computations such as perceiving an object's orientation (Antinucci & Hindges, 2018) or its motion (Kim et al., 2014; Wei, 2018) depend on comparing the output of these two channels in space and time.

This signal bifurcation's anatomical basis lies in the expression of different glutamate receptors at the dendritic tree of BCs (Fig. 1.3, next page), which control the activation of ion-channels in opposing ways (Devries, 2000; Koike et al., 2010).

OFF BCs follow the sign of the PRs by depolarising and releasing glutamate when ambient luminance levels decrease. They express ionotropic α-amino-3-hydroxy-5-methyl-4-isoxazole propionic acid receptor- (AMPA) and kainate-receptors (Devries, 2000) that trigger a pore opening for cations to pass through upon binding of glutamate. In contrast, ON BCs reverse the PRs' sign and express the metabotropic glutamate receptor 6 (mGluR6) (Nomura et al., 1994; Vardi et al., 2000). In the darkness, glutamate binding initiates an intracellular G-protein coupled signalling cascade that causes the closure of the cation-channel TRPM1 (transient receptor potential cation channel subfamily M member 1) (Koike et al., 2010). In bright conditions this process reverses, the channel opens, followed by an influx of cations that causes the cell to depolarise.

The voltage traces shown at the bottom of Figure 1.3 (next page) represent a standard textbook depiction but might lead to the false impression that the response of ON and OFF cells to changes in light intensity can be unipolar only. However, sharp electrode recordings in salamander eye cup preparations

showed that BCs produce graded responses to both negative and positive contrast (Burkhardt et al., 2006).

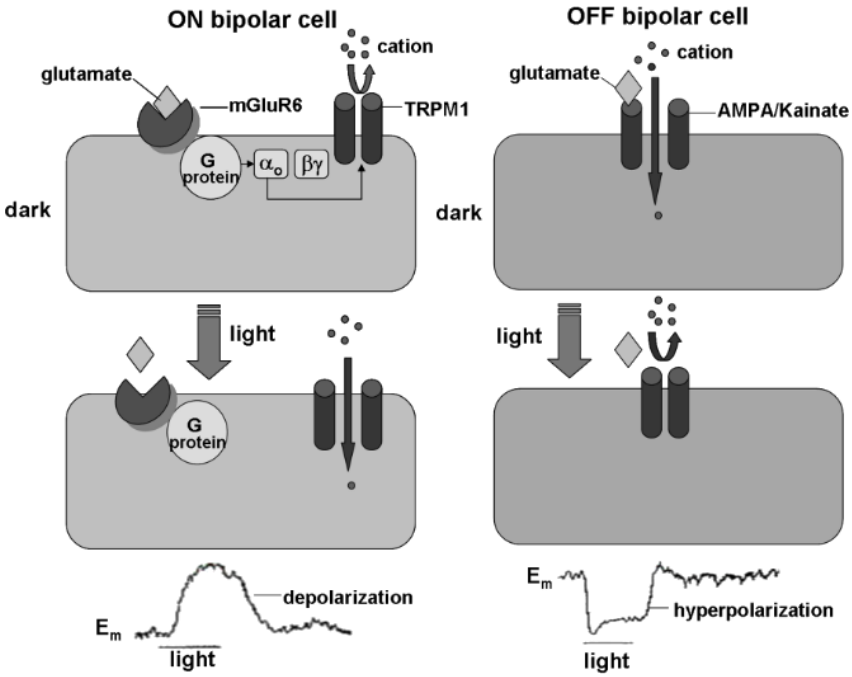

Figure 1.3: Glutamate signalling in ON and OFF bipolar cells

In darkness (upper panel), glutamate binding to mGluRs expressed at the dendritic tree of ON BCs (left panel) initiates an intracellular G-protein coupled cascade that causes the cation-channel TRPM1 to close, leading to a hyperpolarisation. A transition to brighter luminance levels (lower panel) reverses this process and enables the cell to depolarise. OFF BCs express ionotropic glutamate receptors with an inverse glutamate binding behaviour as to ON cells. Here binding of glutamate during darkness triggers the opening of a pore, the influx of cations causes the cells to depolarise in darkness. An increase in ambient light levels reverses the opening of the channel. Figure taken from (Popova, 2015).

Similar observations were made from white noise analyses in catfish BCs in which the cells followed low contrast modulations linearly (Sakai & Naka, 1987). Burkhardt et al. suggest that the ability of BCs to encode positive and negative contrast deflections has been formerly unrecognised due to differences in light adaptation and preparation of the tissue. While the vast majority of investigations into the physiology of BCs by electrophysiological means was based on isolated retinae or retinal slices, which were dark-adapted, Burkhardt et al. obtained their recordings from light-adapted eyecup preparations allowing for preservation of the retinal circuits. The authors conclude that “if the ON and OFF pathways are

truly the substrate for selective processing of negative and positive contrasts, this dichotomy may depend primarily on selective connections and mechanisms beyond the bipolar cells" (Burkhardt, 2011).

ON and OFF BCs are morphologically distinct and tend to project to different depths of the IPL (Fig. 1.2, page 4). OFF terminals are more prevalent in the layers adjacent to the inner nuclear layer (sublamina a), whereas ON cells descent into deeper layers (sublamina b) adjacent to the GC layer (Euler et al., 2014). Within these different layers of the IPL BCs form complex synaptic connections with postsynaptic amacrine and GCs as shown in the electron micrograph of the human and the zebrafish retina in Figure 1.4A and 1.4B, respectively (Dowling & Boycott, 1966; Schmitt & Dowling, 1999).

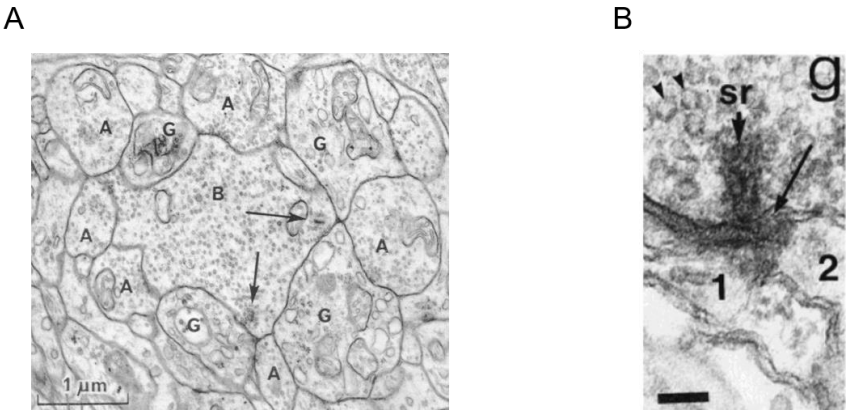

Figure 1.4: Ultrastructure of the inner plexiform layer

A: Electron micrograph of the human retina. A BC terminal (B) with 2 ribbons (arrow) surrounded by GC dendrites (G) and amacrine processes (A). **B:** Electron micrograph of the zebrafish retina. BC terminal filled with synaptic vesicles (arrowhead) and electron-dense material (arrow). Note the presumptive synaptic ribbon (sr) and the two adjacent postsynaptic processes (1, 2). Scalebar = 90 nm. Figure in A and B from (Dowling & Boycott, 1966) and (Schmitt & Dowling, 1999), respectively.

GCs were the sensory neurons in which the ON-OFF dichotomy was first discovered by the seminal work of Haldan Keffer Hartline (Hartline, 1935, 1938). He recorded individual GCs' electrical activity and found that they respond only to the illumination of a small area of the retina - the receptive field (Fig. 1.5A, next page). Three functionally distinct cell types were described: ON types that responded to the onset of light, OFF types that responded to the offset of light and ON-OFF types (mixed types) that signalled both polarities.

Subsequent studies by Kuffler (Kuffler, 1953) and Barlow (Barlow, 1953a) in cats and frogs further revealed that the receptive field of a GC is composed of two regions: the centre-region and the antagonist surround. A stimulus focused on the centre-region elicits a strong response (Fig. 1.5B and C), whereas a stimulus that additionally activates the surround results in a decreased response of the neuron (Fig. 1.5D and E).

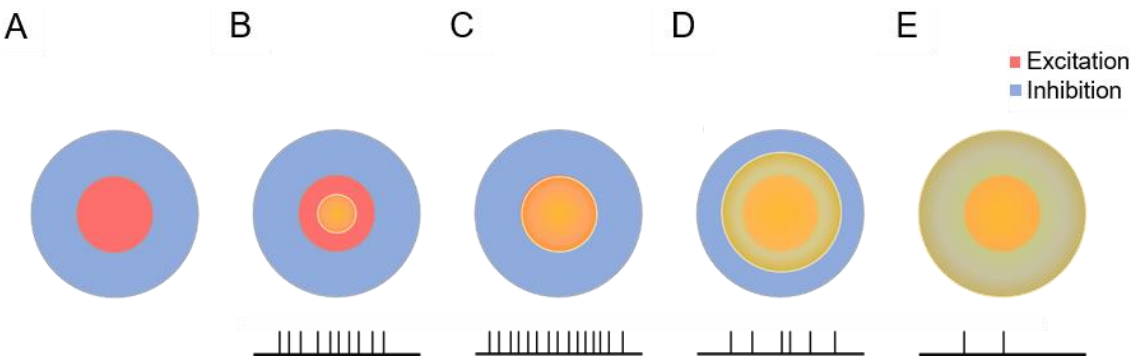

Figure 1.5: Centre-Surround Antagonism

A: Model of a receptive field with excitatory centre (red) and inhibitory surround (blue). **B-E:** Increasing spatial stimulation (yellow) of the receptive field results in an increased response pattern to the point where the inhibitory surround is activated, resulting in a loss of responsiveness. The responses are indicated below the receptive field.

This discovery subsequently led to the question of how the surround antagonism establishes. Two hypotheses were suggested by which either laterally connected horizontal and ACs or convergence of ON and OFF BCs account for the phenomenon. By blocking the ON pathway with the glutamate-analogue 2-amino-4-phosphonobutyrate (APB) and the resulting observation that the centre surround-antagonism of OFF cells is maintained, it was concluded, that lateral connections of inhibitory neurons must indeed provide the surround mechanisms (Schiller et al., 1986). Further studies in many other species established that the centre-surround antagonisms and the described three different response profiles of GCs towards changes in light- levels are a fundamental principle for the visual systems of all vertebrates.

The excitatory input of BC terminals directly drives a GC's receptive field centre's response profile towards light intensity changes. Hence ON GCs and OFF GCs receive inputs from ON and OFF BCs only, respectively, whereas ON

and OFF BCs merge onto ON-OFF GCs. With ON and OFF BCs descending into different layers of the IPL, the stratification of each GC type's dendritic trees follows this pattern: OFF GCs are contacted by BCs in sublamina a whereas ON GCs receive their input in sublamina b. Mixed GCs tend to present a bi-stratified pattern of their dendritic arbour into both sublaminae.

The axons of GCs project to retinorecipient areas of the brain. In mammals most axons ascend to the lateral geniculate nucleus (LGN) of the thalamus which relays information from the retina to the primary visual cortex (V1). Studies by Hubel and Wiesel (Hubel & Wiesel, 1961) showed that there is no transformation of the ON-OFF signalling at the level of the LGN; the centre-surround receptive field organisation of the retina is maintained. However, receptive fields in V1 present various spatial profiles composed of multiple ON and OFF subregions.

In the embryonic and larval zebrafish retina, axonal GC projections form arborisation fields (AFs) which are numbered from 1 to 10 according to their location along the optic tract. While AF1 and AF10 comprise the adult retinorecipient areas of the suprachiasmatic nucleus and the optic tectum, respectively, the matching of the remaining AFs with adult retinorecipient nuclei and their respective function is still under investigation (Baier & Wullimann, 2021).

Since the ON-OFF dichotomy discovery, it has been thought for a long time that both pathways remain strictly separated from each other until they converge onto mixed ON and OFF GCs or converge onto cells in V1. More recent studies revealed that these channels modulate each other presynaptic to the GC layer. The inhibitory network of ACs drives this modulation. Like GCs, these cells can be divided into the ON, OFF or ON-OFF type depending on their input by BCs.

A detailed description of ACs can be found towards the end of this chapter. However, it should be noted here that ON ACs can inhibit the OFF pathway, and vice versa OFF ACs can inhibit the ON pathway. This process is termed crossover inhibition and is essential for several critical retinal computations: it enables GCs to maintain the encoding of temporal contrast during changes of mean luminance in the visual scene (Manookin et al., 2008), it compensates for synaptic rectification (Molnar et al., 2009) - a phenomenon where depolarisation excites a neuron more than hyperpolarisation inhibits, which is prevalent at the transmission level from BCs to GCs (Gollisch & Meister, 2010; James et al., 2019) and it generates the sustained OFF channel in the inner retina (Rosa et al., 2016).

Previous studies have suggested that the ON-OFF-dichotomy evolved to signal changes in light intensity at a lower metabolic cost and in a more rapid manner than a hypothetical one channel system (Gjorgjieva et al., 2014).

1.2.1.2 Axonal composition and inferred mechanisms

Given that BCs are comparatively small neurons, their surface area and low membrane conductance cause little attenuation of the input signal travelling down the axon. However, the presynaptic “equipment”, such as the ribbon and the distribution of various ion channels, shapes the signal transmission in fundamental ways.

1.2.1.2.1 The synaptic ribbon

A specialisation of BC and PR terminals are ribbons that endow the synapse to continuously release glutamate in response to maintained depolarisation instead of synapses where action potential dictate vesicle release (Lagnado & Schmitz, 2015). Ribbons are electron-dense structures that hold glutamate filled vesicles close to the active zone (Fig. 1.6A).

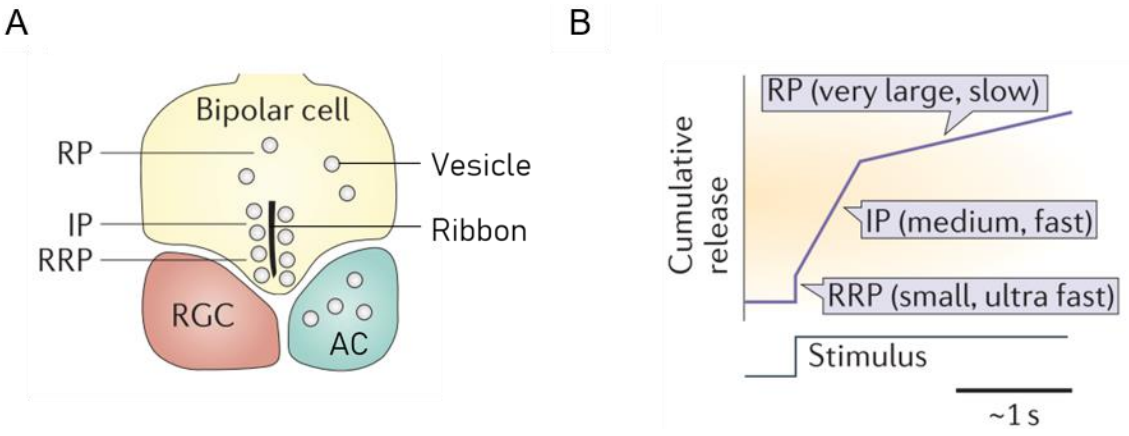

Figure 1.6: Vesicle release dynamics at ribbon synapses

A: Schematic of ribbon synapse of BC presynaptic to dendritic tips of a GC and AC. **B:** Cumulative release versus time plot revealing release dynamics of the different vesicle pools (RRP, readily releasable pool; IP, intermediate pool; RP, reserve pool) during prolonged stimulation at a ribbon synapse. Figure adapted from (Euler et al., 2014).

Vesicles close to the plasma membrane build the ready-releasable pool (RP) and prime for immediate release (<10 ms), those tethered to the ribbon build the intermediate pool (IP) and usually deplete during prolonged light stimulation (Fig. 1.6B, previous page). Untethered vesicles of the reserve pool (RR) refill the depleted vesicles of the ribbon. This system endows the synapses positioned upstream within the visual signalling pathway with release-machinery that can act on a fast timescale and reliably signal subtle changes in membrane potential. This process is useful as the visual system must signal over a broad range of light intensities. The intensities within a visual scene can differ by 4-5 log units (Pouli, 2010; Fred Rieke & Rudd, 2009) and are encoded by graded changes in membrane potential, rather than spikes (Juusola et al., 1996; Odermatt et al., 2012).

The analogue signals that arrive at the BC synapse trigger the release of glutamate-filled vesicles which can occur synchronously and is termed multivesicular release (MVR) (Rudolph et al., 2015; Singer et al., 2004). A recent study brought new insights into how a “quantised” release of vesicles leads to the discretisation of analogue signals arriving at BC terminals into up to 11 sequences of numbers (James et al., 2019). This process enables the synapse to optimise information transfer; the synchronous release of five vesicles transmits four times as many bits of information as five individual release events.

1.2.1.2.2 Ion channels

The terminals of BCs contain various ion channels that are differentially expressed amongst BC subtypes.

The influx of calcium mediates glutamate release in BCs through voltage-gated L- and T-type calcium channels. Most BCs operate at voltages around ~ -70 to -20 mV (Ashmore & Copenhagen, 1983; Saito & Kaneko, 1983; Simon et al., 1975). Modest depolarisations (-40 to -30 mV) activate T-type channels, whereas stronger deflections from rest activate L- and T-type channels (Pan et al., 2001; Tachibana et al., 1993; Von Gersdorff & Matthews, 1994; Zenisek et al., 2003).

For a long time, GCs and ACs were thought to be the only spike-generating neurons within the retina, but it has been shown that BCs are capable of

generating all-or-nothing spikes in addition to graded potentials thus allowing for quick signalling to GCs (Baden et al., 2011; Dreosti et al., 2011). The spike generating mechanism is mainly promoted by L- and T-type calcium channels but some spikes can be generated through voltage-gated sodium channels (Baden et al., 2011).

The size of a bouton can dictate the calcium dynamics and ultimately influence the neurotransmitter release (Baden et al., 2014). A study demonstrated that smaller terminals generate faster and larger calcium transients and thus can follow higher temporal frequencies effectively. The conductance through calcium-gated potassium (Hu & Pan, 2002) and chloride channels (Okada et al., 1995) establishes another form of temporal filtering as the diffusion of calcium ions through the terminal delays membrane hyperpolarisation.

Hyperpolarisation-activated cyclic nucleotide-gated (HCN) channels are enriched in BC terminals (Müller et al., 2003) and comprise unique properties as their activation results in an *influx* of ions into the cell, they have characteristic slow activation times and are not only regulated by changes in membrane voltage but also by cyclic nucleotides (Biel et al., 2009; Wahl-Schott & Biel, 2009). We will describe and discuss these channels' role in detail in chapter 4 to show that these channels endow individual ON BCs with the ability to send an excitatory signal to their postsynaptic partners whenever the polarity of light switches - a previously unrecognized feature of BCs.

1.2.2 Extrinsic properties of bipolar cells

Even though the functional properties of BCs are initially determined by the signals fed into the dendritic tree and subsequently modulated by intrinsic mechanisms mentioned above, it has been shown that the response profile of a BC can differ depending on the spatial structure of the visual input (Franke et al., 2017). Figure 1.7 (next page) shows two different BC-types' responses to a stimulus composed of steps of light followed by periods of increasing temporal frequency and contrast.

Whereas local stimulation (Fig. 1.7A, next page) causes both cell-types to respond similarly, it has been shown that full-field stimulation drastically de-correlates their response profiles with a complete polarity switch (Fig. 1.7B, next

page). At the core of this decorrelation lies the diverse and complex network of inhibitory ACs. In the following section, we will introduce ACs and their role in transforming signals.

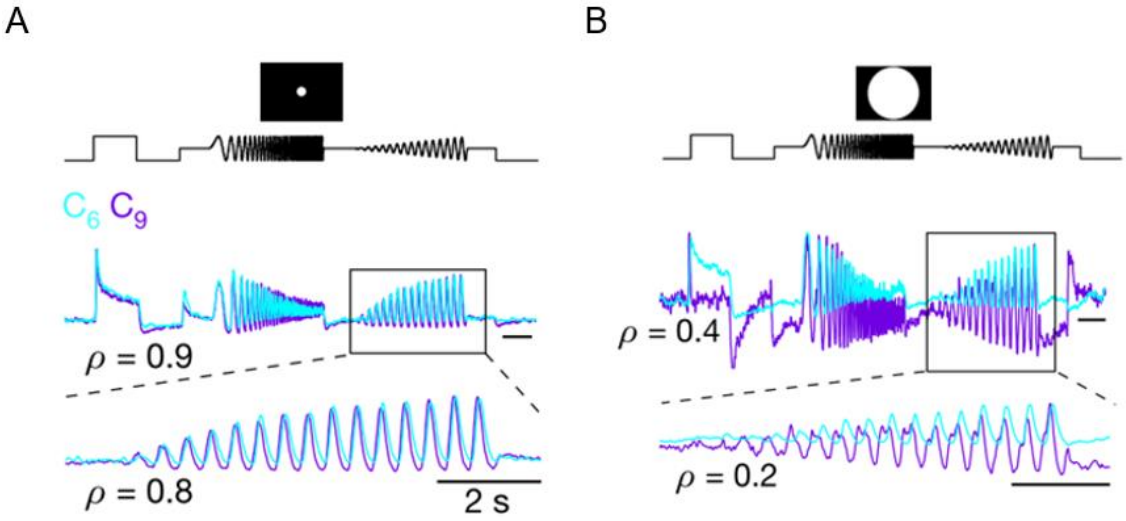

Figure 1.7: Antagonistic surround decorrelates responses of bipolar cells

A: Local field stimulation of two different BC types (pink and blue) with a stimulus consisting of a step of light followed by a chirp of increasing frequency and contrast. **B:** Same as in A but now full-field stimulation. Note the change in polarity and the overall decorrelation. Linear correlation coefficients (ρ) are shown for the whole trace and contrast ramp only. Figure adapted from (Franke et al., 2017).

1.3 Amacrine cells

Within the vertebrate retina, ACs present the most diverse neurons. They provide inhibitory synapses onto GCs (feedforward inhibition), other ACs (lateral inhibition) and additionally build feedback circuits onto BCs (Diamond, 2017; Dowling & Boycott, 1966; Eggers & Lukasiewicz, 2006). The synaptic connections of the ACs to the GC layer outnumber the connections provided by the BCs (Calkins et al., 1994; Freed & Sterling, 1988).

Several striking characteristics reflect the diversity of ACs: in contrast to typical neurons, most of them lack an axon. Their inputs and outputs are distributed along the dendritic tree with each synapse acting as an independent computing unit that allows some of them to perform different computations in parallel. They present diverse morphologies: small-, medium- to wide-field

arborisations cover narrow to broad visual scenes; some maintain their stratification in one layer of the IPL, others extend their processes across varying depths (Kolb et al., 1981; Macneil & Masland, 1998). Figure 1.8 gives an overview of zebrafish ACs observed in five-day-old zebrafish.

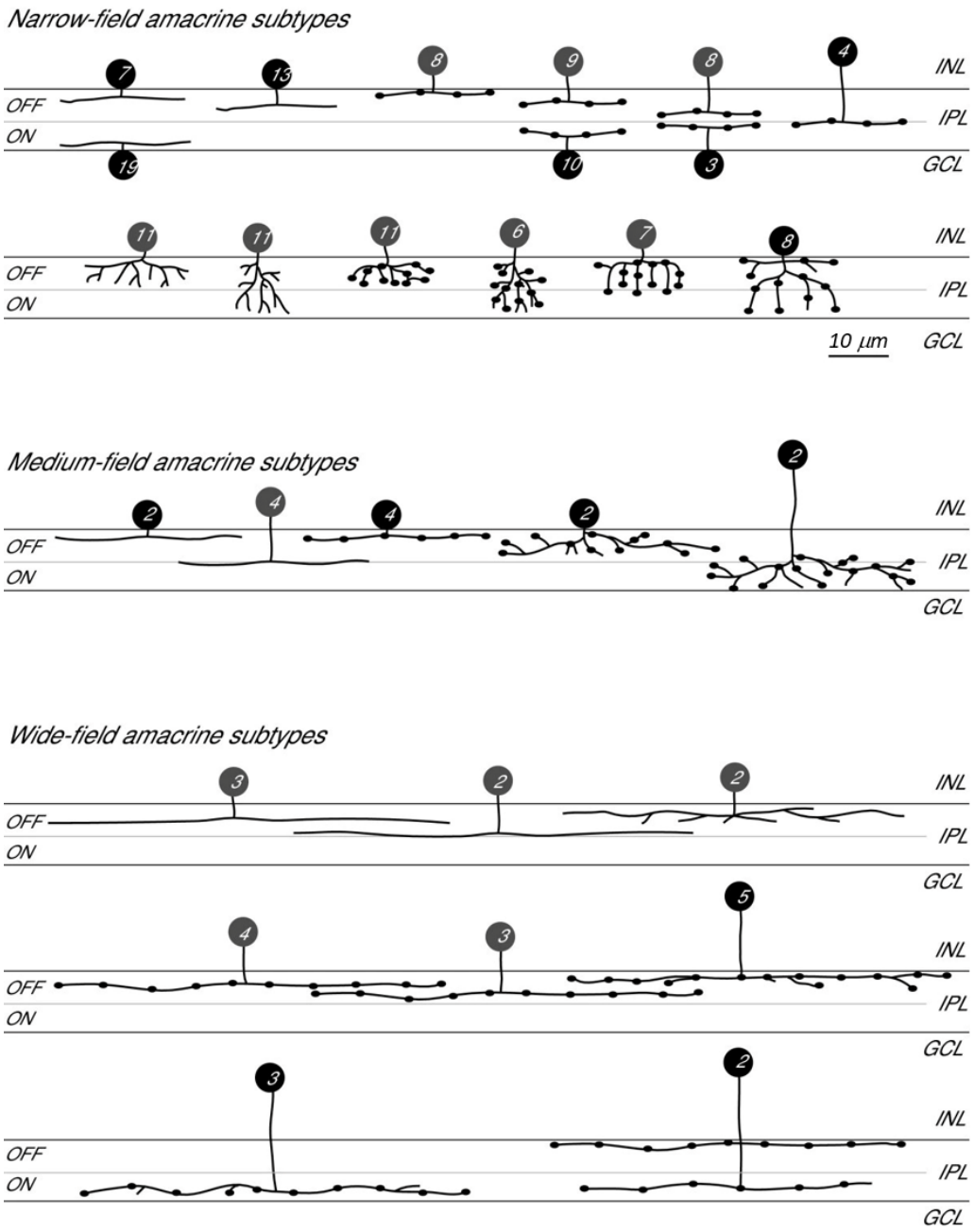

Figure 1.8: Morphological atlas of zebrafish amacrine cells

Schematic showing an atlas of 28 different AC types in zebrafish juvenile retinae (5 dpf). Note the categorization into narrow-, medium- and wide-field cells and the different projection-depths into the IPL. INL, inner nuclear layer; IPL, IPL; GCL, GC layer. Figure from (Jusuf & Harris, 2009).

Small-field ACs modulate the visual signal locally but across all layers of the IPL whereas medium- and large-field ACs process stimuli at larger spatial scales restricted to single layers (Berens & Euler, 2017).

A prominent feature is the co-expression of neurotransmitters: most ACs are either GABA- or glycinergic but many co-express other neurotransmitters (e.g. acetylcholine or dopamine), neuropeptides (e.g. substance-P or vasoactive intestinal peptide) or nitric oxide (Kolb, 1995; Masland, 2012b; Vielma et al., 2012; Villette et al., 2019).

While some AC circuits have been dissected to completion (Bloomfield & Dacheux, 2001; Borst & Euler, 2011), most of their functional roles within microcircuits remain elusive since they are difficult to access for physiological recordings, possess independent processing units and their genetic profiling is incomplete. Moreover, each cell type is thought to drive distinct and specialised functions (Diamond, 2017) and thus might be more difficult to discover.

Nevertheless, studies aiming for more general categorisation of AC activity across the inner retina have revealed fundamental retinal processing principles. A study in salamander investigating the excitatory input from individual BCs to GCs, in which properties like kinetics, adaptation, and rectification at the BC-GC synapse were analysed, showed that ACs lie at the basis of the observed signal divergence (Asari & Meister, 2012).

1.4 Ganglion cells

GCs are the output neurons of the retina. Each type extracts specific visual scene features by integrating visual information over its receptive field in space and time. Since the dendritic tree of a BC is much smaller than the spatial extent of a GC, hundreds of BC signals can converge onto a single cell (Barlow, 1953b; Hartline, 1940). The integration of this multitude of excitatory signals can occur in either linear or non-linear fashion before the signals are ultimately sent in the form of a spike code along the optic nerve to downstream areas in the brain.

Morphologically GCs are usually distinguished by their dendritic field characteristics and stratification within the IPL as shown for the atlas of the 14 morphologically distinct zebrafish GCs shown in Figure 1.9 (next page). However, recent studies suggested that further division based on the axonal projection

patterns into the brain might be useful since, e.g. in mice, it was shown GCs can project to up to ~40 distinct areas (Morin & Studholme, 2014). Similarly, it has been shown that axons of zebrafish GCs that possess identical dendritic tree morphology diverge onto 10 different arborization fields of the tectum (Robles et al., 2014).

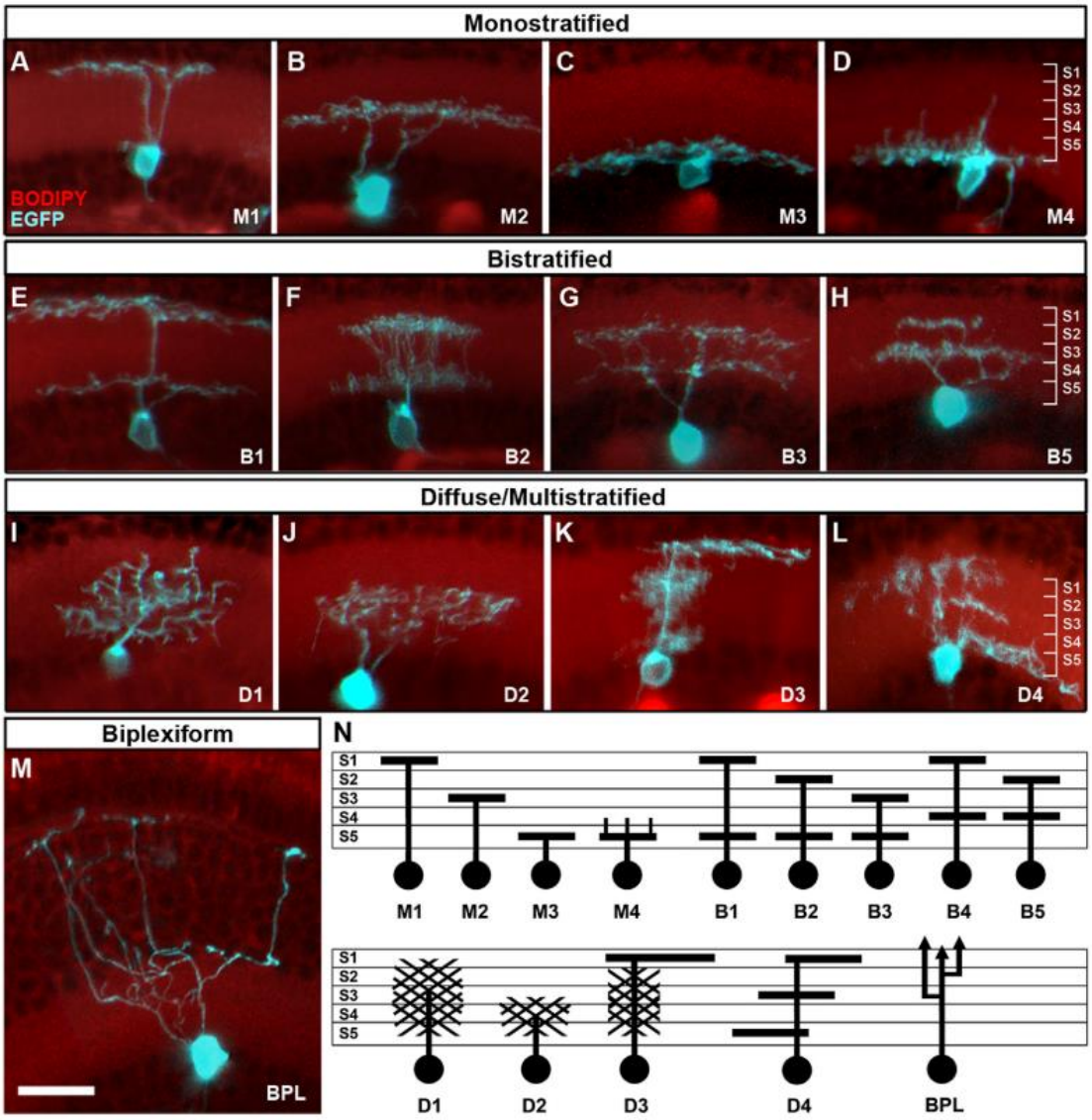

Figure 1.9: Morphological atlas of zebrafish ganglion cell stratification within the inner plexiform layer

Schematic of 14 different GC types present in 6-7 dpf-old juvenile zebrafish retinae. **A-D:** Examples of monostratified cells**. E-H:** Example of bistratified cells. **I-L:** Examples of multistratified/diffuse GCs. **M:** Biplexiform cell, characterized by the dendritic tree's projection into both synaptic layers of the retina. **N:** Schematic summary of 14 RGC classes defined by IPL stratification. Scalebar = 12.5 µm. Figure from (Robles et al., 2014).

Some GC types project their dendrites into one stratum (Fig. 1.9A-D, previous page) while others can cover two (Fig. 1.9E-H) or more strata (Fig. 1.9I-M) of the IPL. Interestingly, in zebrafish, one type shows a stratification within both synaptic layers of the retina (Fig. 1.9M).

Whereas early functional classifications divided GCs into ON, OFF and ON-OFF types based on their response to decreases and increases of light, recent studies have revealed a more nuanced and diverse census of subtypes. For example, an approach in which thousands of GCs were functionally analysed by calcium-imaging under two-photon illumination showed that 32 functionally different cell types can be distinguished from each other in mice (Baden et al., 2016). In zebrafish, more than 50 GC types were identified based on their pre- and postsynaptic structure (Robles et al., 2013, 2014) and 30 different types based on their transcriptional profile (Kölsch et al., 2021). However, despite many efforts, a complete functional classification has not been revealed yet (Nikolaou et al., 2012; Semmelhack et al., 2014; Zhou et al., 2020).

1.5 Aims of this thesis

This thesis comprises an investigation of the computational power of BCs. While some fundamental feature-extracting pathways emerge at the dendritic tree, we will focus on the synaptic compartments that form the neuron's output. In terms of studies to date, there is an active debate as to whether:

1. The various outputs of individual BCs can transmit qualitatively different information to their postsynaptic partners or if the responses are homogenous across all synapses.
2. The outputs of BCs display some degree of selectivity towards stimuli that either move into a specific direction or possess a specific spatial orientation.

This thesis aims to provide answers to both of these questions. We use larval zebrafish *Danio rerio* that express functional reporters of neuronal transmission in different cell types of the inner retina. This method allows us to study individual

neurons' physiology and their involvement in the circuitries of the retina *in vivo* under two-photon illumination.

Chapter 2
Methods

2. Methods

2.1 Animals

All animal procedures were carried out under the UK Animals (Scientific procedures) Act of 1986 (PPL 70/8851) and in accordance with the UK Home Office guidelines and approval of the University of Sussex Animal Welfare and Ethical Review Board. Genetically modified zebrafish strains were either generated at the University of Sussex or imported from other licenced establishments. Line maintenance and breeding were conducted at the Biological Research Facility (BRF) at the University of Sussex. Animals were housed under standard conditions on a 14h light cycle (light onset: 8 am, light offset: 10 pm; 15 minutes of ramping up and down, respectively). Larval zebrafish were housed in incubators at 28°C. The same light cycle as for adult fish was applied; however the transition from light to dark and vice versa was immediate.

2.2 Two-photon excitation microscopy

2.2.1 The principles of two-photon microscopy

The development of two-photon excitation microscopy (Denk et al., 1990), when combined with genetically encoded fluorescent reporters, serves as a powerful alternative to electrophysiological approaches in studying the physiology of neurons *in vivo*. The technique is based on the principle of two-photon absorption (Göppert-Mayer, 1931) whereby a fluorophore is excited by the simultaneous absorption of two photons of lower energy in the same way as it is excited by the absorption of one photon of higher energy only. Since the timescale of molecular absorption is extremely short (~10^{-16} seconds) and the event of simultaneous absorption of photons depends on a high density of photons focused at the probe, Titanium-Sapphire lasers are typically used. These lasers deliver highly repetitive infrared light pulses of short duration (10^{-15} seconds). In contrast to the conventional laser scanning confocal microscopy, which is based on one-photon absorption, two-photon excitation depends on the square of light intensity which means that a doubling of the excitation intensity quadruples the rate of emission. Additional benefits of using two-photon excitation microscopy lie in the spatial

confinement of fluorophore excitation to a small volume. Only the focal point of the objective delivers the photon density needed for the two-photon effect to occur. There is no emission from regions that lie out of focus and thus no photobleaching outside the excitation volume. Furthermore, the use of infrared light allows for deeper optical penetration of the tissue and less scattering due to the lower energy content of the longer wavelength.

2.2.2 Technical details of two-photon setup

Imaging was carried out using a two-photon microscope (Scientifica) equipped with a mode-locked titanium - sapphire laser (Chameleon II, Coherent) tuned to 915 nm. Excitation was delivered through a 20x water immersion objective (Olympus, XLUMPlanFL) with a numerical aperture of 0.95. Emission was captured both by the objective and a substage oil condenser (Olympus; NA of 1.4) and filtered through GFP filters (green emission: HQ 525/50, red emission: HQ 620/60 Chroma Technology) before detection using GaAsP photomultipliers (H7422P-40, Hamamatsu). The signal from each multiplier passed through a current-to-voltage converter, and then the two signals were added by a custom-made summing amplifier before digitization. Scanning and image acquisition were performed using the software ScanImage (v.3.8)(Pologruto et al., 2003). Functional imaging was typically performed at a framerate of 100 Hz (256 × 20 pixels per frame, 0.5 ms per line), while high resolution images were acquired at 512 x 512 pixels or 256 x 256 pixels per frame, 1 ms per line.

2.2.3 Preparation of larval zebrafish for imaging

All experiments were performed at room temperature (20°C – 25°C) from 11 a.m. to 8 p.m. All fish used for imaging experiments were between six and nine days-post-fertilisation (dpf) old. Hetero- or homozygous *casper* mutant fish (White et al., 2008) were used to improve the signal-to-noise-ratio (SNR) of in-vivo multiphoton recordings. Treatment with 1-phenyl-2-thiourea (200 µM final concentration; Sigma) from 10 hours-post-fertilisation (hpf) reduced pigmentation further. Prior to imaging larvae were embedded in 3% Hi-Strength™ LMP Agarose (Biogene) and mounted in a chamber on top of a glass cover slip (thickness 0) where they were superfused with E2 fish medium (Westerfield,

2000). The ocular muscles were immobilized by injection of ~ 1 nl alpha-bungarotoxin (2 mg/ml, Alomone Labs) to prevent eye movement.

2.2.4 Light stimulation with lightguide

For the experiments presented in chapters 3 and 4 full-field stimuli were delivered through a lightguide positioned in proximity to the fisheye, as shown in Figure 2.1A. The light source consisted of an amber light-emitting diode (LED) (l_{max} = 590 nm, Thorlabs) filtered through a 590/10 nm bandpass filter (Thorlabs). To study the kinetics of the responses, steps of light (318 nW/mm2) of different duration (1 s, 0.5 s and 0.25 s) were repeated for ten times each with an interstimulus period of 3 s of darkness in between each step. The stimulation with temporal frequencies at 0.5 or 1 Hz consisted of square wave modulations around the mean (159 nW/mm2) at 100 % contrast for 24 s. Three seconds of constant light illumination preceded and followed the flicker. The same mean intensity was used in experiments in which we varied contrast.

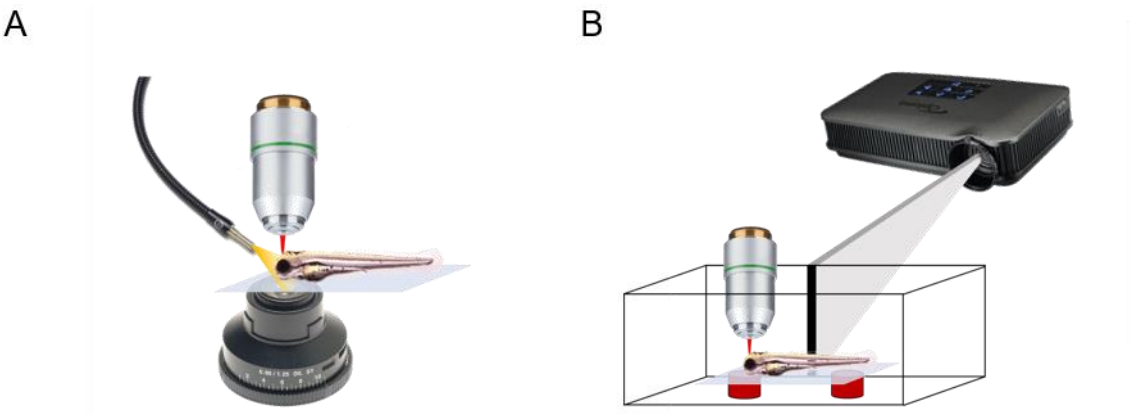

Figure 2.1: Methods of light stimulation

A: **Stimulation with a LED lightguide.** A fish larva embedded in agarose mounted on a glass slide (slide holder not shown) and covered by a drop of fish water (E2). A LED lightguide positioned close to the eye stimulates the fisheye. Excitation occurs through the object above. Photons are collected through both, the objective at the top and condenser at the bottom. **B: Stimulation with the fish cinema**. In agarose embedded fish larvae mounted on a stage that is made out of a glass slide sitting on top of two magnets. The stage is positioned within a small chamber filled with fish water (E2). All sides of the chamber are made of black plastic except one side that consists of a screen onto which movies of moving bars (here vertical black bar) or static gratings (not shown) are projected by a pico projector. Excitation and photon collection occur through the objective, note that this setup lacks photon collection through a condenser.

2.2.5 Light stimulation with LED projector

For the orientation selectivity experiments presented in chapter 5, we build a fish “cinema” shown in Figure 2.1B (previous page). Sequences of moving bars or static gratings were projected onto a screen through a pico projector (Optoma PK320, Watford, Hertfordshire, U.K.) with the red LED enabled only. The code for stimulus delivery was written in MATLAB (MathWorks, Natick, MA, U.S.A.) using the Psychophysics Toolbox software (Brainard, 1997). Visual stimulation was synchronised with imaging using custom-written code and a U3 LabJack digital-to-analogue converter (Labjack, Lakewood, CO, U.S.A.).

The moving bars stimulus consisted of -100% contrast bars with a width of 4.1° of visual angle and a height matching the screen’s height moving across a background of 12.7 nW mm^{-2} irradiance at 18.6° s^{-1} in 8 different directions in a pseudo-random order. The representation of different directions was repeated 5 times with each bar being spaced 6 s apart from each other in time. A visual representation of the stimulus is shown in Figure 5.1, chapter 5, page 86.

The static grating stimulus comprised a full-field grating of 0.03 cycles per degree reversing contrast from minus to positive 100% at a frequency of 5 Hz. The grating stimulus started with 10 seconds of mean illumination followed by alternating representations of horizontal (90 °) and vertical bars (0 °) reversing contrast for 10 seconds each, repeated twice in total. A visual representation of the stimulus is shown in Figure 5.3, chapter 5, page 88.

The stimulus to map the receptive fields consisted of a -100% contrast bar projected onto the screen at 5 orientations ranging from 0 ° to 144 °. Each bar covered 6.2 ° of visual angle and was presented with 50 % overlap, resulting in a spatial resolution of 3.2 °. Bars were presented 2 s apart in a pseudo-random manner for a period of 0.5 s.

2.3 Genetically encoded reporters of neural activity

Imaging genetically encoded fluorescent reporters has emerged as a powerful alternative to study the physiology of neurons compared to the traditionally used electrophysiological recordings. These sensors enable researchers to study individual cells or whole populations *in vivo* and assess their physiology on timescales from milliseconds to months (James et al., 2019; M. Li et al., 2017).

2.3.1 Genetically encoded calcium indicators (GECIs)

GCaMP-sensors have become one of the most widely used reporters in functional imaging (Chen et al., 2013; Rose et al., 2014). These indicators are calcium sensors which contain a circularly permuted green fluorescent protein (GFP), or a derivative form, fused to calmodulin (CaM) and the M13 domain of the myosin light chain kinase. Binding of calcium ions to the CaM-domain induces conformational changes within the chromophore which results in increased fluorescence. Since the binding of calcium occurs cooperatively, CaM-based calcium-sensors can exhibit a non-linearity depending on the prevalent calcium concentration. Thus, even though continuous genetic engineering has brought forward improved versions of GCaMPs over the past decade, that can compete with previously used synthetic reporters in kinetics, dynamic range and sensitivity, precaution and thorough evaluation should be taken into consideration prior use. In the present work GCaMP3.5 (Tian et al., 2009) and GCaMP6f (Chen et al., 2013) reporters were employed.

2.3.2 The glutamate sensor iGluSnFR

In 2013 a new powerful genetically encoded sensor was made available to the scientific community which enabled researchers to study neuronal transmission from a different angle (James et al., 2019; Johnston et al., 2019). The newly developed glutamate sensor iGluSnFR (Marvin et al., 2013) allows the investigation into glutamatergic transmission between neurons. The genetic design, as with previously mentioned GCaMPs, is also based on a circularly permuted GFP. The fusion of a bacterially derived periplasmatic glutamate binding protein GltI to the chromophore and the anchoring of the resulting protein to the extracellular membrane equips this sensor with the ability to report changes in glutamate concentration. The reporter exhibits a large dynamic range (~ 4.5 $\Delta F/Fmax$) and reports changes in glutamate concentration in a linear manner (Borghuis et al., 2013). Notable are the sensitivity and kinetics. A recent study investigating the release of glutamate in BC terminals demonstrated that this sensor can detect the release of single quanta and distinguish between release events with a time resolution of only 12 ms (James et al., 2019).

In the present work the superfolder variant of iGluSnFR (SFiGluSnFR) was used (Marvin et al., 2018). In this improved version of the glutamate sensor, the GFP was replaced with a superfolder version of the protein (Pédelacq et al., 2006), resulting in a faster maturation and export from the endoplasmatic reticulum along the vesicular pathway ultimately resulting in increased expression levels of the protein.

2.4 Transgenesis

Microinjection of DNA into fertilized oocytes serves as a standard method in order to generate transgenic vertebrates. In the early days of generating transgenic animals, DNA constructs were directly injected into eggs. Recent advances in transgenesis have brought forward methods that improve transient and germline integration. The transgenic lines generated in this thesis were based either on the I-SceI-Meganuclease (Thermes et al., 2002) or the Tol2-transposase system (Suster et al., 2009). Briefly, both methods are based on the principle of flanking the transgenic DNA by recognition sequences. The I-SceI-Meganuclease-system comprises flanking sequences which are recognized by the I-SceI-enzyme, which aids integration into the genomic DNA. The Tol2-based system contains flanking regions that are recognized by the Tol2- RNA-transposase.

2.5 Targeting reporters of neural activity to cell populations

Standard procedures for transgenesis are based on introducing plasmid DNA into fertilised oocytes at the one-cell stage. A standard design of a transgenic sequence comprises a promoter region localised upstream to the coding region of a protein of interest. A polyA-signal which ensures the stability, correct localisation and translation of the transcribed RNA follows the protein sequence.

As mentioned previously, studying neuronal activity by imaging reporters of neural activity is a powerful method, but some limitations to this method should be considered prior use. Firstly, to study a specific cell population, it is crucial to identify a promoter that allows for targeted expression of the transgene. Secondly, fluorescent imaging relies on the sensor's high expression-levels to achieve a good signal-to-noise ratio (SNR). The expression of a reporter gene

depends on the promoter's strength; if a promoter is too weak, the sensor's resulting expression levels might be too low to distinguish a signal from noise.

The Gal4/UAS system (Brand & Perrimon, 1993) offers an alternative in driving expression of a transgene if expression levels are too low. This system consists of two parts: the transcriptional activator protein Gal4, brought under the control of a promoter of choice, and an array of upstream activation sequences (UAS) that enhance the transcriptional activity of a downstream positioned basal promoter when Gal4 is bound to them. The basal promoter ultimately drives the expression of any protein sequence brought under its control. Since increasing the number of UAS elements has been shown to result in increased transcriptional activity of the basal promoter (Distel et al., 2009), weak promoters can still drive robust expression within targeted cells.

Studies have shown that targeting reporters to sub-cellular components increases local reporter concentration and thus increases the signal-to-noise ratio. Tethering calcium-sensors to the vesicle protein synaptophysin increases these reporters' linear range (Dreosti et al., 2009). Rather than detecting bulk changes in calcium concentration, the reporter's positioning in the vicinity to the active zone leads to detection of transient changes that represent the voltage-gated influx of calcium ions.

2.6 Transgenic zebrafish lines and constructs

The transgenic lines listed in Table 2.1 on the next page were used within this thesis. The ptf1a:gal4 (Parsons et al., 2009) and UAS:SyGCaMP3.5 (Lowe et al., 2013) lines were generated by other research groups; all other lines were generated within this study. The following sections will give an overview of each line.

Transgenic Line	Expression within retina	Chapter
Ribeye:Gal-BH	Photoreceptors, **Bipolar Cells**	3 and 4
10 x UAS:SFiGluSnFR-MH	Subject to driver-line	3 and 4
HuC:KalTA4-BH [only transiently labelled fish were used]	Horizontal, **Amacrine** and **Ganglion Cells**	3 and 4
Ribeye:SyGCaMP6f	Photoreceptors, **Bipolar Cells** [Reporter targeted to synaptic compartment]	3,4 and 5
Ptf1a:Gal4	Horizontal and **Amacrine Cells**	5
UAS:SyGCaMP3.5	Subject to driver-line [Reporter targeted to synaptic compartment]	5

Table 2.1: Transgenic lines and their expression within the zebrafish retina

Column 1 contains the transgenic lines that were used in this study. Column 2 lists the labelled cell types within the retina; cells of interest for this study are labelled in bold. Column 3 lists chapters in which lines were used. BH/MH: Bleeding heart and mossy heart, respectively.

2.6.1 Ribeye:Gal4-bleeding heart

This line was generated with the purpose to target the transcriptional activator Gal4 to BCs of the retina. The promoter of the zebrafish gene *ribeye a* was identified in a previous study (Odermatt et al., 2012), and it was demonstrated that 1.8 kb of the sequence upstream the start codon of the *ribeye a* gene contains all regulatory elements to drive the expression of transgenes in all ribbon synapses of the eye, vestibular organ, lateral line and pineal gland. However, the expression of the transgenes is stronger in BCs than PRs. Since the Gal4 protein cannot be detected visually, a short heart-specific promoter sequence (cmcl2), driving the expression of a red fluorophore (mcherry), was added to the plasmid. Thus, screening of founder fish could be performed visually under whole field fluorescence by searching for offspring with a red heart (bleeding heart).

2.6.2 10 x UAS:SFiGluSnFR-mossy heart

Our previous attempts to drive expression of the glutamate sensor under the direct control of the ribeye promoter resulted in low expression levels in the early days of development followed by a complete loss of expression by seven days-post-fertilisation. Thus, we employed the previously described Gal4/UAS system in order to increase expression levels. We generated and tested three different UAS-constructs with increasing numbers of UAS-repeats (4 x UAS, 10 x UAS and 14 x UAS). The stable transgenic line with 10 UAS elements resulted in robust expression levels of the sensor in BCs. However, the expression pattern comprises mosaic labelling since the Gal4/UAS system in zebrafish is prone to silencing, resulting in sparse labelling of cells within tissues (Akitake et al., 2011). This sparse labelling allowed for imaging of single BCs. The screening for founders under wide-field fluorescence was unsuccessful initially due to low basal fluorescence of the reporter. Since no green, fluorescent cells could be detected visually, we added the cardiac promoter cmcl2 driving the expression of a green fluorophore (GFP) to the transgene. To obtain double transgenic larvae for imaging, we bred Ribeye:Gal4-BH fish with 10xUAS:SFiGluSnFR-MH fish and selected for red (bleeding) and green (mossy) expression in the heart. Figure 2.2A (page 30) shows the expression pattern within the larval zebrafish eye on seven days-post-fertilisation.

2.6.3 HuC:KalTA4-bleeding heart

The HuC promoter (also termed elavl3) is commonly described as a pan-neuronal promoter. In the retina, we find that expression of proteins under this promoter is excluded from cells that contain ribbon synapses (BCs and PRs) but drives expression in amacrine and GCs. We generated a Gal4-based construct which we injected into incrosses of UAS:SFiGluSnFR fish and led to a robust expression of the sensor. In contrast, crossing the stable line to UAS:SFiGluSnFR fish resulted in weak labelling insufficient for prolonged imaging. Previous attempts to image glutamatergic inputs into amacrine or GCs by using cell-specific promoters (Ptf1a and Islet2b) combined with the Gal4/UAS-system did result in weak or no expression. The new HuC driver line comprises an optimized version of the Gal4 protein, namely KalTA4 (Distel et al., 2009). Figure 2.2B (page 30) shows the

mosaic expression of ACs and GCs in the retina of a 7 dpf old larva. A colleague under supervision cloned the plasmid.

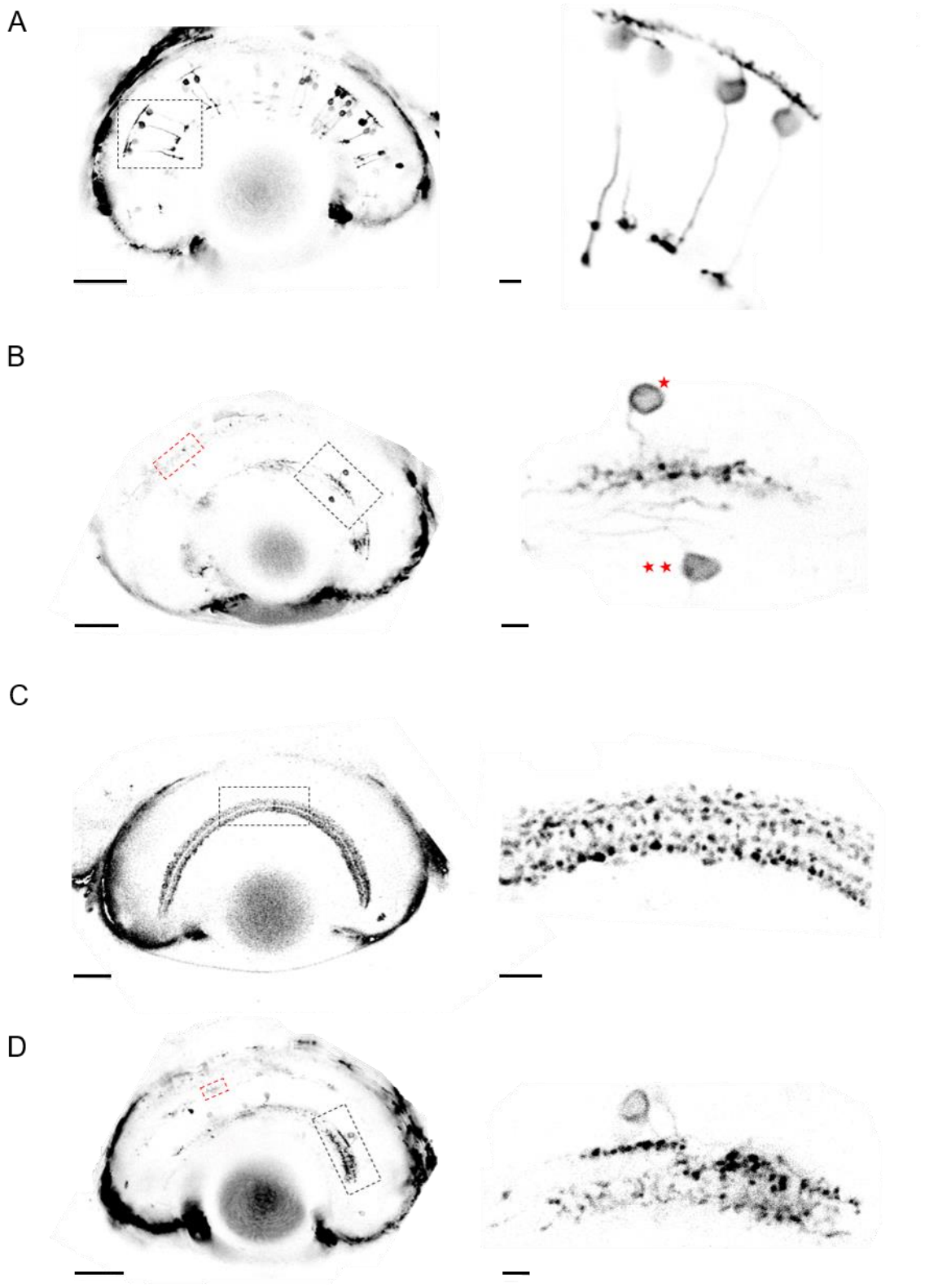

Figure 2.2: Expression of functional fluorescent reporters in the larval zebrafish eye

Pictures comprise average intensity projections of a single plane in 7 dpf old fish. Left column shows whole eyes, right column the insets (dashed boxes). → *bottom next page*

2.6.4 Ribeye:SyGCaMP6f-bleeding heart

Since the development of the first GCaMP sensor in 2001 (Nakai et al., 2001), improved versions were engineered by mutagenesis and targeted design. The engineering of GCaMP6 resulted in three different versions, each displaying different kinetics: GCaMP6-fast, -medium and -slow (Chen et al., 2013). Our lab received a plasmid of the GCaMP6-fast version before the new series was published. The plasmid has one different amino acid to the published version but possesses the same properties. This version was initially named GCaMP6 v.10.500, but in the following, we will only refer to it as GCaMP6f. To improve the signal-to-noise ratio and obtain a report on transient changes in calcium-concentration at the BC terminal GCaMP6 was fused to the vesicular protein synaptophysin as described previously (Dreosti et al., 2009).

Figure 2.2C (previous page) shows the expression of the reporter in a larval zebrafish day at seven dpf. Figure 2.3 (next page) compares the kinetics of the sensors employed in the present work. GCaMP3.5 (Lowe et al., 2013) is an older version of the GCaMP series, and even though the rise time is comparable to the one of GCaMP6f, the decay is significantly slower.

The kinetics of the glutamate sensor iGluSnFR, particularly the rise-time, outperforms both calcium sensors' kinetics and as of now, there are no calcium-sensors available that can compete with this sensor if one wants to assay the kinetics of synaptic activity.

Bars in left and right column equal 50 and 5 microns, respectively. **A:** Ribeye:Gal4 x UAS:SFiGluSnFR double transgenic larvae; Line shows mosaic expression of the glutamate sensor across the membrane of BCs. Note that the entire neuron is labelled, thus glutamate input and output can be measured. **B:** UAS:SFigluSnFR injected fish with HuCKalTA4. Injection results in transiently labelled amacrine (red star) and GCs (two red stars). Note, the ptf1a promoter also drives weak expression in HCs (red dashed box). **C:** Ribeye:SyGCaMP6f; Line shows the targeted expression of the GCaMP6 sensor in the terminals of BCs. No axons, cell bodies or dendrites are labelled. **D:** Ptf1a:Gal4 x UAS:SyGCaMP3.5 double transgenic larvae; Line shows targeted expression of the GCaMP sensor to the synapses of ACs. Note, the ptf1a promoter also drives weak expression in HCs (red dashed box).

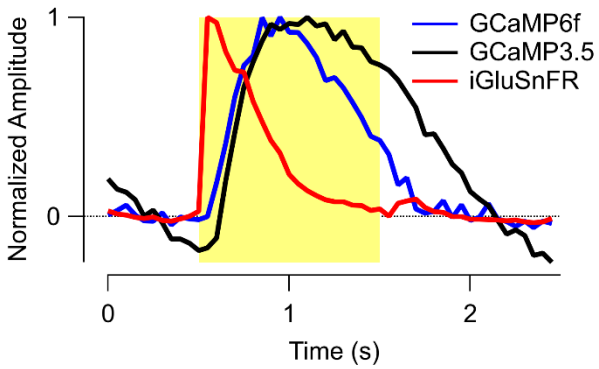

Figure 2.3: Kinetics of calcium- and glutamate sensors

Averaged responses of GCaMP6f-, GCaMP3.5- and iGluSnFR-labelled BC terminals (n=5 for each) to 0.5 Hz temporal contrast (square waveform). The responses were normalized to $peak_{max}$.

sensors employed in the present work. GCaMP3.5 (Lowe et al., 2013) is an older version of the GCaMP series, and even though the rise time is comparable to the one of GCaMP6f, the decay is significantly slower.

The kinetics of the glutamate sensor iGluSnFR, particularly the rise-time, outperforms both calcium sensors' kinetics and as of now, there are no calcium-sensors available that can compete with this sensor if one wants to assay the kinetics of synaptic activity.

2.6.5 Ptf1a:Gal4 and UAS:SyGCaMP3.5-mossy heart

The Ptf1a-promoter targets the transcriptional activator to all amacrine and HCs of the zebrafish retina (Jusuf & Harris, 2009). We used this line in combination with the UAS:SyGCaMP3.5-line to study the physiology of the inhibitory neurons in the IPL. GCaMP3.5, as mentioned previously, is an older sensor of the GCaMP-series with slower kinetics than the GCaMP6f. Our attempts to establish a UAS:SyGCaMP6f line were unsuccessful, the stable transgenes showed no expression. Figure 2.2D (page 30) shows the expression pattern of the eye in the double-transgene. Note that there are still some cell bodies labelled where targeting of the sensor to the synapses only was incomplete.

2.7 Image Analysis

2.7.1 Analysis of movies in signal decomposition study (chapters 3 and 4)

We analysed movies, imported from Scanimage as .tiff-files, in Igor Pro 8.04 (Wavemetrics) using the custom-written software SARFIA (Dorostkar et al., 2010) which allows for the semi-automated assignment of regions of interest (ROIs). ROIs were defined by (a) manually thresholding the Wavelet Transform of an averaged image sequence and (b) by removing ROIs that are smaller than a definable number of pixels (Fig. 2.4). The background was subtracted by manually choosing a “background” area in the averaged image. The average value of the selected background region was subtracted from each frame of the time series. We calculated responses as the change in fluorescence relative to the baseline measured in the preceding 0.125 s before the stimulus started and smoothed them with a binomial filter (=2). Responses that had a threshold of 3*SD above the baseline were used for subsequent analysis only.

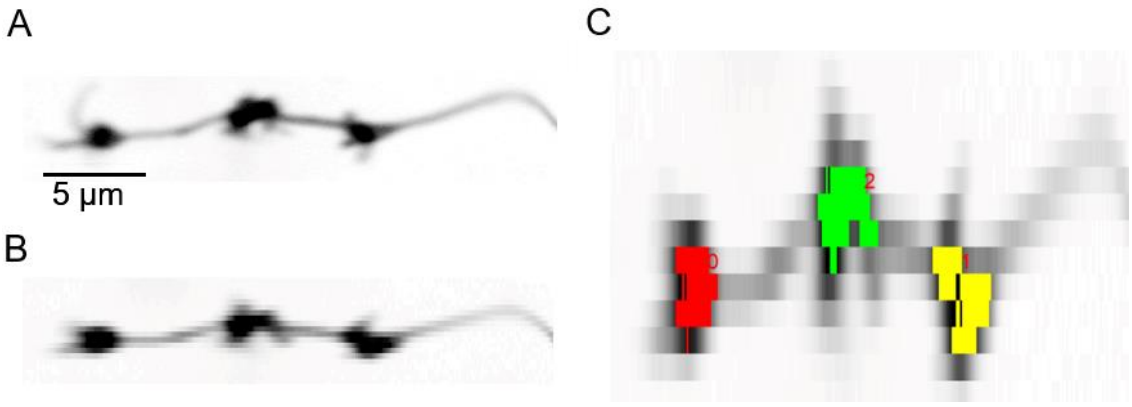

Figure 2.4: ROI assignment with SARFIA

A: Averaged movie of high-resolution recording (256 x 200 pixels) of BC axon with 3 boutons. **B:** As in A but here low-resolution recording (256 x 20 pixels) which served as a standard to record glutamatergic responses typically at a framerate of 100 Hz. **C:** Mask showing regions of interest after semi-automated thresholding with SARFIA.

2.7.2 Analysis of movies in orientation selectivity study (chapter 5)

Similar to the previously described segmentation method employed by SARFIA, we used another custom-written algorithm to assign regions of interest to analyse BCs responding to moving bars or static gratings. Prior to analysis, some movies were registered to correct for motion artefacts which can occur during long recordings. Igor Pro contains an inbuilt image registration algorithm which was employed. Again a custom-written semi-automated algorithm named “Advanced ROI Tools (ART)” was used to assign regions of interest, as described by Portugues et al., (2014). First, pixels with strong signals and high temporal correlation were designated as “seeds”. Pixels surrounding these seeds were added until the correlation value reached sub-threshold (Fig. 2.5). Threshold values were chosen by the user and were consistent across all analysed fish.

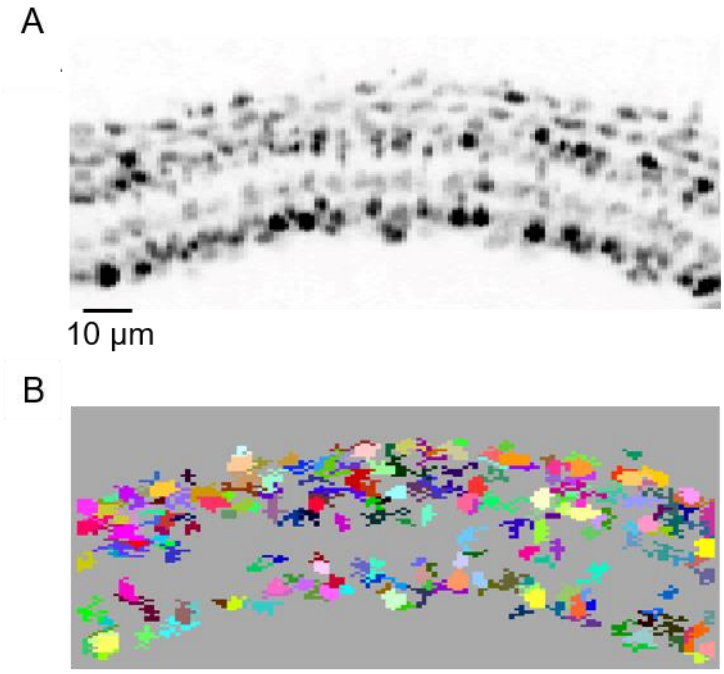

Figure 2.5: ROI assignment with Advanced ROI Tool

A: Averaged movie showing a stretch of the IPL labelled by the calcium sensor GCaMP6 expressed at BC terminals. Typically stacks were recorded at a resolution of 128 x 100 pixels and 10 Hz frame rate. **B:** Mask showing regions of interest after semi-automated thresholding with the Advanced ROI Tool algorithm.

Baseline fluorescence in the moving bars experiments was calculated by taking the average of the data collected within 2 seconds before each start of trial, which is 5 trials in total (see Figure 5.1, chapter 5, page 86 for visualisation of stimulus).

Only terminals that had responses > 4*SD of the baseline were included for analysis. To define terminals as orientation- or direction-sensitive, we used an approach similar to that described by Mazurek et al., (2014). A vector sum was computed in orientation space for each of the 10 trials. Terminals were then classified as orientation-selective based on the result of Moore's version of Raleigh's test. The false-positive rate was determined by measuring shuffled angle data and using a critical value of 1 %.

The orientation selectivity index was calculated by comparing the median response amplitude (R) from the vertical (90°) and horizontal (0°) grating (see Figure 5.3, chapter 5, page 88 for visualisation of stimulus) using the following equation 1:

$$(|R0° - R90°|) / (|R0°| + |R90°|) \qquad \text{(Equation 1)}$$

To avoid adaptation effects, we calculated the median response from only the last two angle representations of the stimulus protocol. We only used indices for further analysis when the difference between the orthogonal angles was twice the medium absolute deviation (MAD) of the smaller response. To test for direction selectivity, we used the "direction dot product" (Mazurek et al., 2014). We first found the preferred angle as described above, then calculated the magnitude of the 5 directional vector projection sums on the preferred angle, giving a one-dimensional distribution of direction dot product values. We tested the distribution against a mean of zero using Student's T-test and found that 3% of terminals showed a directional preference only slightly higher than the rate expected by chance. The receptive fields were recovered by employing the filtered back-projection technique (Johnston et al., 2014). The ellipticity of a receptive field was calculated by comparing the length of the minor and major axis using equation 2:

$$1 - (\text{minor axis} / \text{major axis}) \qquad \text{(Equation 2)}$$

2.8 Pharmacology

We co-injected all drugs with the red dye AlexaFluor 594 (1mM) into the eye's vitreous chamber. Prior data collection, we imaged the mix's distribution throughout the retinal tissue in the microscope channel that detects red emission (Fig.2.6). Injection of the solution without drug resulted in maintained responses as in control conditions. The estimated volume of a seven dpf fisheye, excluding the lens, is five nanolitres based on a measurement of the eye-radius of ~135 microns subtracted by the lens-radius (~ 50 microns). With an average injection bolus equal to the size of the fish lens (0.5 nanolitres), the injected drug's dilution factor is approximately 1:10. The stock concentrations of the various drugs were the following: HCN channel blocker ZD7288 (Abcam, 100 mM), strychnine hydrochloride (Sigma, 50 mM), SR 95531 hydrobromide (GABAzine, Tocris, 10 mM), dopamine hydrochloride (Sigma, 100 mM), dopamine (D1)-antagonist R(+)-Sch23390 hydrochloride (Sigma, 10 mM), L-AP4 (Tocris, 50 mM).

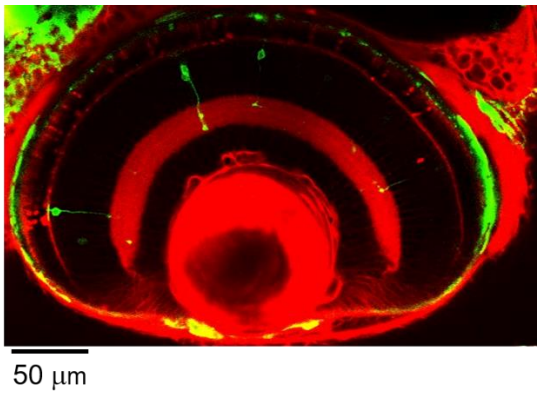

Figure 2.6: Zebrafish eye injected with AlexaFluor594

Eye of a transgenic zebrafish (UAS:SFiGluSnFR x Ribeye:Gal4) injected with AlexaFluor594. Note the spread of the dye through the IPL and OPL. Individual BCs are expressing SFiGluSnFR.

2.9 Molecular Biology

2.9.1 Cloning

Plasmids were cloned via the Gibson-Assembly-Method (Gibson et al., 2009). Table 2.2 (next page) provides information on the primers and templates used to amplify the vector and inserts with Q5 polymerase via a polymerase chain reaction (PCR).

Destination Plasmid	Template	Primers 5'-3'
Rib: Gal4-BH	Rib: SyGCaMP6-BH	GGCGCTCTGGATATGTAGC Ggcggccgcgactctagatca
		CTTTCAGGAGGCTTGCTTCA ggtggctcgagatctgagtcc
	Brn3c: Gal4	GACTCAGATCTCGAGCCAC Ctgaagcaagcctcctgaaagatgaag
		TGATCTAGAGTCGCGGCCG CCGCTACATATccagagcgcc
10xUAS: SFiGluSnFR-MH	10xUAS: iGluSnFR-MH	CCGCTCGAGATCAGCCTCG Aaattatcgatgatgatccagacatgata agatacattg
		AGGAGTGTGTCTGTCTCCAT tcttcgaggtcgagggaattcg
	pCMV: SFiGluSnFR	AATTCCCTCGACCTCGAAGA atggagacagacacactcctg
		TGGATCATCATCGATGAATTt cgaggctgatctcgagcg
Huc: KalTA4-BH	14xUAS: pT2KXIGin	GGGGCCCGGTACCCAATTA Caagatctgcgaagatacggc
		AAATTCAAATTAGTGAATTctt atcgataccgtcgacctcg
	P5E-HuC	GAGGTCGACGGTATCGATA Agaattcactaatttgaatttaaatgcatt atctttctattcc
		GCGTACGTAAGGGGCCTAT Cgatccggtccttcgatttgca
	pCH-MCS-KalTA4GI	GCAAATCGAAGGACcGGAT Cgataggccccttacgtacgc
		GAGGGGGACGTGAATGAGA Ggatgcatgctcgagtccac
	Rib: SyGCaMP6-BH	AGTGGACTCGAGCATGCAT Cctctcattcacgtccccctcc
		GCCGTATCTTCGCAGATCTT gtaattgggtaccgggcc

Table 2.2: Primers for Gibson Assembly

Column one denotes destination plasmid. Column two lists plasmids that were used as a template for the PCR reaction. Column three lists primers. Note, forward primers are listed on grey background. Small letters comprise sequence that will anneal to template DNA, whereas capital letters comprise sequence that will align to the fragment to be fused during Gibson reaction.

2.9.2 Gene Expression Analysis via Reverse Transcriptase PCR

Information on number and sequence of HCN genes in the zebrafish genome were retrieved from the Ensemble genome browser database, Ensemble release 101, using the Genome Reference Consortium Zebrafish Build 11 (GRCz11). Information on designed primers, the sequences they target, expected amplicon length, and annealing temperature is shown in Table 2.3 (next page). We prepared complementary DNAs (cDNAs) from 7 dpf old nacre wildtype fish. The total amount of 200 larval eyes was dissected with an 18 gauge-needle in batches of 5 larvae directly stored on dry ice to prevent RNA degradation. Furthermore, we processed the tissue of 50 whole larvae as a control library. The RNA total extraction kit from Agilent and the iSript cDNA kit from BioRAD was used to extract RNA and synthesize cDNA. To amplify cDNA per RT-PCR, Q5 polymerase, 100 ng/ml cDNA per reaction and following cycle conditions were employed: 98 °C for 30 s initial denaturation, 98 °C for 5 s, 66 °C for 20 s, 72 °C for 7 s, the cycle repeats 35 times followed by 72 °C for 2 min to finalize reaction. We used two primers couples for each HCN gene and ran amplicons on a 2% agarose gel. The results are shown in chapter 4, Figure 4.5, page 67.

Ensembl gene ID, Targeted transcript, Amplicon length [bps], Targeted exons	Primers 5'-3'
ENSDARG00000104480, HCN1_203, 233 and 219, exons 3 and 4	ATCTGATTGGCATGATGCTG
	GAGCATGGTGATCCAGAGGT
	ATGCTGCTGCTCTGTCACTG
	GAGCATGGTGATCCAGAGGT
ENSDARG0000061665, HCN2b_201, 225 and 203, exons 2 and 3	GCGTTTCACCAAGATCCTCA
	GACACCCAACAGTCCGAAG
	GATTGTCCAGGCTGATTCGT
	CACCATCTTGTTAAGGGACACC
ENSDARG00000027192, HCN3_201, 230 and 253, exons 2 and 3	GGATGTTTGGGAGCGCTAAA
	GGCCAGGAAAAGTGTGTCAG
	GTTTGGGAGCGCTAAAGGG
	GCCAGTGCGAAAGTTGAAGA
ENSDARG00000061685, HCN4_202, 229 and 218, exons 2 and 3	AGGATGTTTGGGAGCGAGAA
	TCAGGAAGAAAGTGTCGGAGA
	CTGAGGATGTTTGGGAGCGA
	TCGGAGACCACGTTAAAGAC
ENSDARG00000074419, HCN4l_202, 207 and 203, exons 1 and 2	CACGCATCGACTCGGATTTC
	TGGCACAGCAACAACATCAT
	ACTGAGTCTGCTTCGGTTGT
	AGCAGTCTGAAGGGAAATCC
ENSDARG000077382.5, HCN5_201, 244 and 216, exons 2 and 3	TGGTGGCCATAACATTTCTCA
	AAAGCTGCCACCAAATCAGG
	ACTATATTATGTGCATGGTGGCC
	GGTGACGGATGCTTTTCAAATC

Table 2.3: Reverse transcriptase PCR primers

Column one lists the Ensembl Identifier, which transcript was targeted, the length of the PCR products and the exons that were targeted by the primers. Column two comprises primer sequences. Note, two combinations of forward and reverse primers were designed if one combination results in an unsuccessful amplification.

Chapter 3

Decomposition of ON and OFF signals at the output of individual bipolar cells

Phenomenon

3. Decomposition of ON and OFF signals at the output of individual bipolar cells: Phenomenon

3.1 Introduction

BCs are the only neurons that relay information from the outer to the inner retina. At the input, their dendritic tree collects mixed signals from converging PRs. All information passes along a single cable - the axon- to multiple synaptic outputs, which GCs and ACs sample. The question is now if these different boutons of an individual BC “stream” different information to their postsynaptic partners, or if all boutons of an individual cell perform as one entity.

Sensory- and motor-system studies in invertebrates (Gaudry et al., 2013; Guerrero et al., 2005) revealed that individual neurons are able to decompose signals at their outputs, but direct evidence in vertebrate systems lacks so far. However, using paired recordings of bipolar and GCs in the salamander retina, it has been shown that the transfer function of synapses between GCs and different boutons of the same BC can differ (Asari & Meister, 2012). How these differences arise, whether presynaptic events, such as feedback inhibition of BC terminals by ACs, or mechanisms at the postsynaptic membrane, such as feedforward inhibition, or differences in glutamate receptor activation are at work, could not be addressed by electrophysiological means.

The present and following chapter revolve around investigating whether BCs employ strategies in which different components of a signal are extracted, separated, and propagated to their postsynaptic partners. We started this examination by probing and comparing individual BCs' outputs for their responses towards changes in light intensity. These changes are known to be detected by the ON-OFF system described in detail in chapter 1. Briefly, the expression of different classes of glutamate receptors at the dendritic tree of BCs leads to a divergent response behaviour towards changes in light amongst these cells. PRs that signal onto BCs continuously release glutamate in darkness. Ionotropic glutamate receptors expressed at the dendritic tree of OFF BCs bind glutamate, which leads to subsequent depolarisation of these neurons; thus, the sign of the PRs is maintained. In contrast, ON BCs invert the sign. The presence of metabotropic glutamate receptors at their dendritic tree triggers the closure of

downstream cation channels which results in a hyperpolarisation upon glutamate binding.

The recent development of the glutamate sensor iGluSnFR (Marvin et al., 2013) enabled us to study the output of BCs and make a distinction between pre- and post-synaptic events. We developed several transgenic lines and DNA-constructs (see methods, chapter 2, pages 26-32) that allowed us to study the excitatory input and output of all major cell types of the inner retina. This chapter will describe the observation we made when studying the glutamatergic signalling at the different outputs of individual BCs and their input into amacrine- and GCs under two-photon illumination. The following chapter (chapter 4) will describe how we systematically dissected the underlying mechanisms of the observations made in chapter 3.

3.2 Results

3.2.1 Decomposition of ON and OFF signals at the outputs of individual bipolar cells

Do the synapses of an individual BC have the potential to transmit different signals to their postsynaptic targets? To answer this question, we studied transgenic zebrafish larvae that express the glutamate sensor SFiGluSnFR in BCs in mosaic fashion (Fig. 3.1A, next page) under two-photon illumination. The reporter's expression was driven by employing the Gal4/UAS-system and the BCs' specific reporter RibeyeA (see methods, chapter 2, page 27). An amber LED lightguide (wavelength 590 nm) provided a simple full-field stimulation in the form of squarewave-modulations at 0.5 Hz around a mean light intensity.

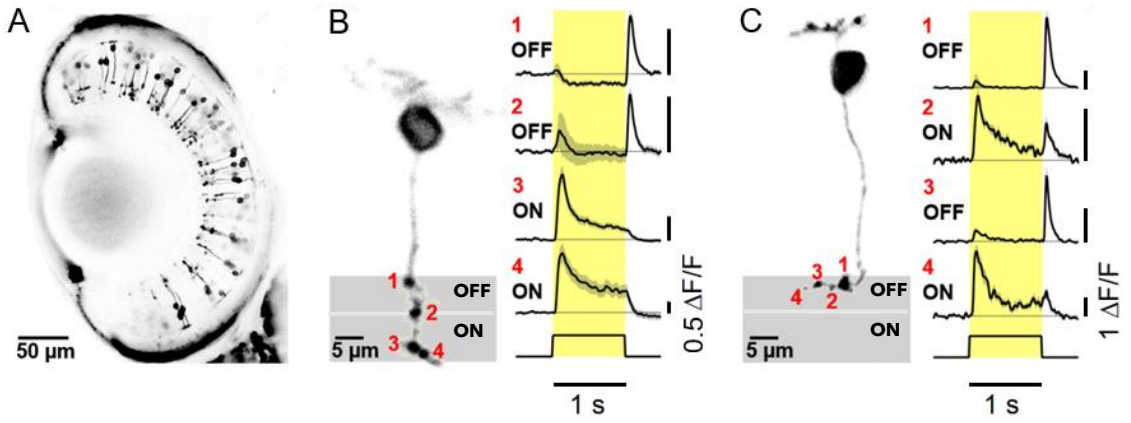

Figure 3.1: Decomposition of ON and OFF signals at the outputs of individual bipolar cells

A: Mosaic expression of SFiGluSnFr in retinal BCs. **B, left:** BC with four synapses (red numbers) located along an axon that vertically projects into the IPL (grey). **C, left:** BC with four synapses (red numbers) located along an axon that horizontally projects into the IPL (grey). **B and C, right:** Corresponding averaged responses of synapses to 0.5 Hz temporal flicker, note the differing responses in polarity and kinetics.

The example in Fig. 3.1B (left) shows a BC with a vertical projection of the axon, containing four prominent boutons, throughout the IPL. The averaged responses of each terminal to one cycle show a divergence of signals coming from the neuron: terminals one and two, proximal to the soma, generate weak ON responses to an increase in light intensity, but large and transient OFF responses to a decrease in intensity.

However, the distal terminals three and four generate strong and sustained ON signals and remain silent during the OFF phase. The outputs of this cell, therefore, transmit signals differing in both polarity and kinetics. While graded changes in membrane potential measured at the soma of BCs in response to both negative and positive contrast changes have been reported in the literature (Burkhardt, 2011; Burkhardt et al., 2006; Sakai & Naka, 1987), an excitatory response at the outputs of individual BCs in response to both transitions of light, ON and OFF, presents a formerly unknown, property of BCs. Please note that throughout this thesis the terms “ON” and “OFF signal” will denote an excitatory response whenever there is a light increment or decrement, respectively.

Might these differing responses arise because each terminal resides within different depths of the IPL, or can similar observations be made at BC terminals that are mono-stratified? Figure 3.1C shows an example of a cell that projects

several terminals horizontally within one layer but also conveys ON and OFF signals in a qualitatively similar manner.

To investigate if this phenomenon arises only within few BC types or appears only in some layers of the IPL, we analysed several BCs with different morphologies and stratifications pattern under the same conditions. Differing responses from individual BCs were observed within all layers of the IPL and across diverse BC subtypes (Fig. 3.2).

On average ~60 % of BCs (26 out of 44 randomly recorded cells) with two or more synaptic compartments responded to both polarities from mid-day to evening (12 noon – 8 pm).

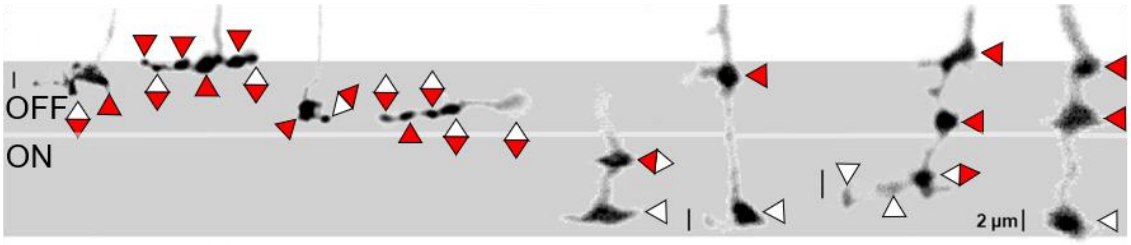

Figure 3.2: Decomposition of ON and OFF signals by individual bipolar cells across the inner plexiform layer

Representation of BPCs with different morphologies and stratification patterns that decompose ON and OFF signals across the IPL (grey, layer 1-5); red triangle (ON response), white triangle (OFF response); red-white diamond (ON and OFF response). Note that scalebars are indicated to the left side of each cell, cells with no scalebar have the same dimensions as cells shown to their left side.

These observations contradict the classical view that excitatory ON and OFF responses can only be conveyed from ON or OFF BCs, respectively. Different excitatory response polarities arise at the level of an individual neuron and its different subunits: the release of glutamate at some terminals is activated by one stimulus polarity, whereas other terminals of the same neuron respond to both increases and decreases of light intensity.

3.2.2 Dependence of polarity switch on preceding stimulus duration and synapse location

Some analysed terminals (Fig. 3.1B, terminal 1, page 43) showed a reduction of glutamate release during the ON phase of the stimulus, followed by a

pronounced, transient OFF response. Might this OFF response be generated due to a rebound depolarisation occurring after a release from inhibition during the ON phase? This hypothesis implies that the strength of the rebound depends on the duration of the light step. We probed cells with flashes of light of increasing duration (0.25 s – 1 s) to test this possibility (Fig. 3.3A-C).

A comparison of the response amplitudes to the ON and OFF phases reveals a linear dependence of the rebound response on the stimulus duration (Fig. 3.3D and E): whereas there are prominent ON response towards increases of light

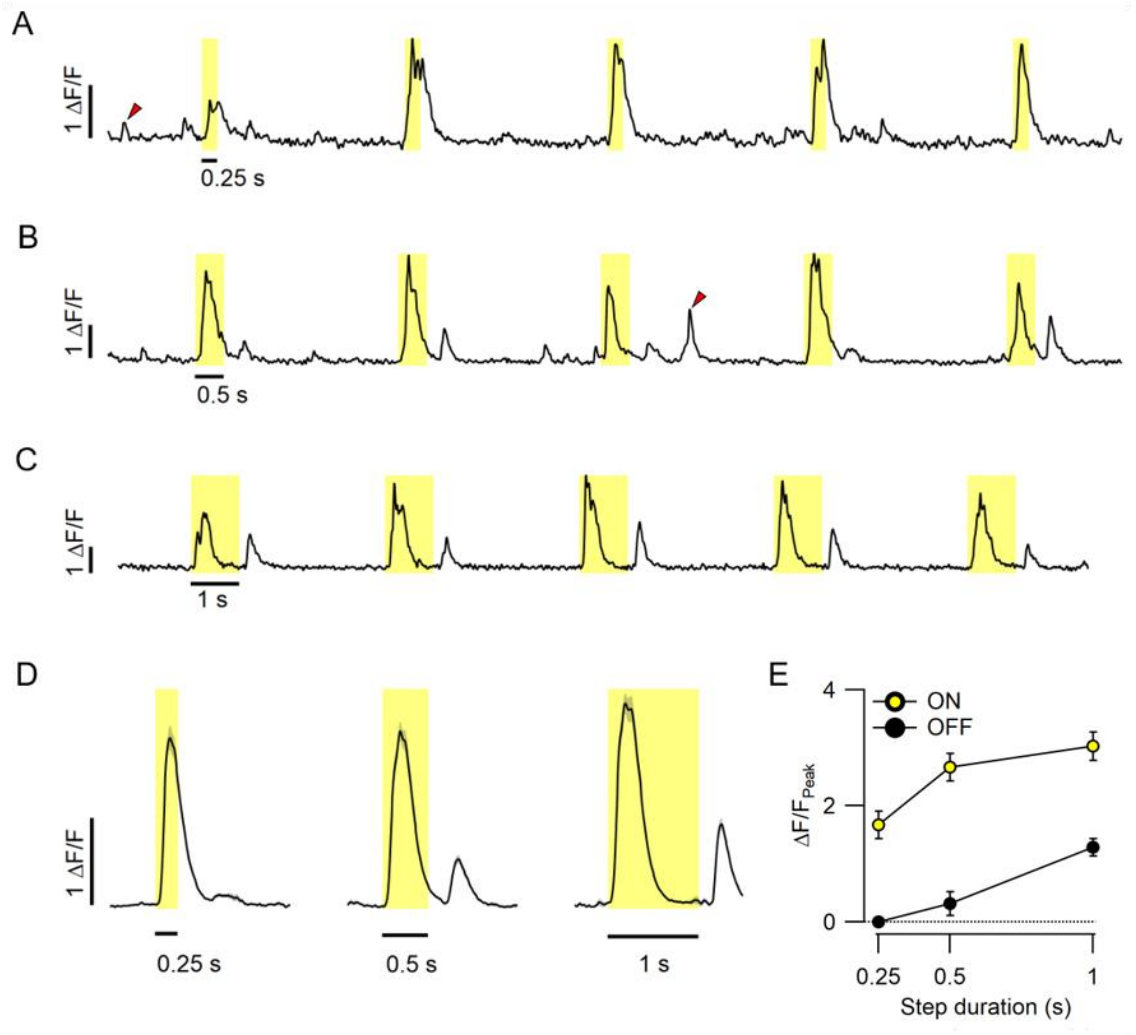

Figure 3.3: Dependence of rebound strength on preceding stimulus duration

A - C: Traces of a BC terminal responding to repeating flashes of different duration. Red triangles highlight spontaneous release events. **D:** Averaged responses +/- SD from A-C. E: Peak amplitudes +/-SD of the ON and OFF responses at different stimulus durations from data presented in A-D. Note the decreasing OFF response amplitudes with decreasing light flash duration.

throughout the recordings, stronger OFF responses start emerging with extended periods of light stimulation only.

A population analysis of 19 BCs that follow this response pattern (Fig. 3.4) shows

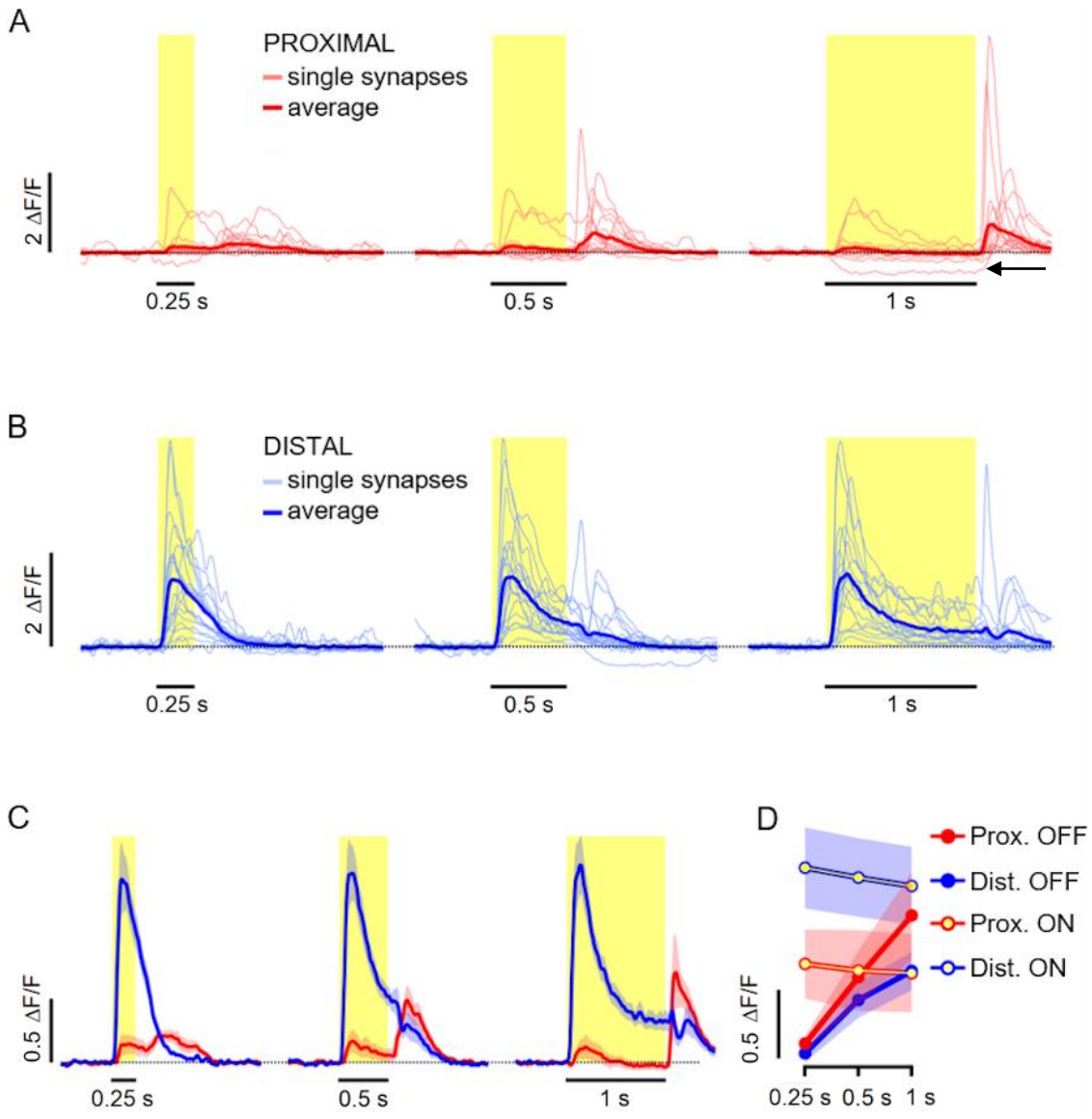

Figure 3.4: Dependence of rebound strength on synaptic location

A and B: Single and averaged responses of 19 proximal synapses (red) and 19 distal synapses (blue) obtained from 13 different retinae to light steps of different duration (0.25 s – 1 s). **C:** Comparison of population averages of proximal versus distal synapses as shown in A and B. **D:** Category plot presenting amplitudes +/-SEM of the ON- and OFF responses at different stimulus durations from data presented in B. Note the decreasing OFF- response amplitudes with decreasing light-flash duration.

that the responses of terminals located closest to the soma (proximal) differ to the responses of the most distant terminals (distal): rebound responses are more pronounced at the proximal synapse, whilst responses to the ON phase are smaller in comparison to the distal terminal. A decrease in glutamate release during the light step was observed in 4 proximal boutons (Fig. 3.4A, previous page, black arrow) but never in the distal boutons of the same neuron.

A mixture of predominantly OFF responses in proximal terminals and ON responses in distal terminals immediately begs the question – What is each BC's inherent polarity? The inherent polarity is determined by the glutamate receptor expressed at that neuron's dendrites, as described in chapter 1. Chapter 4 will provide evidence that BCs that decompose ON and OFF outputs are inherently ON, expressing metabotropic glutamate receptors. The ability of proximal terminals to release glutamate upon a decrease of light depends on the integration time of the preceding stimulus and the terminal's position along the somato-axonal axis (Fig.3.3 and 3.4; pages 45 and 46, respectively).

What electrophysiological events cause proximal and distal terminals to generate outputs of opposing signal polarity? These observations point to either a prevalent inhibitory gradient along the axon or a differential distribution of ion channels promoting rebound depolarisation. Chapter 4 will provide evidence that glycinergic inhibition suppresses the ON response and HCN channels generate a rebound depolarisation that stimulates glutamate release.

3.2.3 Encoding of contrast by bipolar cells that decompose ON and OFF signals

We probed cells with different contrasts to assess how individual BCs' segregation of ON- and OFF signals can encode these changes. Two representative examples of cells (Fig. 3.5A and B, next page) show that individual BCs and even individual boutons can increase their glutamate release in response to both negative and positive contrasts. The contrast-response functions for each cell (Fig. 3.5C and D, next page) show an increase over a broad range of negative and positive contrasts.

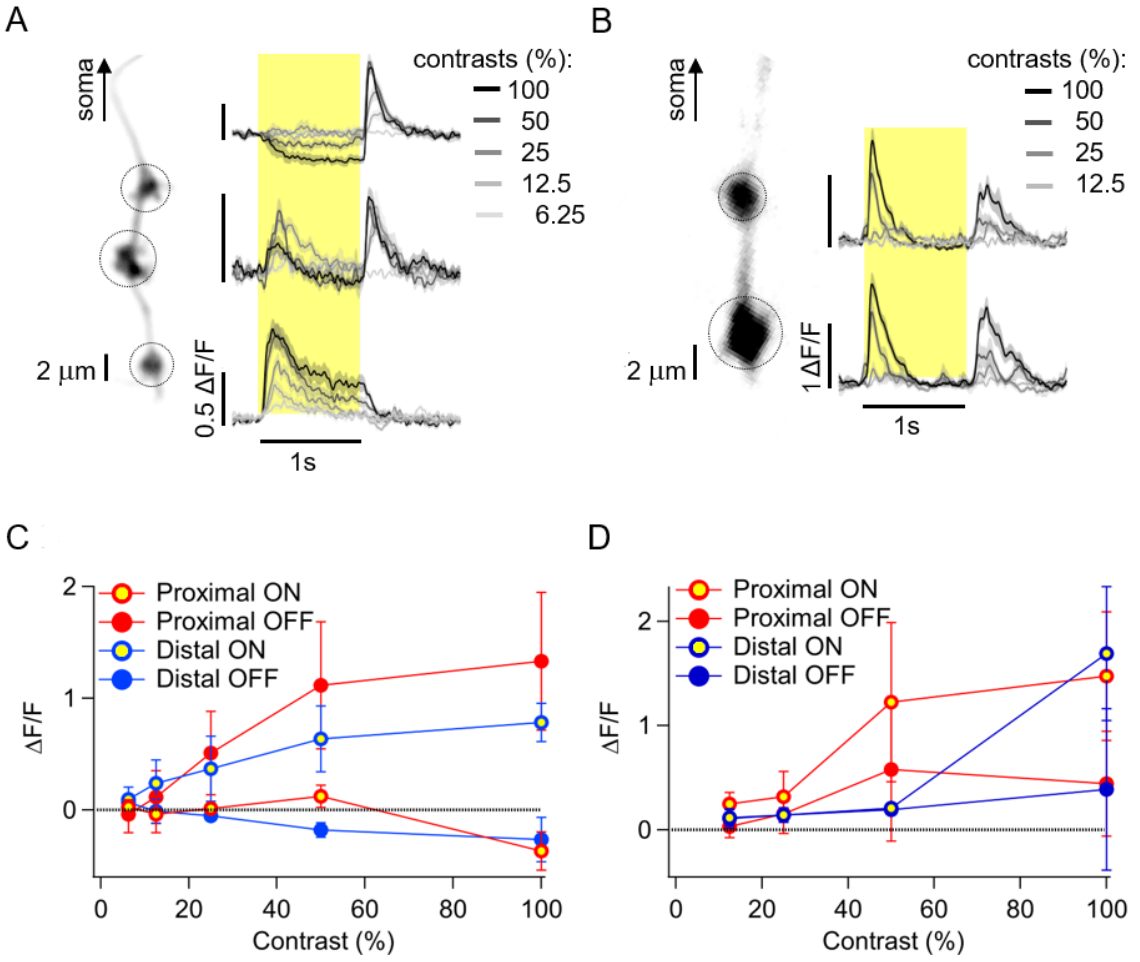

Figure 3.5: Encoding of ON and OFF responses across various contrast levels by individual bipolar cells

A and **B**: Example of two cells with 3 and 2 synaptic compartments respectively probed with 0.5 Hz square frequency at different contrasts (6.25 to 100%), to the right average responses+/-SD. **C** and **D**: Contrast-response-function measured as mean amplitude (+/-SD) of ON- and OFF responses of the proximal versus distal terminal presented in the two cells in A and B.

3.2.4 ON-OFF signalling at individual inputs of amacrine and ganglion cells

Amacrine and GCs' responses towards changes in light are commonly classified either as ON, OFF or ON-OFF. These properties are commonly established based on the excitatory input they receive at their dendritic tree: ON and OFF cells receive inputs from ON or OFF BCs only, whereas ON-OFF cells receive inputs from both types of BCs.

Based on our previous observation that individual synaptic terminals of BCs can release glutamate in response to both polarities of light, we questioned if this response profile is propagated to and received by postsynaptic boutons of amacrine- and GCs. Injection of a Gal4-variant under the control of the HuC-promoter into transgenic UAS:SFiGluSnFR zebrafish resulted in transient labelling of individual amacrine- and GC (see methods, chapter 2, pages 28-30).

We probed multiple inputs into both cell types for their light response physiology. To avoid the merging of spatially distinct ON and OFF responses, we assigned the size of ROIs to range around two microns.

The AC shown in Figure 3.6A (next page) has a narrow dendritic spread (20-25 µm) but stratifies across all layers of the IPL. The various inputs measured at one depth of the dendritic tree present diverse response profiles: most of the inputs are ON-OFF (34 of 54 inputs), whereas only a few are ON or OFF (5 and 14, respectively) (Fig. 3.6B and C, next page). A representative example for measurements at the dendritic tree of GCs (Fig. 3.6D, next page) shows a similar pattern with some inputs consisting of the pure ON or OFF type, whereas others are mixed (9 out of 36) (Fig. 3.6E and F, next page).

Further analysis of more amacrine and GCs (Fig. 3.7, page 51) shows that most have some individual synaptic inputs that signal both ON and OFF excitatory signals: 7 out of 8 probed ACs received mostly pure OFF driven inputs (ranging from 49 to 92%) but also pure ON driven (from 3 to 22%) or ON-OFF driven inputs (from 8 to 33%) were observed. One AC (Fig. 3.6A, next page and cell 3 in Fig. 3.7A, page 51) did receive mostly ON- and OFF-driven inputs (63%) whereas 2% were unresponsive, and 9 and 26 % of analysed ROIs consisted of pure ON and OFF responses, respectively. The analysis of 7 GCs (Fig. 3.7B, page 51) showed that 3 of these cells were driven mostly by ON inputs (ranging from 52 to 80%) with some OFF and ON-OFF inputs (ranging from 10 to 19% and 10 to 29%, respectively). 4 out of 7 GCs received mostly OFF inputs (ranging from 39% to 93%) accompanied by ON and ON-OFF responses (ranging from 5 to 33% and 16 to 38%, respectively).

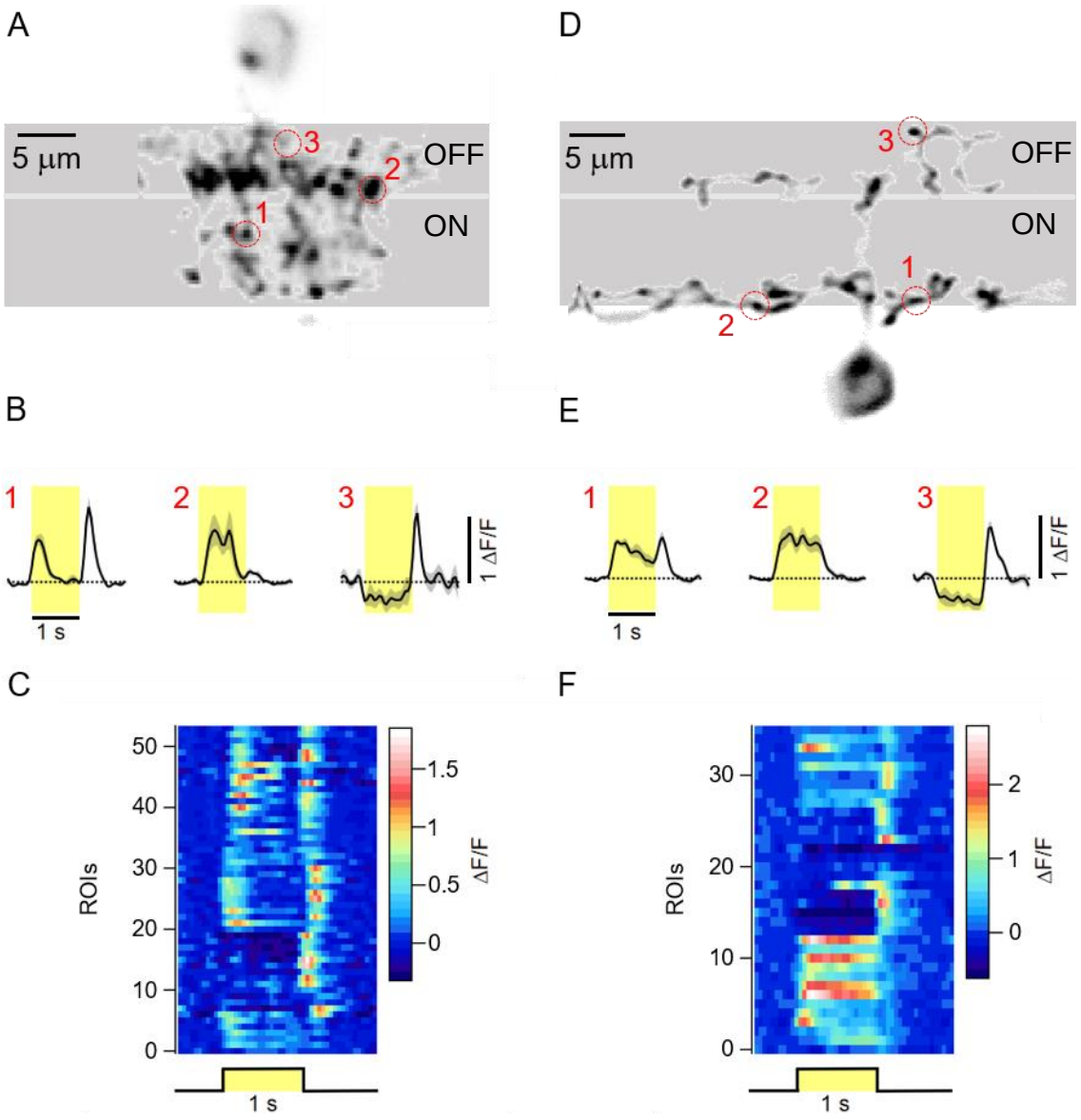

Figure 3.6: Imaging the excitatory input into individual amacrine and ganglion cells

A: Average intensity projection of AC. Note the narrow spread of dendritic tree and stratification throughout the IPL. Red, numbered circles denote analysed synapses in B. **B:** Averaged responses of synapses to 0.5 Hz temporal flicker; yellow presents ON-phase of the cycle, dashed line the baseline. Note the responses to the ON and OFF phase of synapse 1. **C:** Raster plot of the responses of 54 analysed synapses of cell presented in A to full-field stimulation with 0.5 Hz temporal flicker. Of 54 synapses, one synapse showed no significant response (ROI 1), five responded to the ON phase (ROI 2-6), 14 to the OFF phase (ROI 7-20) and 34 to the ON and OFF phase (ROI 21-54). **D:** Average intensity projection of a GC. Note the large spread of the dendritic tree (~50 µm) and the bi-stratification within the ON and OFF layer. Red, numbered circles denote analysed synapses in E. **E:** As in B. **F:** Raster plot as presented in C. Of 36 synapses, one synapse showed no significant response (ROI 1), 12 responded to the ON phase (ROI 2-13), 14 to the OFF phase (ROI 14-27) and nine to the ON and OFF phase.

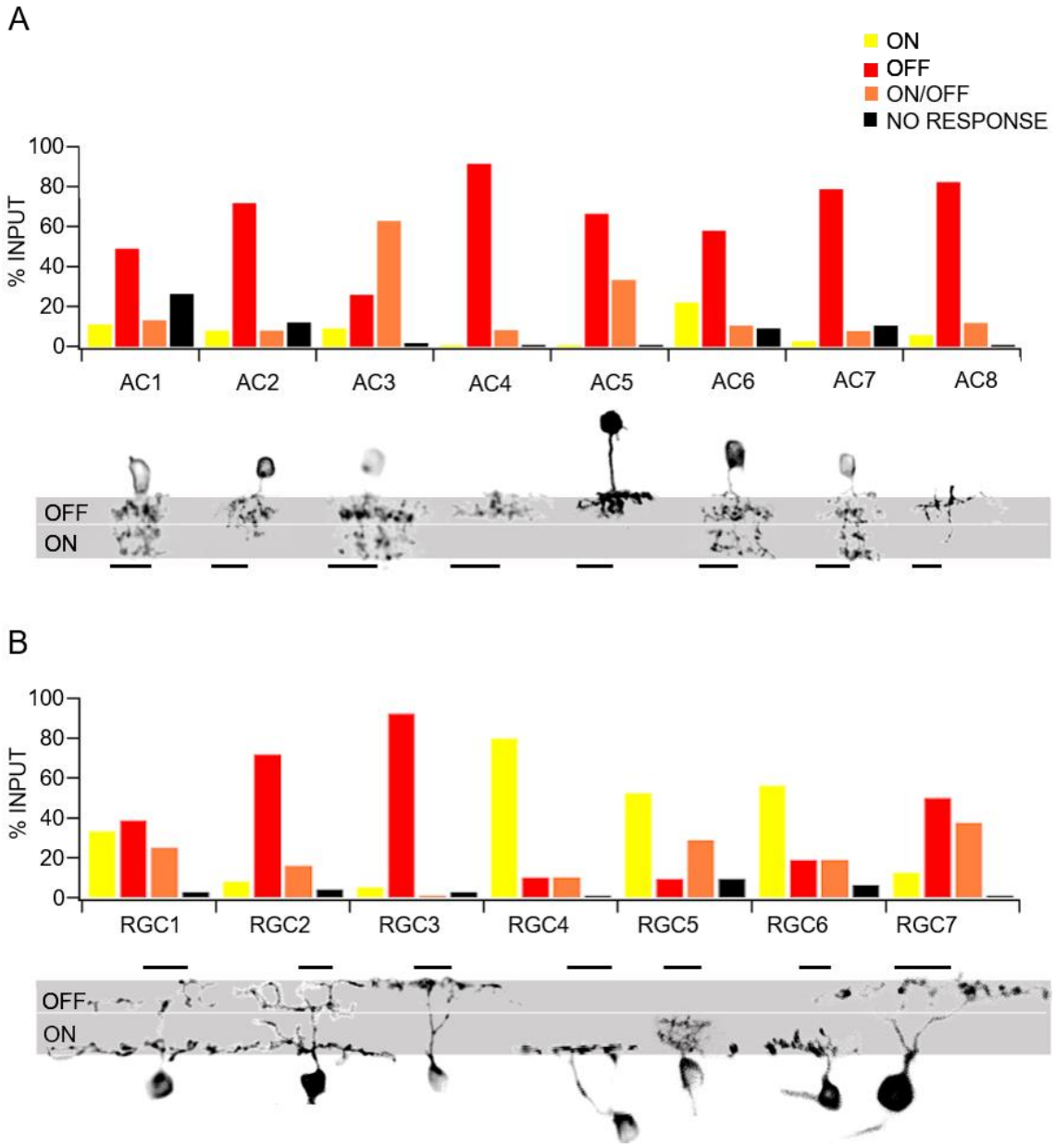

Figure 3.7: Survey of excitatory drive into multiple amacrine and ganglion cells

A: Results of a survey of the excitatory drive into ACs responding to 0.5 Hz temporal flicker. The histogram shows the percentage of each input type (ON, OFF, ON-OFF and non-responsive). Note that seven out of eight cells receive mostly inputs from synapses that respond to the OFF phase of the stimulus, whereas the inputs to AC3 consist of synapses responding to both light polarities. **B:** The same as in **A** but here, the analysis was performed on seven GCs out of which four received mostly ON responses and four OFF responses. Scalebars = 10 µm

3.2.5 Distribution of differing signals across dendrite

We investigated how close boutons with differing responses could reside within the dendritic spread of a GC. We analysed a multi-stratified GC (Fig. 3.8A) by focusing on the responses of several regions of interests within the OFF layer (Fig. 3.8B). We find that boutons, located as close as one micron from each other, have differing response profiles towards changes in light intensity and therefore a spill-over of signals from neighbouring synapses is unlikely.

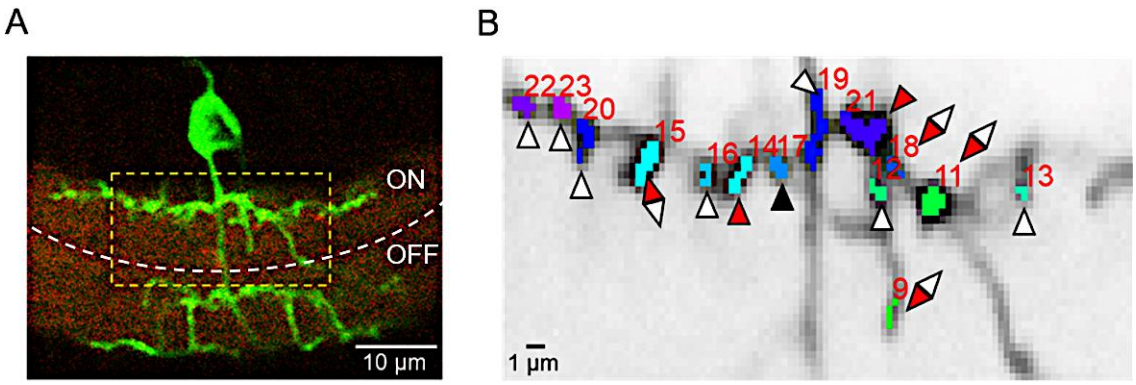

Figure 3.8: Spatial distribution of differing response profiles across neurite

A: Image of GC expressing SFiGluSnFR sending projections to the OFF and ON layer of the IPL labelled in red with Alexa Fluor 594. Yellow inset demarks analysed region in B. **B:** Region of the dendritic tree within the OFF layer showing numbered regions of interests. Triangles/diamonds encode differing response profiles: red triangle (ON response), white triangle (OFF response), black triangle (no significant response) and red-white diamond (ON and OFF response).

3.2.6 Efficacy of calcium reporter GCaMP6f in reporting rebound responses

A change in presynaptic calcium concentration precedes the release of neurotransmitter in BC synapses. We investigated whether an increase in calcium concentration in response to increases and decreases of light could be detected in synapses of BCs. Transgenic zebrafish, which express the genetically encoded calcium sensor GCaMP6f at the terminals of BCs (see methods, chapter 2, pages 30-31), were used to study the calcium dynamics. Figure 3.9 (next page) shows the averaged responses of ~275 terminals from 3 retinae to a light-step (1 s) out of which 22 showed no significant response, 91 and 152 were pure ON and OFF, respectively, and only ten were ON-OFF.

Could a calcium-independent neurotransmitter release account for the inability of the calcium sensor to report the phenomenon? Studies showed that glutamate uptake carriers - usually clearing the extracellular space off glutamate - can run backwards and pump the neurotransmitter extracellularly (Adam-Vizi, 1992; Bernath, 1992). However, a theoretical treatment, considering a high density of uptake carriers at a presynaptic bouton during normal synaptic transmission, showed that the resulting release of glutamate ions would equal only ~5% of a single vesicle's content (Attwell et al., 1993). Therefore, the differing results between the reporters are more likely due to a limitation of genetically encoded calcium sensors to detect the underlying changes in calcium concentration.

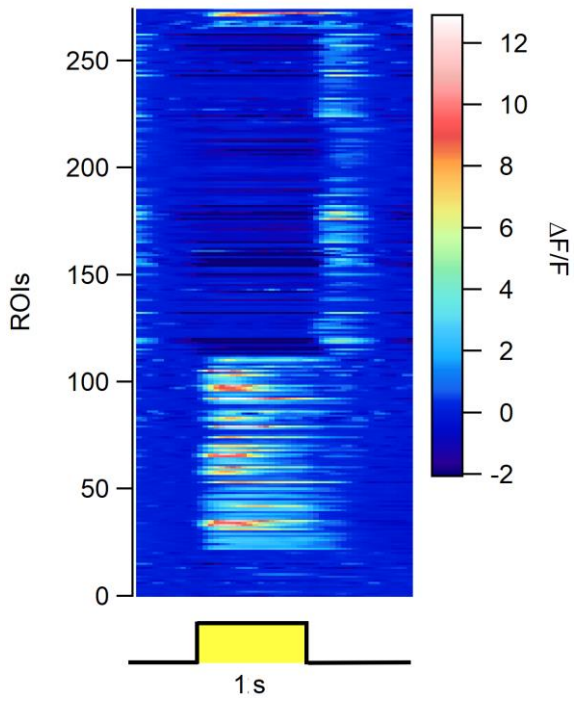

Figure 3.9: Response of bipolar cell terminals labelled with calcium sensor GCaMP6f towards steps of light

Raster plot of the responses of 275 analysed BC terminals to full-field stimulation with 0.5 Hz temporal flicker. Of 275 synapses, 22 synapses showed no significant response (ROI 1-22), 91 responded to the ON-phase (ROI 23-113), 152 to the OFF-phase (ROI 114-265) and 10 to the ON- and OFF-phase (ROI 266-275).

3.3 Discussion

The findings presented here describe a new property of BCs and their downstream targets. The ability of individual BCs to send excitatory ON and OFF signals to their postsynaptic partners (Fig. 3.1, page 43) appears to be a feature of many BCs (~60%) across the entire IPL (Fig. 3.2, page 44). Moreover, the differing excitatory response polarities were visible over a broad range of contrasts (Fig. 3.5, page 48).

Previous investigations into the physiology of BCs by electrophysiology (Asari & Meister, 2012) or calcium imaging (Fig. 3.9, previous page) failed to give a direct insight into this newly identified feature. However, the glutamate sensor iGluSnFR allowed us to directly assess the glutamatergic output of zebrafish BCs at the level of individual terminals *in vivo* and to study the ability of BCs to segregate ON and OFF signals. Moreover, we were able to distinguish presynaptic events controlling glutamate release from postsynaptic events such as receptor activation or feedforward inhibition by ACs to the BC axon.

The observed heterogeneity at the outputs of individual BCs suggests that the computational power of these neurons might be much larger than previously assumed and poses the question which other features of a stimulus might be conveyed.

Moreover, synaptic decomposition of ON and OFF signals through individual BCs increases the coverage factor (Masland, 2012a) of ON an OFF responses across a retinal patch, especially when taking into account that even an individual synapse can release glutamate upon both transitions of light.

The ON and OFF channels are conventionally thought to run in two parallel, separated streams before they either merge at the dendritic tree of ON-OFF ganglion and ACs or at cells of the primary visual cortex. Here we demonstrated that many individual BC terminals send excitatory signals to their postsynaptic targets in response to positive and negative contrast modulations (Fig. 3.6 and 3.7, page 50 and 51) and that these different inputs are spatially concise with ON and OFF responses appearing as close as one micron from each other (Fig.3.8, page 52). Therefore a misinterpretation of the mixed signals due to spill-over seems unlikely.

Can switching in the polarity of synaptic responses be detected in GCs transmitting the retina's output? Interestingly, multielectrode array recordings (MEA) from mouse and pig retinae (Tikidji-Hamburyan et al., 2015) reported the occurrence of opposite response polarities within GCs that were either classified as the ON or OFF type based on their linear filter. The opposing signals emerged during presentations of contrast-steps lasting two seconds or representations of naturalistic movies and were visible across a wide range of ambient light levels but varied in their presence and response kinetics. Moreover, recordings of qualitatively similar nature were retrieved from the lateral geniculate nucleus (LGN). These findings have several implications for our study: (1) They suggest that the heterogeneous signals we studied at the output of individual BCs might lie at the source of the phenomenon observed at the output of GCs. (2) These signals are implemented in the retina's neural code and sent to visual centres in the brain. (3) This phenomenon is prevalent across many species and not only restricted to zebrafish.

How are the differing response polarities towards changes in light intensity generated at the output of individual BCs? The partially visible hyperpolarisation below baseline during the ON phase (Fig. 3.1B, page 43; Fig. 3.4A, page 46; Fig. 3.5A, page 48 and Fig. 3.6B and E, page 50) points to the activation of ACs. If this is the case, this poses the question of whether GABAergic or glycinergic ACs are providing inhibition. Glycinergic small-field ACs tend to spread over several layers of the IPL and are the ideal candidate to provide spatially confined but differing levels of inhibition along the axonal axis of individual BCs. We will investigate this possibility in the chapter to follow and debate compartmentalisation in the discussion.

Rebound depolarisation relies on hyperpolarisation dependent activation or de-inactivation of channel currents. Previous studies showed that various ion channels mediate rebound depolarisation (Alviña et al., 2009; Van Hook & Berson, 2010; Zheng & Raman, 2009).

Hyperpolarisation-activated cyclic nucleotide-gated (HCN) channels are of particular interest as these channels are characterized by slow channel activation - up to hundreds of milliseconds - and a peculiar voltage dependence: they open upon hyperpolarisation (Biel et al., 2009; Wahl-Schott & Biel, 2009). We showed that increases in light lasting hundreds of milliseconds (> 250 ms) resulted in the

emergence of excitatory ON and OFF signals at BC synapses (Fig. 3.3 and 3.4, pages 45 and 46), whereas shorter light intervals led to monopolar responses only. Might HCN channels and their slow kinetics form the molecular basis of the observed rebound depolarisations? The following chapter will give further insights into HCN channels and their involvement in signal divergence at BC terminals.

Chapter 4

Decomposition of ON and OFF signals
at the output of individual bipolar cells

Dissection of Circuitry

4. Decomposition of ON and OFF signals through individual bipolar cells: Dissection of circuitry

4.1 Introduction

In the previous chapter, we described the phenomenon that the output of individual BCs can be heterogeneous. Some terminals are responding to increases or decreases in light intensity, whereas others signal both changes. We hypothesized that some terminals along the axon of a BC are hyperpolarised during a rise in light intensity, whereas others are excited. After the release from inhibition, the previously hyperpolarised terminals respond with rebound depolarisation. We suggested that hyperpolarisation-activated and cyclic nucleotide-gated (HCN) channels might form the rebound's molecular basis. Their characteristic slow activation times could account for the observation that ON and OFF responses arise only during prolonged steps of light.

HCN channels are a class of voltage-gated ion channels discovered in the heart's pace-making tissues (Brown et al., 1979; 1977; DiFrancesco, 1981a, 1981b). Subsequent studies revealed they exist throughout the whole central nervous system and form the molecular basis for the generation of auto-rhythmicity in pace-making cells (Halliwell & Adams, 1982; Maccaferri et al., 1993). They are characterized by a reverse voltage dependence, a conductance of an inward current consisting of sodium ions and potassium ions (ratio 4:1), and slow activation times (hundreds of milliseconds)(Biel et al., 2009; Wahl-Schott & Biel, 2009). Upon activation, the inwardly directed current (designated I_f or I_h) slowly depolarises the cell towards the threshold for firing action potentials. In addition to the pace-making properties, HCN channels contribute to setting the membrane potential. They are partially open at rest and thus control cells' excitability by counteracting membrane hyperpolarisation and depolarisation. A hyperpolarising current initiates the characteristic slow activation of the channels, allowing for an influx of positive charge. This conductance counteracts further hyperpolarisation by driving the membrane potential back towards the resting potential, as seen in the voltage sag (Figure 4.1 A, next page). A sudden release from inhibition causes the membrane to generate a depolarising rebound. In contrast, depolarisation triggers the closing of HCN channels. The membrane

potential hyperpolarises towards the resting membrane potential. The release from excitation now causes the membrane to generate a hyperpolarising rebound (Fig 4.1 B).

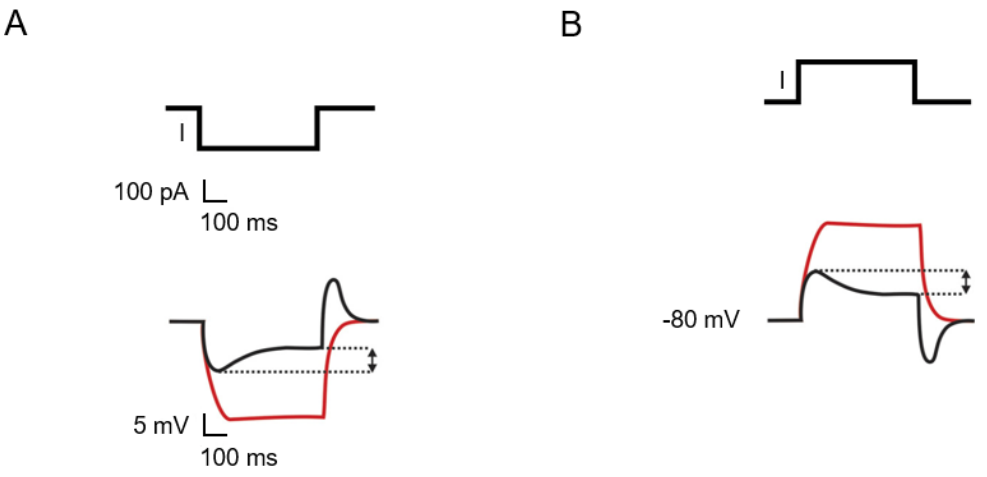

Figure 4.1: HCN channels control the resting membrane potential

Schematic of current clamp experiment. **A:** A hyperpolarising current (top) triggers the slow opening of HCN channels. The conductance of positive charge into the neuron drives the membrane potential back towards rest and appears as a depolarising voltage sag. The release from inhibition generates a depolarising rebound (bottom). **B:** A depolarising current (top) causes the closing of HCN channels that are partially open at rest. A hyperpolarising voltage sag drives the potential back to rest. The release from excitation generates a hyperpolarising rebound (bottom). Note, blocking HCN channels (red trace) causes the membrane to hyperpolarise/depolarise further. In both scenarios, no voltage sags and rebounds appear. Figure adapted from (Biel et al., 2009).

In mammals, four genes (HCN1-HCN4) encode for HCN channels. Structurally they belong to the superfamily of voltage-gated K+ and cyclic nucleotide-gated channels. Each channel comprises a homo-tetramer with distinct biophysical properties, and each monomer consists of six transmembrane domains that form the ion pore and contain a voltage-sensing domain (Figure 4.2, next page). The C-terminus encompasses a cyclic nucleotide-binding domain that allows for a modulation of the channel by the second messenger cyclic adenosine monophosphate (cAMP) in addition to voltage. An intracellular rise in cAMP concentration shifts the voltage-dependence of channel activation to more positive values and increases conductance at any given voltage. The four

different isoforms are highly conserved in their transmembrane regions and the cyclic nucleotide-binding domain. Each channel has distinct biophysical properties: HCN1 channels activate at more positive voltages with comparably fast kinetics (tenths of milliseconds). They are less sensitive to cAMP than HCN4 channels, which, in contrast, are slowly gating (hundreds of milliseconds) and activate at more negative voltages. HCN2 and HCN3 have intermediate properties (Biel et al., 2009; Wahl-Schott & Biel, 2009).

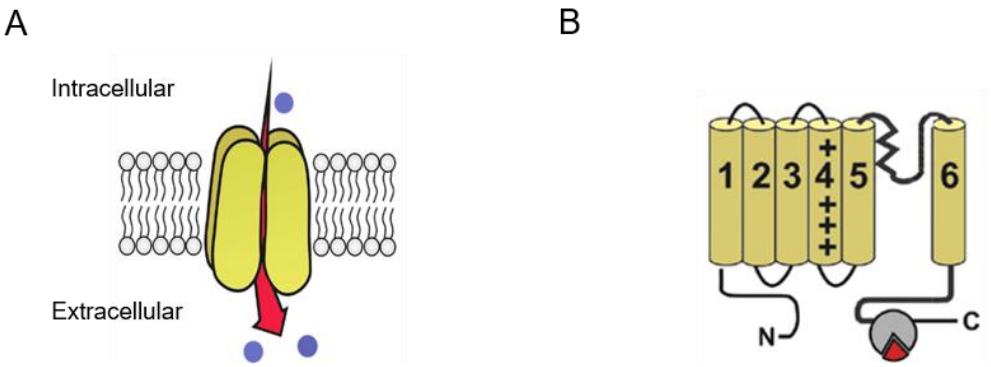

Figure 4.2: Structure of HCN channels

A: Schematic of tetrameric structure of HCN channel-forming pore in cell membrane allowing for an influx of sodium and potassium ions (in a ratio of 4:1). **B:** Structure of monomer consisting of six transmembrane domains. One comprises the voltage-sensing domain (number 4 in picture) and two form the pore region (numbers 5 and 6 in picture). Note the cyclic nucleotide-binding domain at the C-terminus. Figure adapted from (Wahl-Schott & Biel, 2009).

The mammalian retina, as part of the central nervous system, expresses all four HCN channel isoforms (HCN1–4). Immunostainings of the rat retina, with antibodies specifically targeting the different channel isoforms, revealed a differential expression in the retina: HCN1 expresses throughout the retina with particularly robust labelling in the inner segments of PRs. HCN2 shows a more targeted expression pattern with dense labelling of ON BC axon terminals in the proximity of ribbons. HCN3 appears to be most prominent in cone pedicle synapses whereas staining with an HCN4 antibody resulted in labelling of two types of BCs that terminate in the OFF layer and of some ACs. Interestingly, different isoforms can be expressed within one neuron as type 5 BCs express

HCN1 and HCN4 (Müller et al., 2003). Type 5 BCs terminate in the middle of the IPL at the intersection between the ON and OFF sublamina and are thought to play a role in motion detection pathways (Hellmer et al., 2016).

What is the functional role of HCN channels within the retina? The increased prevalence of HCN1 channels in the inner segments of PRs suggests involvement in shaping the light response (Knop et al., 2008). Indeed, studies of HCN channels and their function in rod and cone PRs showed that the channels activate with increasing light intensity and slowly depolarise the neuron towards the dark potential thus rendering the light response more transient (Baylor et al., 1984; Fain et al., 1978; Hestrin & Korenbrot, 1987). Moreover, HCN channels improve the visual system's ability to filter perceptually relevant signals from intrinsically generated noise. Intrinsic noise is prevalent across different retinal levels, from spontaneous rhodopsin isomerisation within PRs (Baylor et al., 1984; F. Rieke & Baylor, 1996) to spontaneous firing of GCs (Brivanlou et al., 1998). The activation of HCN channels is thought to diminish the responses towards these noisy signals and has been confirmed experimentally by multielectrode recordings of GCs under a pharmacological block of HCN channels. Overall, GCs showed slower response kinetics and reduced sensitivity towards higher temporal frequencies. ON cells responded less strongly, whereas the gain of OFF cells remained similar but showed an increased response threshold (Bemme et al., 2017).

Might there be a yet undiscovered role of HCN channels in the retina? Their strong expression and localisation in the proximity of the ribbons of BC terminals, suggests involvement in controlling neurotransmitter release. This chapter will lay out the investigation into their potential role in generating the observed rebound polarisations. If HCN channels are the factor determining rebound excitation, which isoforms are prevalent in zebrafish, and more specifically, within the retina?

4.2 Results

4.2.1 The effect of blocking HCN channels on the rebound excitation at the bipolar cell terminals

We performed a set of experiments where the HCN channel-specific blocker ZD7288 (~ 10 mM final concentration) was administered to the retina by intravitreal injection. We confirmed the drug's successful application by the addition of a red fluorophore (Alexa Fluor 594) to the injection mix. Prior to data collection, we imaged the mix's distribution throughout the retinal tissue in the microscope channel that detects red emission (see methods, chapter 2, page 36).

A comparison of the responses of the most distal synapse with the proximal synapse shows that distal synapses that respond to the ON and OFF phase continue responding to the ON phase only after treatment with the channel-blocker (Fig. 4.3A-C, page 64 and Fig.4.4A-F, page 65). The gain of the ON phase remains similar (except Fig.4.4F, page 65) but with a delay in the onset of the response. Proximal synapses that respond with an OFF response only during the control condition show a reduced gain or complete loss of the OFF response and hyperpolarisation below baseline after the channel block. Finally, yet importantly, no BCs were observed that continued responding with the OFF phase only. All cells responded to the ON phase only (except Fig.4.4F, page 65). As a result, the cell's intrinsic property, as defined by the expression of glutamate receptors in the dendrites, is revealed.

Figure 4.3 (page 64) shows the averaged responses of BCs and their population average before and after drug treatment. Each cell's response differs in its waveform, which raises the question of whether the observed differences might be artefacts caused by inappropriate averaging methods, noise, distortions, or changes in responsivity? Firstly, Figure 4.4 (page 65) shows the responses of the same synapses as analysed in Fig.4.3 (page 64) to the 22 repetitions of the stimulus accompanied by the averaged response. The responses of the distal terminals that are shown in Fig. 4.4A and B (page 65, bottom panel) differ in the release kinetics of glutamate in response to the increase of light: whereas the bouton in panel A releases glutamate in a sustained manner, the bouton in panel B responds only transiently. The distinction between sustained versus transient response kinetics comprises another fundamental characteristic of BCs (Kaneko,

1970; Werblin & Dowling, 1969). While the transient channel is established by the cone PRs acting as band-pass filters in the outer retina (Schnapf et al., 1990), the sustained channel is thought to arise within the inner retina (Dong & Werblin, 1998; Rosa et al., 2016; Sagdullaev et al., 2006). All pharmacological data presented throughout this thesis was collected and sorted the following way: (1) We randomly imaged and subsequently analysed BCs for their responses towards the on- and offset light. (2) Only cells with a heterogeneous response profile comprising a minimum of 2 boutons at their axon were included in the database. (3) Since the responses of boutons which are located nearest (proximal) to the soma comprise a pronounced OFF response -only a few exceptions showed an additional weak, negligible ON response as presented in Fig.4.4B and E – we averaged responses despite the differing kinetics of glutamate release. We followed the same logic by averaging the responses of boutons that were located furthest from the soma (distal) and which either showed an ON *and* OFF response or only an ON response. After applying the HCN-channel blocker all OFF responses were abolished (Fig.4.3 and 4.4, pages 64 and 65, respectively) except at one proximal terminal (Fig.4.4F, page 65) where the amount of drug might not have been sufficient to suppress the rebound but where the distal terminal showed a switch from OFF to ON.

Finally, might the responses be a result of noise, distortions, or changes in responsivity? Even though there is some variability in the kinetics and strength of responses to each repetition of the stimulus (Fig.4.4, page 65), the onset of the responses occurs in a distinct time frame so that the average has a pronounced amplitude rather than being “nulled” by the averaging process. Distortions in form of potential bleaching of the reporter are unlikely since we rarely observed a bleaching of the reporter due to short recording times (30 s) and dismissed recordings in which the baseline showed a decay. Furthermore, due to the short recording times, changes in responsivity were not registered with boutons responding to the same polarity throughout all repetitions of the stimulus.

These results support the notion that HCN channels are the molecular determinant that mediates the observed rebound depolarisation. They equip terminals with the ability to respond to polarity switches at low temporal frequencies. Moreover, we have already shown that the rebound's strength

correlates to the light phase duration (chapter 3, Fig. 3.3 and 3.4, pages 45 and 46). Therefore, HCN channels can be thought as "integrators" of preceding stimuli

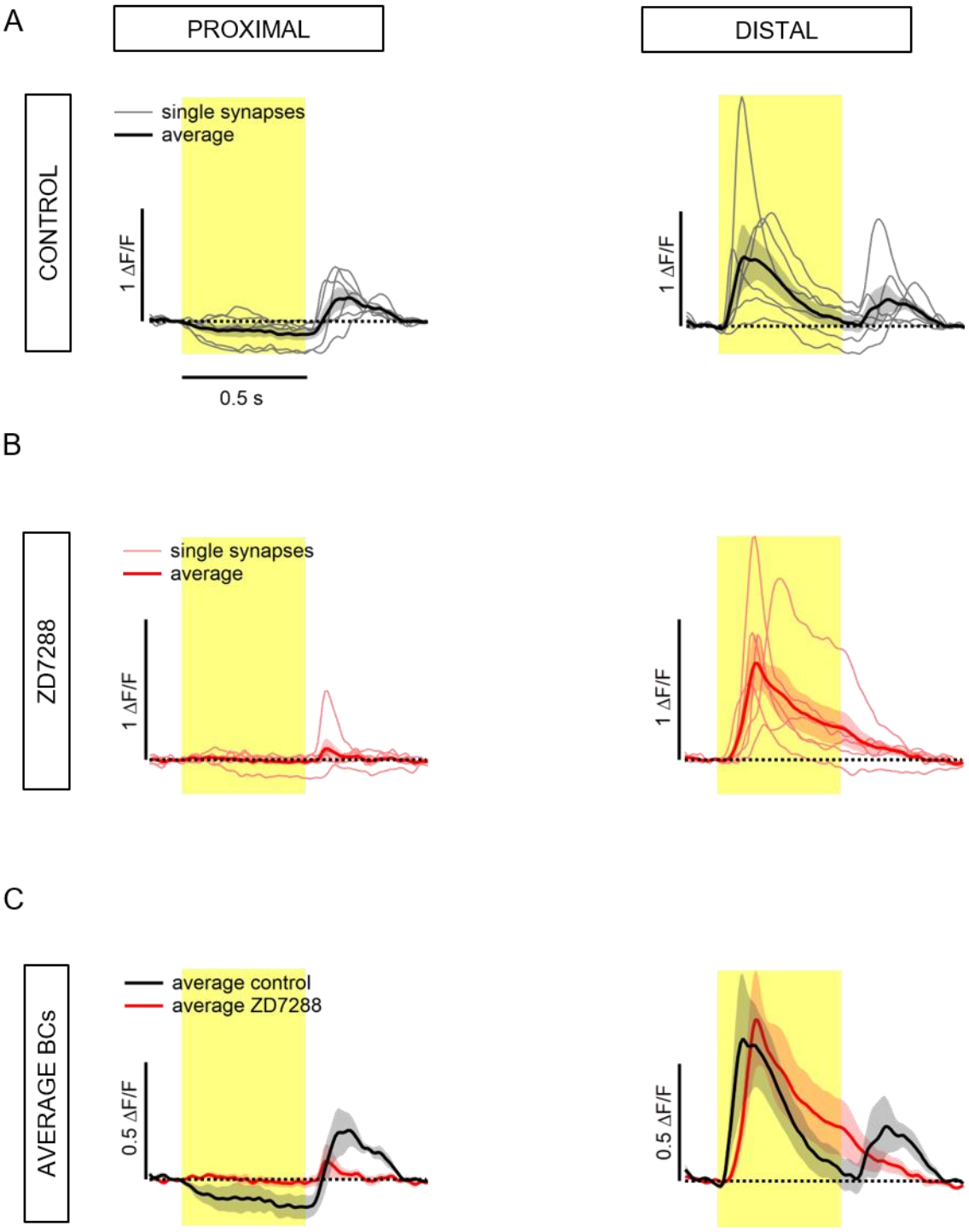

Figure 4.3: Pharmacological block of HCN channels with ZD7288

A: averaged responses +/- SD of 6 proximal and distal synapses stimulated with 1 Hz frequency **before** ZD7288 treatment. **B**: same as in A, here responses **after** ZD7288 treatment. **C:** Averaged responses (+/- SEM) from populations shown in A and B.

that allow for the encoding and processing of inhibitory signals by translating inhibition into excitation.

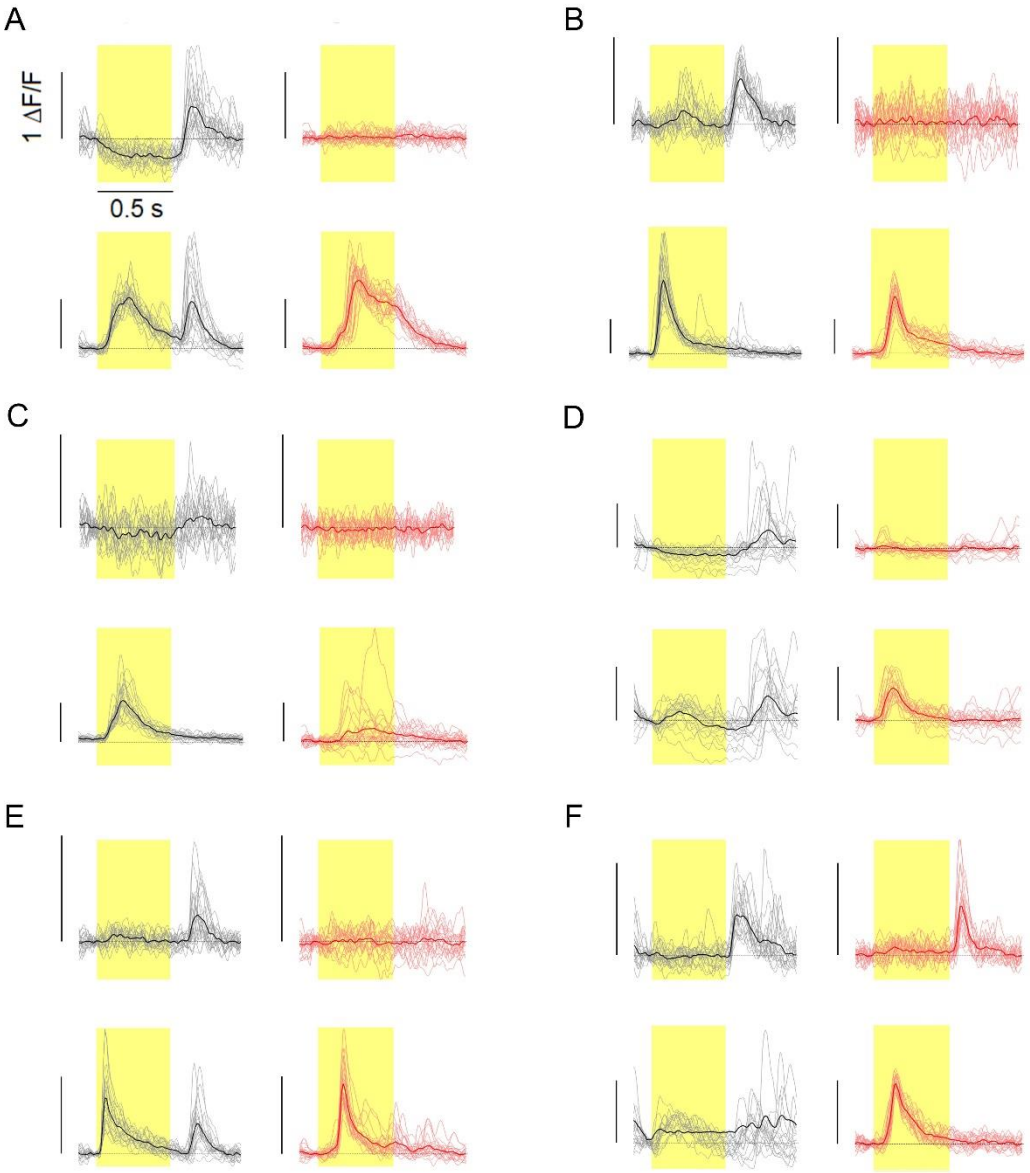

Figure 4.4: Responses of single synapses to repeated stimuli before and after HCN channel block

Responses of the synapses before (grey) and after administration of ZD7288 (light red). Note, that as opposed to Figure 4.3. the responses to each repetition (grey) of the stimulus plus the averages (black) for each of the six synapses (A-F) are plotted. **A-F:** Top panels show black/grey traces of proximal synapse and the responses after drug application (light-red/red). Bottom panels show black/grey traces of distal synapse and the responses after drug application (light-red/red).

4.2.2 HCN channel expression in the zebrafish retina

Four HCN genes have been identified in mammals (Ludwig et al., 1998, 1999; Santoro et al., 1998; Seifert et al., 1999). A query of HCN gene prevalence in the Ensemble zebrafish genome database (Yates et al., 2020) showed that six genes have been identified so far (Table 4.1.).

	Homology between zebrafish and orthologue sequence [%]	**Expression in zebrafish [ZFIN and Alliance database]**
HCN1	mouse [72.36] rat [71.92]	confirmed in hair cells (Trapani & Nicolson, 2011)
HCN2b	restricted to fish	no info
HCN3	restricted to fish and sauropsids	no info
HCN4	mouse [62.92] rat [55.84]	myocardium and circulatory system
HCN4l	mouse [58.86] (to HCN4) rat [58.37] (to HCN4)	Neuromasts (Trapani & Nicolson, 2011)
HCN5	restricted to fish	Otic sensory epithelium, hair cells (Erickson & Nicolson, 2015)

Table 4.1: Overview of zebrafish HCN genes

Column one and two show curated HCN genes and their sequence homology to respective orthologues retrieved from Ensemble genome browser (Yates et al., 2020). The **third column** provides information on expression data retrieved from ZFIN (Ruzicka et al., 2019) and Alliance (Agapite et al., 2020).

A comparison of sequence homology between the zebrafish genes and their orthologues in mice and rats shows a homology ranging from 56 to 72% within HCN1, 4, and 4l (Table 4.1). Interestingly, genes HCN2b, 3, and 5 were restricted to the species of fish and sauropsids only. Thus no homology with rat and mouse genes was found. A further query on curated expression data (Agapite et al., 2020; Ruzicka et al., 2019) only provided information on the expression of these

genes within the heart, circulatory and lateral line system (Table 4.1, previous page).

To investigate which of the six genes are expressed in the zebrafish retina, we extracted RNA from whole zebrafish larvae and the eyes only (see methods, chapter 2, page 38). Complementary DNA was synthesized from both RNA pools and used as a template for a reverse transcriptase-polymerase chain reaction (RT-PCR). We found that all genes, except HCN5, are expressed in the retina of seven-day-old zebrafish.

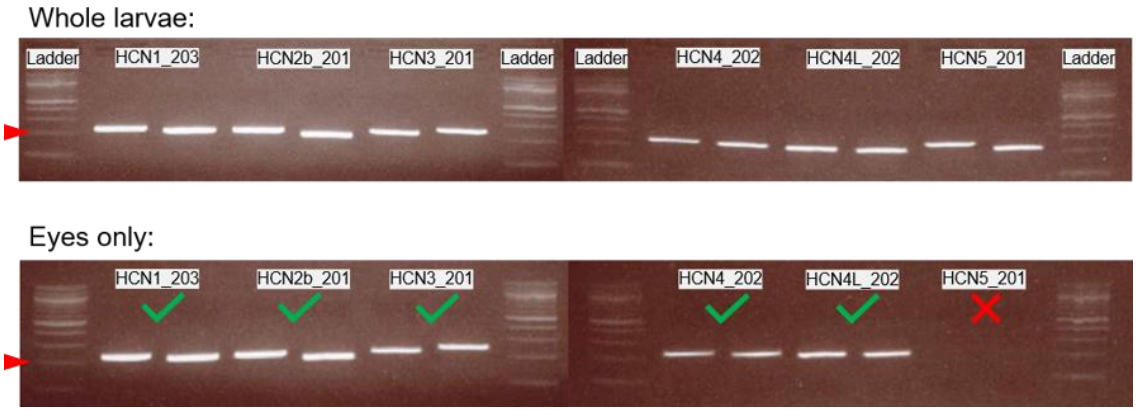

Figure 4.5: Electrophoresis of RT-PCR

Gel-electrophoresis pictures of RT-PCR products. The upper panel shows results from where cDNA from whole larvae was used as the template, whereas cDNA synthesized from the eyes only was used in the bottom panel. Note, that for each HCN gene, two primer pairs were used and designed to amplify ~200 base pairs (bps) of the genome. Red triangle denotes 200 base pairs band of DNA ladder.

4.2.3 The differential effect of blocking glycinergic and GABAergic transmission on rebound depolarisations

For HCN channels to open, inhibitory signals must drive the membrane to more hyperpolarised values. We have observed a hyperpolarisation below baseline in some recordings, especially in traces obtained from proximal to the soma positioned boutons (see chapter 3, Fig. 3.1B, page 43; Fig. 3.4A, page 46; Fig. 3.5A, page 48 and Fig. 3.6B and E, page 50). We hypothesized that glycinergic transmission might be the source of inhibition. Glycinergic small-field ACs tend to stratify across all layers of the IPL and therefore offer the anatomical structure to

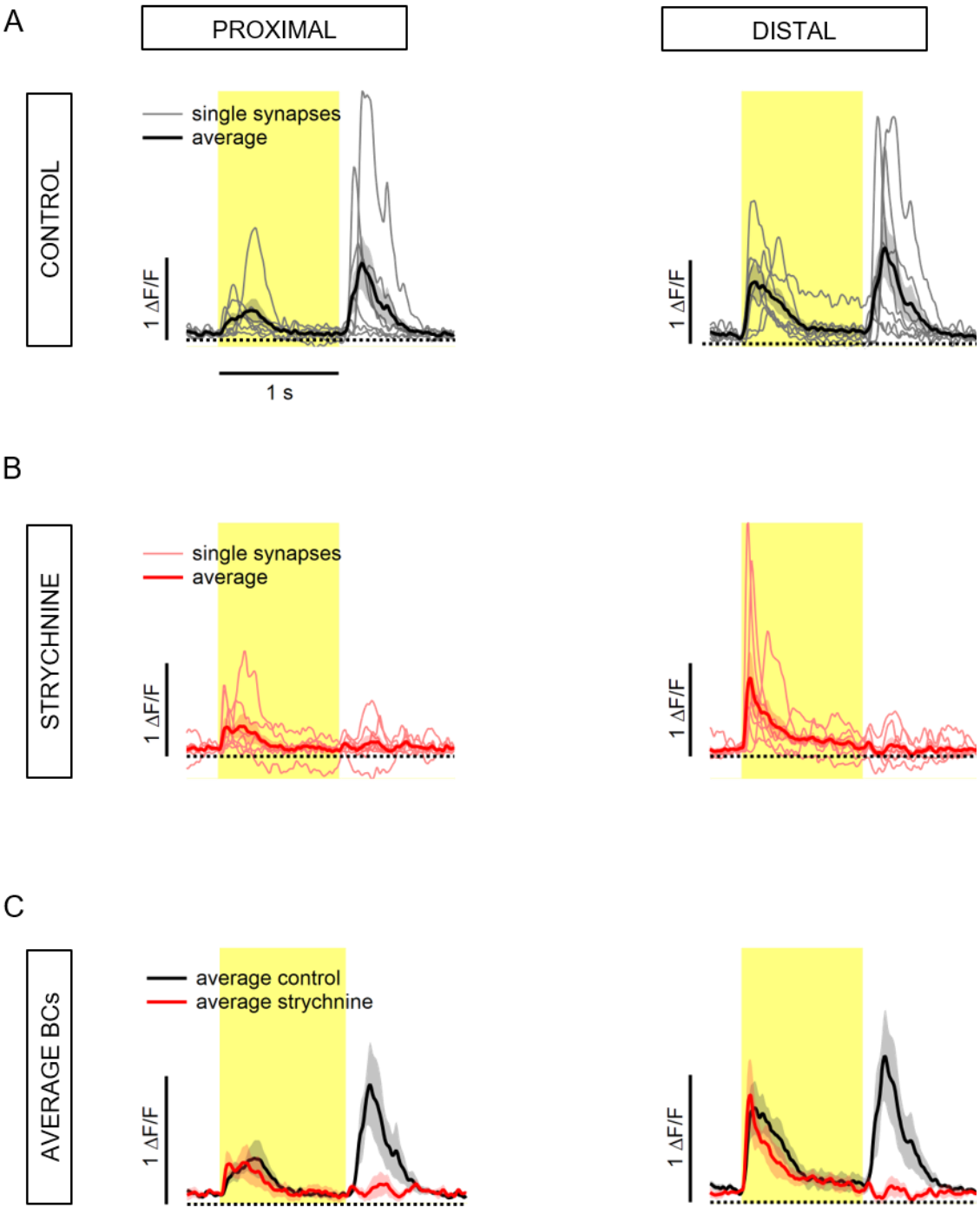

Figure 4.6: Pharmacological block of glycinergic Amacrine cells with strychnine

A: averaged responses +/-SD of 7 proximal and distal synapses stimulated with 0.5 Hz frequency **before** strychnine treatment. **B**: same as in A, here responses **after** strychnine treatment. **C:** Averaged responses (+/- SEM) from populations shown in A and B.

provide inhibition to boutons of individual BCs positioned at different depths of the IPL. Indeed, we find that blocking glycinergic transmission with strychnine (~5 mM final concentration) results in the loss of rebound polarisations (Fig. 4.6, previous page).

In contrast to the previous experiments with the HCN channel blocker ZD72188 (Fig. 4.3 and 4.4, pages 64 and 65, respectively), a complete loss of rebounds in both terminals, proximal and distal, is noted, whereas the intrinsic ON response's strength remains similar. Moreover, all cells treated with strychnine continued responding to the ON phase only. Conversely, blocking GABAergic transmission (~1 mM final concentration) showed no change in the response polarity towards changes in light polarity as both transitions were still sensed but with an overall increase in gain (Fig. 4.7).

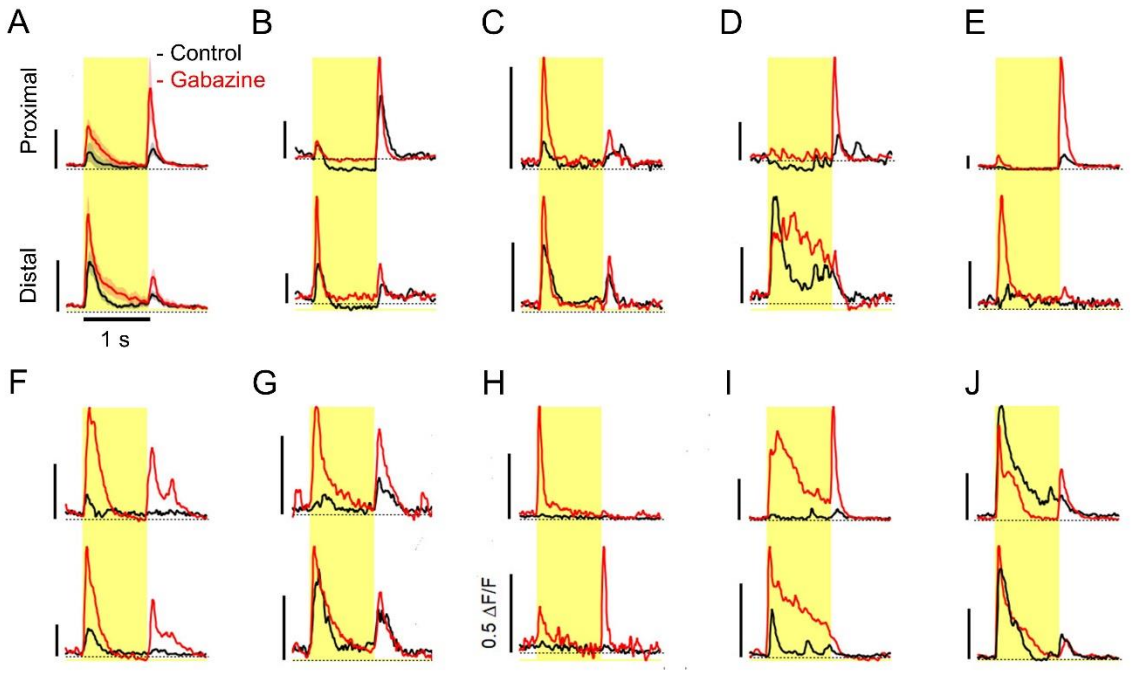

Figure 4.7: Pharmacological block of GABAaergic Amacrine cells with GABAzine

A: Population averages of responses (+/-SEM) of 9 proximal and distal synapses responding to 0.5 Hz frequency before (black) and after (red) GABAzine treatment. **B – J:** Averages of individually analysed BCs, which were pooled in A, before and after GABAzine treatment. Note that all vertical bars show a change of 1 ΔF/F unless annotated differently.

These findings show that wide-field ACs, which tend to send their projections only within one or few layers of the IPL, are not involved in providing local inhibition to BCs that segregate ON and OFF signals. The increase of gain for both ON and OFF responses is coherent with GABAergic ACs' general function in providing surround inhibition globally; thus, BCs signal stronger after a release from inhibition.

4.2.4 Dynamic reconfiguration of polarity switch by the neuromodulator dopamine

The cyclic nucleotide-binding domain at the C-terminus of the HCN channel protein allows for modulation of channel activation and kinetics by cyclic AMP. This property enables the channels to integrate chemical inputs provided by neurotransmitters and hormones in addition to the integration of electrical signals (Biel et al., 2009).

In the retina a subset of ACs releases the neurotransmitter dopamine, which modulates the activity of neuronal circuits through light-adaptive and circadian processes, and acts on target neurons through G-protein coupled receptors that regulate adenylyl cyclase activity (Doyle et al., 2002; Kolb et al., 1981; Yazulla & Studholme, 2001). Activation of the D1-receptor results in an increase in cellular cAMP concentration.

A previous study showed co-localisation of D1-receptors and HCN4 channels in rat BCs and postulated that HCN4 channel activity might be modulated by dopamine due to increased cAMP levels triggered by D1 receptor activation (Müller et al., 2003). We questioned if dopamine could have a similar effect in the zebrafish retina and be coupled to the cAMP metabolism, ultimately regulating HCN channel activity in BCs. We performed two sets of experiments to test this hypothesis, where we either injected dopamine or the dopamine antagonist SCH23390 (~10 and ~1 mM final concentration, respectively).

We find that dopamine administration turns BCs responding with just one polarity into neurons that respond to both phases (Fig. 4.8, next page) with the gain of the ON phase remaining similar before and after dopamine application. Administration of the dopamine antagonist to cells that respond to both light phases results in a loss of the OFF response (Fig. 4.9, page 72) additionally

providing evidence that intrinsic dopamine levels are prevalent during daytime in the zebrafish retina.

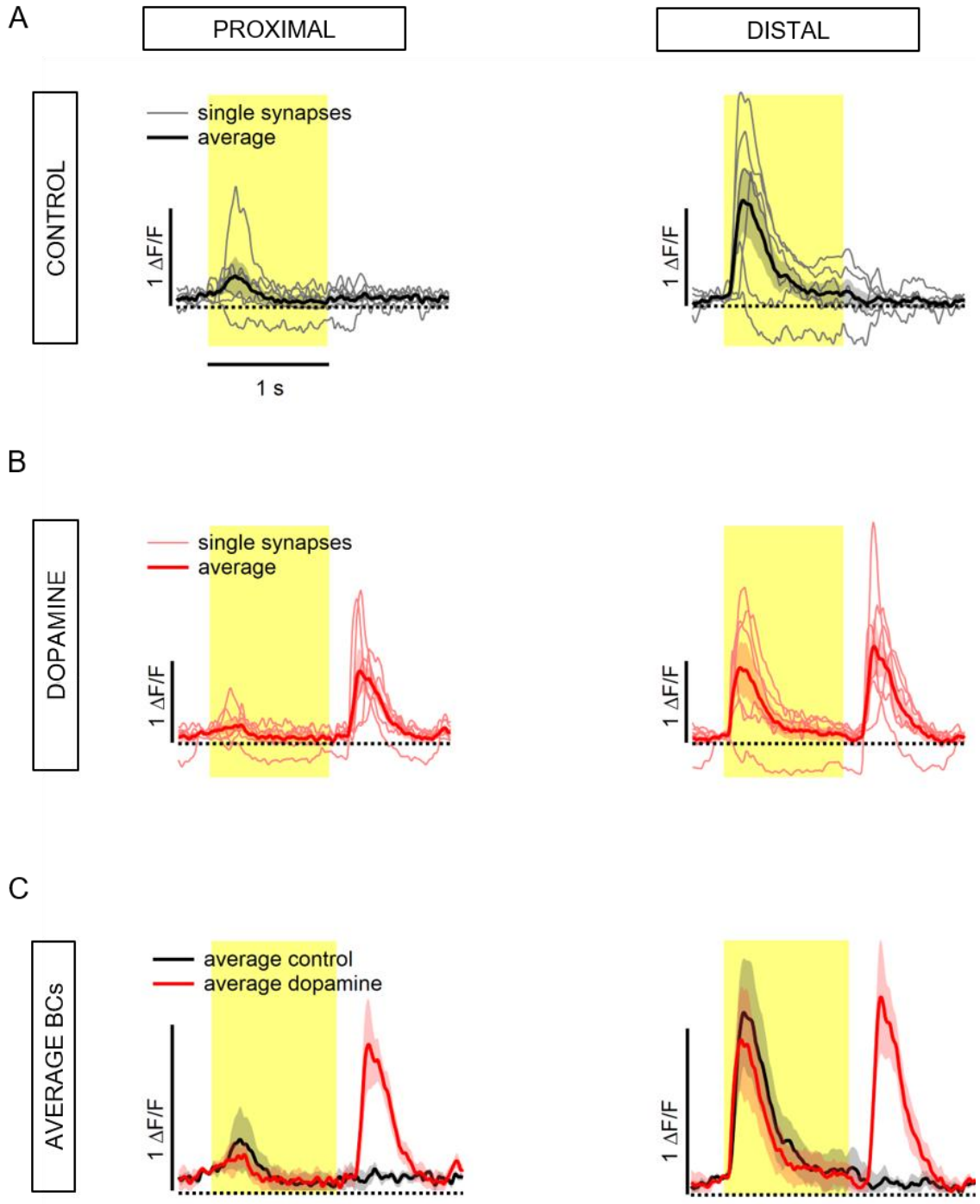

Figure 4.8: Effect of dopamine on polarity switches

A: averaged responses +/-SD of 6 proximal and distal synapses responding to 0.5 Hz frequency **before** dopamine treatment. **B**: same as in A, here responses **after** dopamine treatment. **C:** Averaged responses (+/- SEM) from populations shown in A and B.

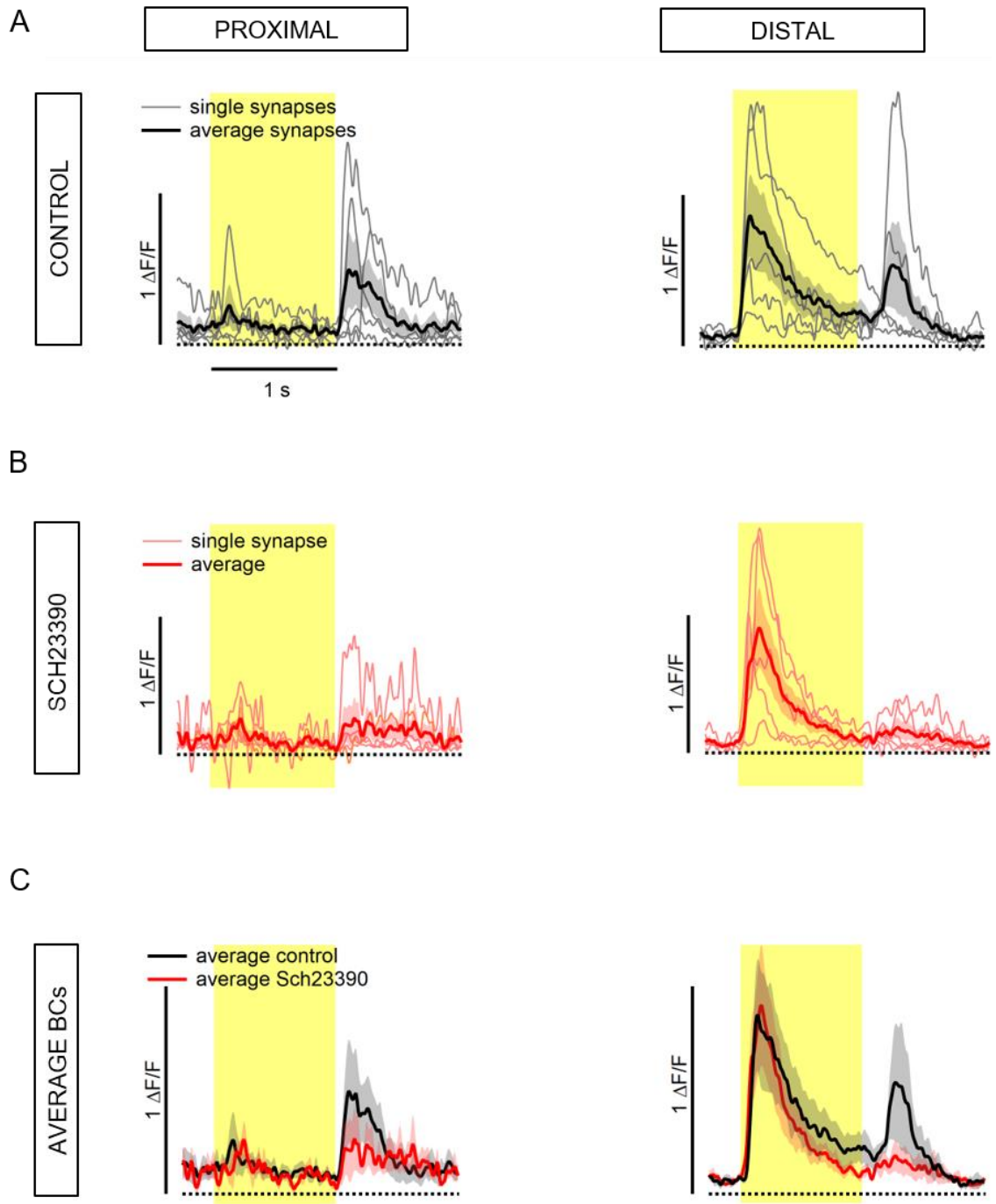

Figure 4.9: Effect of dopamine antagonist Sch23390 on polarity switches

A: averaged responses +/-SD of 5 proximal and distal synapses responding to 0.5 Hz frequency **before** Sch23390 treatment. **B**: same as in A, here responses **after** Sch23390 treatment. **C:** Averaged responses (+/- SEM) from populations shown in A and B.

4.2.5 Proof for intrinsically generated mechanism and against spill-over

The observation that the emergence of additional OFF responses arises only after prolonged intervals of light stimulation (chapter 3, Fig. 3.3 and 3.4, pages 45 and 46), and that these responses disappear after blocking HCN channels (Fig. 4.3 and 4.4, pages 64 and 65, respectively), and glycine receptors (Fig. 4.6, page 68) suggests that BCs are inherently ON cells. To prove that this property is generated intrinsically within ON BCs and to rule out that extrinsic factors such as spill-over from the OFF pathway generate the observed OFF responses, we recorded from retinae in which the ON pathway was blocked by the injection of L-AP4, a specific agonist for the type III metabotropic glutamate receptor expressed on ON BCs (Shiells et al., 1981).

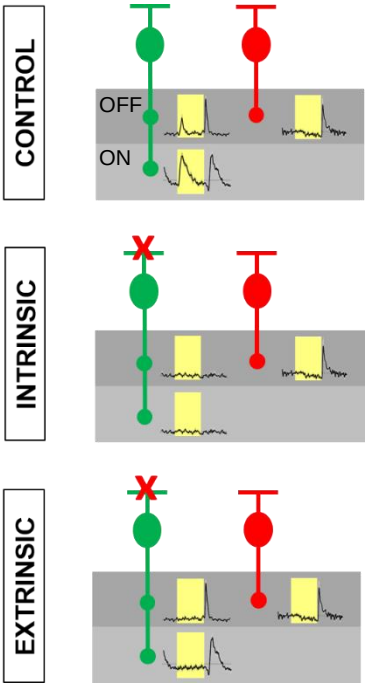

Figure 4.10: Predicted effect of blocking the ON pathway with L-AP4

The three panels show an ON (green) and OFF cell (red) projecting their terminals into the ON and OFF and OFF layers of the IPL, respectively. In the control condition, the ON cell terminals also signal the offset of light, whereas the OFF cell responds to the OFF phase only. Administration of L-AP4 mutes the ON cell's output since the metabotropic glutamate receptor on their dendrites is blocked (red cross), whereas the response of the OFF cell is unaffected. An intrinsically generated mechanism would predict that the ON and OFF responses of the ON neuron disappear, whereas an extrinsically generated mechanism would result in a loss of the intrinsic ON response, but with a maintained OFF response caused through spill-over of the OFF pathway.

Figure 4.10 (previous page) depicts a schematic showing the block's predicted outcomes, assuming that the OFF responses originate intrinsically or extrinsically. We find that after injection of L-AP4 (~5 mM final concentration) terminals that responded to both phases were completely (Fig. 4.11A) or almost silenced (Fig. 4.11B and C), whereas the OFF cells' responses were not inhibited. These results prove that the OFF signals arise within intrinsic ON cells. Therefore we can dismiss the idea of spill-over by neighbouring OFF cells.

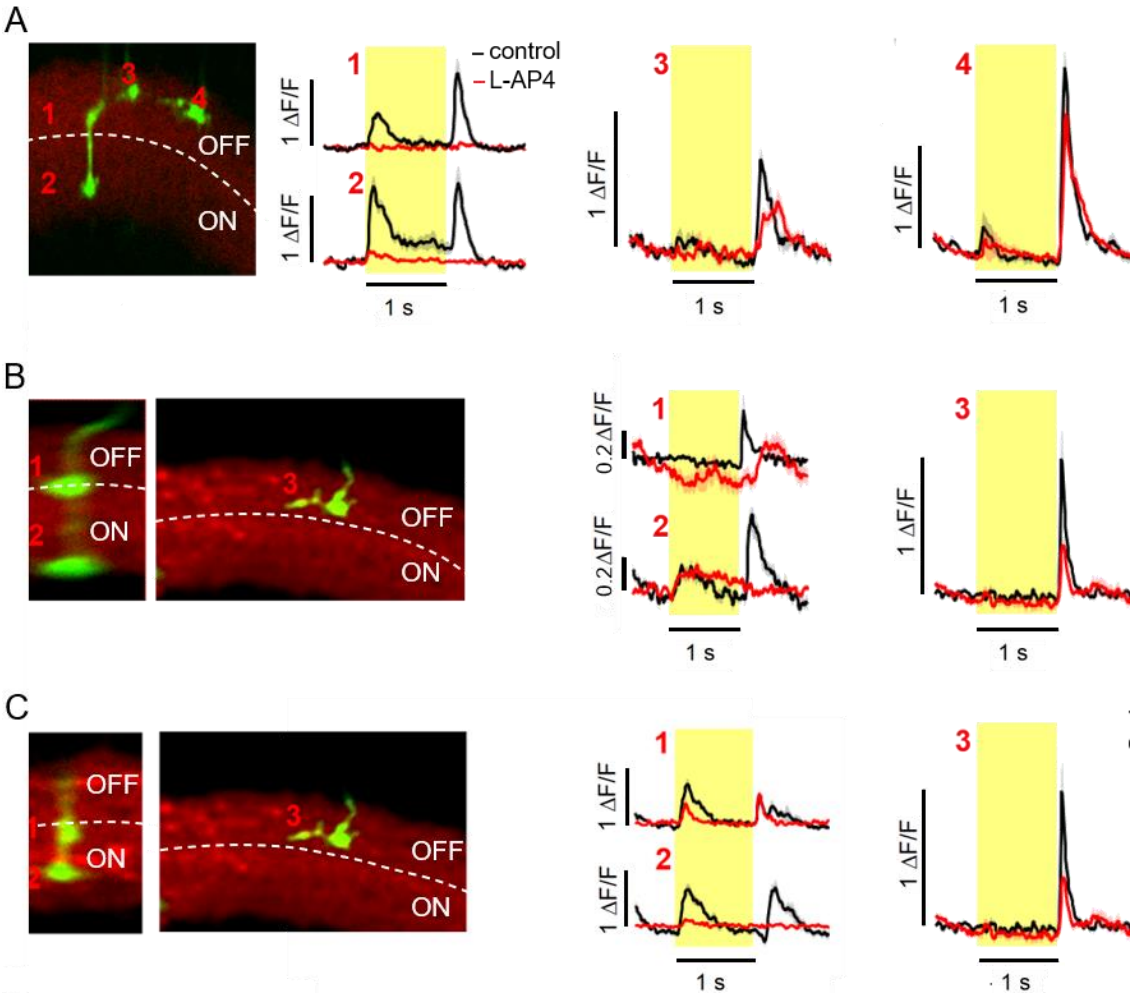

Figure 4.11: Blocking the ON pathway with L-AP4

Images show analysed BCs expressing SFiGluSnFR (green) and their location within the IPL (labelled with Alexa594). Graphs to the right show the responses of boutons before (black) and after administration of L-AP4. **A:** terminals 1 and 2 belong to an ON cell, they fail to respond after drug injection, whereas OFF cells 3 and 4, with one terminal each, continue responding to the OFF phase. **B and C:** Same as in A but here individual OFF cell was located in different field of view and used as OFF control for both cells in B and C.

4.3 Discussion

This study challenges the classical view of retinal BCs segregating fundamental properties of a stimulus - such as light increments and decrements - into distinct, parallel operating channels. Here we showed that this operation can already be achieved within an individual BC, thus revealing an increased, previously unknown, level of granularity within the processing units of the IPL.

We showed that the mechanism involves HCN channels (Fig. 4.3 and 4.4, pages 64 and 65) and corroborated these findings by confirming their expression in the zebrafish retina (Fig. 4.5, page 67). ON and OFF signals' divergence along the axons of BCs arises because some boutons containing HCN channels are inhibited by increases of light while other synaptic compartments are excited. A decrease in luminance switches each bouton's state to the opposite: previously active synapses are muted whilst boutons that are disinhibited respond by rebound depolarisation.

Notably, only glycinergic and not GABAergic transmission lies at the source of inhibition within this circuit (Fig. 4.6 and 4.7, pages 68 and 69, respectively), indicating involvement of small-field ACs and implying that this mechanism operates on a spatially small scale. Intriguingly, switches in synapse polarity are enabled by dopamine (Fig. 4.8 and 4.9, pages 71 and 72, respectively) therefore adding a level of plasticity. The signal flow can be adjusted according to efferent signals which reflect the internal state of the animal.

In chapter three, we argued that spill-over is unlikely to account for the appearance of mixed ON/OFF signals at the individual inputs into amacrine and GCs. We demonstrated that signals with opposing response polarity were localized as near as 1 μm from each other (chapter 3, Fig. 3.8, page 52). We substantiated this idea further by showing that silencing the ON-pathway by pharmacological means did result in a total loss of responses across the axons of individual BCs (Fig. 4.11, previous page). Therefore, ruling out that the rebound depolarisations comprise of spill-over from the OFF pathway.

4.3.1 Compartmentalisation of boutons

How can a distally located ON signal of an intrinsic ON BC still be ON, if the proximal synapse is strongly suppressed during the ON phase (Fig.3.1.B and C,

chapter 3, page 43)? Closer inspection of the responses of the BC in Fig.3.1A (chapter 3, page 43) shows that synapse 1 starts to release glutamate at the onset of light but that this release is reduced below baseline quickly before a pronounced transient OFF response appears upon the change in polarity. Similar observations can be made at synapse 2 and shows that the signal is initially an ON signal. We need to understand now the kinetics of the sustained glutamate release at synapses 3 and 4. Many studies have shown (Lagnado et al., 1996; Neves & Lagnado, 1999; Snellman et al., 2011; Von Gersdorff & Matthews, 1994) that the vesicle release at ribbon synapses can have fast and transient or more sustained release dynamics and that the residual increase in intracellular calcium can outlast the duration of the signal and trigger vesicle release lasting several hundreds of milliseconds. Furthermore, many traces throughout all experiments show a strong rebound response at the light offset even though there is no visible hyperpolarisation during the ON phase or even a pronounced ON response visible. Might inhibitory currents be counteracting the excitatory drive? The analysis of the individual synapses before and after administration of strychnine (Fig. 4.6, page 68) show that out of the 7 proximal and distal terminals, 2 proximal and 4 distal terminals respond with an increased ON amplitude in comparison to the control condition. This observation supports the notion of counteracting forces; however, the ON amplitude of the remaining 8 synapses responded with a weaker gain. Similar expectations can be applied to the experiments in which we applied the HCN channel blocker ZD7288 (Fig. 4.3 and 4.4, pages 64 and 65). Since HCN channels open during phases of hyperpolarisation and thus the influx of cations drives the membrane potential towards the potential at rest, a blockage of these channels not only results in a loss of the rebound response at light offset but also in a reduced gain of the ON amplitude since the blocked HCN channels cannot counteract the hyperpolarising current. However, the responses of all synapses analysed in Fig.4.4. (page 65) show various outcomes with stronger, weaker or similar profiles in gain. Given the complexity of the IPL, other circuits might be involved or generate the observed phenomenon. A biophysical multi-compartment model might provide a better understanding of the underlying circuitries; however, this lies outside the scope of this thesis.

4.3.2 An unsuspected mode of adaptation

The retina continually adjusts the way stimuli are processed according to the previous stimulus history. Adaptation in the form of gain change is a commonly used strategy to prevent the system's saturation and allow for future registration of strong stimuli (Johnston et al., 2019; Kastner & Baccus, 2013; Nikolaev et al., 2013). The observed appearance of rebound responses after an extended stimulus duration represents a new and more complex form of adaptation: a retuning of synapses instead of a simple gain change - driven by an external stimulus rather than the intrinsic synaptic machinery. These externally driven changes present a form of "predictive coding" (Hosoya et al., 2005; Kastner & Baccus, 2013). The changes are predictive because they retune specific connections to respond if there is a future change in the stimulus in the opposite direction, from ON to OFF or vice versa.

4.3.3 Efficient Coding of ON and OFF signals

Might the findings that ON and OFF signals can be transmitted by an individual BC support the notion of efficient coding? The efficient coding hypothesis (Attneave, 1954; Barlow, 2013; Sterling & Laughlin, 2015) postulates that sensory systems encode information in a neural code that efficiently represents sensory information whilst economizing the usage of space, material and energy. How might the signal decomposition of ON and OFF signals at the output of individual BCs support this notion, if at all? A recent theoretical study suggested that the splitting of ON and OFF signalling into parallel pathways evolved to signal changes in light intensity at a lower metabolic cost and in a more rapid manner than a one channel system (Gjorgjieva et al., 2014). Experimental discoveries support this hypothesis; the transmission of information is more efficient when signalled through small neurons that transmit at a low rate than through large neurons that transmit at a high rate (Niven et al., 2007). Our finding that individual BCs transmit ON and OFF signals to their postsynaptic partners seems to violate this aspect of efficient neuronal coding. However, other aspects of coding efficiency might be met by the facts that: (1) The density of ON-OFF signalling within the IPL is increased. Since natural scenes contain more negative than positive contrasts (Balasubramanian & Sterling, 2009), the increased coverage

factor of OFF signals optimizes the representation of the visual scene. (2) The flow of ON and OFF signals is not hard-wired. Dopamine is in control of the signal flow across individual BCs. Therefore, the system can "stream on-demand" if needed but turn down transmission if unnecessary. (3) Not all synapses convey the same information; some get predictively tuned towards new stimuli, therefore preparing the system to signal future changes while reducing redundancy.

4.3.4 Neuromodulation of ON-OFF signalling

Reports have shown that dopamine increases the retina's visual acuity and contrast sensitivity (Jackson et al., 2012). Investigations into the underlying mechanisms have revealed various actions such as modulation of electrical coupling between PRs and HCs in the outer retina (Ribelayga et al., 2008; Thoreson & Stella, 2000) and lowering of the voltage threshold for activation of voltage-gated calcium channels in BC terminals (Heidelberger et al., 1994). Our findings provide further insights into how these increases in acuity and contrast sensitivity are achieved.

In zebrafish, dopamine is released by interplexiform cells (IPCs) (Li & Dowling, 2000; Popova, 2014). These cells comprise a unique subset of ACs that reside within the inner nuclear layer and extend their processes into both plexiform layers and thus modulate neuronal transmission at the outer and inner retina level. Dopamine release and synthesis are regulated by direct light input and the circadian clock (Doyle et al., 2002; Iuvone et al., 1978). Concentrations are high during daytime and low at night (McCormack & Burnside, 1993; Ribelayga et al., 2004). Interestingly, a recent study found that olfactory stimulation results in alteration of retinal sensitivity mediated through variation in dopamine concentration (Esposti et al., 2013). Efferent signals from the olfactory bulb are relayed onto IPCs in the retina. Therefore, the release of dopamine is under additional control of olfactory stimulation. For example, the food-related amino acid methionine induces a response cascade in which dopamine regulates the activation of presynaptic calcium channels. This effect occurs only in OFF BCs and increases their sensitivity towards luminance and contrast (Esposti et al., 2013). These findings lead to further questions: Do other sensory modalities modulate the decomposition of ON and OFF signals? Which other

neuromodulators or molecules control this circuit? How do behavioural and internal state (fear, arousal, hunger, stress, hormone levels) influence this pathway?

4.3.5 Species-specific differences and the need for standardization of experimental procedures

We demonstrated that the segregation of ON and OFF signals is a characteristic of ON cells. We did not find any OFF cells with ON rebound depolarisations. These findings are supported to some extent by a study undertaken in rat retinae in which immunolabeling with antibodies specifically designed to target the 4 HCN isoforms, showed immunoreactivity of all ON BCs. In contrast, just one out of the four existing OFF BC types in rats was labelled with an antibody targeted against HCN4 (Müller et al., 2003). However, studies investigating light responses in mice and pigs by functional imaging and multielectrode recordings reported contrasting results. Here, an appearance of ON responses in OFF bipolar and GCs occurred often whereas reverse response patterns were rare.

However, our and other studies highlight the difficulty in characterizing the response profiles of cells or even entire circuitries (Tikidji-Hamburyan et al., 2015; Vlasits et al., 2014). We demonstrated that most terminals which are localized proximal to the soma tend to give OFF responses only (Figure 3.4 A, page 46), whereas terminals distal to the soma show ON or ON and OFF responses (Figure 3.4 B, page 46). Furthermore, we showed that terminals that are silent or respond to the ON phase only, start responding to the OFF phase when dopamine levels increase (Fig. 4.8, page 71). Accordingly, each study should be designed carefully by considering the neural network's plasticity; a standardization of protocols and procedures would be useful, especially when comparing data from different studies and research groups.

4.3.6 Anatomical aspects of retinal microcircuits

The larval zebrafish retina encompasses a functional and anatomical asymmetric structure that matches the animal's natural chromatic statistics and behavioural requirements (Yoshimatsu et al., 2020; Zimmermann et al., 2018). For instance, the area temporalis (Schmitt & Dowling, 1999) comprises the retinal patch that

surveys the front and slightly upward visual field of the fish. This area is also termed "strike zone" because its circuits are optimized for prey-capture due to the high density of UV-sensitive cones which enable larval zebrafish to detect and hunt small microorganisms like *Paramecia* which appear as UV-bright spots to the fish retina (Yoshimatsu et al., 2020; Zimmermann et al., 2018). These structural differences might allow for another level of complexity if the decomposition of signals is implemented regionally. It is tempting to speculate that the segregation of ON and OFF signals is more prevalent within the strike zone, facilitating prey recognition and capture by increasing the spatial resolution but under permissive control of dopamine reflecting the fish's hunger state. We observed that individual BCs across the entire IPL (dorso-ventral, nasal-temporal) signal excitatory ON and OFF responses, however an in-depth analysis of regional differences regarding the density of these cells will be addressed in future experiments.

Further anatomical aspects are of interest: In chapter 3, we illustrated that the various boutons' responses along the BCs' axon are different (Fig. 3.1 and 3.2, pages 43 and 44, respectively). The proximal terminal sometimes showed a hyperpolarisation below baseline during the ON phase, followed by a strong rebound at the light offset. Only a few recordings presented responses towards both phases (chapter 3, Fig. 3.4, page 46). However, the distal terminal rarely hyperpolarised below baseline but responded in most cases to both polarities. How are these differences generated? Are different levels of inhibition provided to each terminal, with stronger inhibition at the proximal terminal? Or are more glycine-receptors expressed at the proximal synapse? Alternatively, the degree of inhibition might be similar, but the expression levels of ion channels different. For example, ACs that encode the direction of moving stimuli were found to have dendritic compartmentalization of the chloride cotransporter essential for the computation (Gavrikov et al., 2006). In our model, a higher density of HCN channels at the proximal synapse might explain the appearance of more robust rebounds and possibly also the occasional weak ON responses as these channels counteract both deflections of the resting membrane potential. The experiments in which we blocked rebound depolarisation by either using the HCN channel-specific blocker ZD72188 or strychnine to block glycinergic transmission showed some interesting differences. Whereas strychnine entirely blocked the

responses at both, proximal and distal, terminals (Fig. 4.6, page 68), ZD72188 administration only blocked the rebound at the distal terminal, but rebound responses were still visible at the proximal synapse (Fig. 4.3 and 4.4, pages 64 and 65). This observation might indicate an increased expression of HCN levels at the proximal synapse. Moreover, a differential expression of voltage-gated calcium channels along the axon might account for the regional differences.

Further experiments could involve controlling inhibition through optogenetic strategies, however these are challenging to achieve currently because of the lack of a glycinergic AC-specific promoter in zebrafish. Recent optimizations in the design of genetically encoded voltage sensors might soon enable us to study local voltage changes across the BC membrane and provide insights into neurons' compartmentalization and electrical compactness (Villette et al., 2019; Yang et al., 2016).

Chapter 5

The emergence of orientation selectivity in the retina

5. The emergence of orientation selectivity in the retina

5.1 Introduction

The visual system of many animals comprises a subset of neurons that is tuned to edges of a particular orientation. These cells respond strongly to elongated stimuli oriented along a “preferred” axis but respond weakly to stimuli oriented orthogonally to the preferred axis (Hubel & Wiesel, 1959, 1962). These orientation selective cells are organized into functional columns in the cortex of some animals such as primates (Hubel & Wiesel, 1962, 1968; Humphrey et al., 1980), whereas in others such as rodents there is no spatial organisation, yet many cells show strong orientation tuning (Girman et al., 1999; Ohki et al., 2005; Van Hooser et al., 2005). Many orientation-selective cells can additionally be selective for stimuli moving in one direction in contrast to movements in any other direction (Barlow & Levick, 1965; Hubel & Wiesel, 1962; Weliky et al., 1996).

Where does orientation- and direction-selectivity emerge within the visual system? For a long time, these properties were thought to arise within the primary visual cortex (Hubel & Wiesel, 1959). However, later studies revealed that they can emerge at earlier stages. Selective responses were found in the lateral geniculate nucleus (Cheong et al., 2013; Marshel et al., 2012), the superior colliculus and the retina (Levick, 1967; Venkataramani & Taylor, 2010). Interestingly, studies suggest that orientation- and direction-selectivity emerges through different pathways (Antinucci et al., 2016).

In the retina direction- and orientation-selective amacrine (Antinucci et al., 2016; Euler et al., 2002) and GCs (Barlow et al., 1964; Levick, 1967) have been described.

Two mechanisms are essential in generating the direction-selective outputs of GCs: (1) Starburst ACs (SACs) co-release GABA and acetylcholine in response to stimuli that move in the centrifugal direction - that is from the soma to the distal dendrites - but not to the opposite direction (Euler et al., 2002). (2) SACs provide spatially asymmetric inhibition. SAC processes that point into the null direction of direction-selective GCs release GABA and acetylcholine, whereas processes that point into the preferred direction only release

acetylcholine (Briggman et al., 2011; Lee et al., 2010). Furthermore, fewer synapses form on the preferred side (Briggman et al., 2011).

Similarly, the connectivity of amacrine and GCs dictates the emergence of orientation-selective responses in GCs: GABAergic ACs with elongated receptive fields evoke large inhibitory postsynaptic currents (IPSCs) in GCs when the orientation of a stimulus coincides with the orientation of their receptive fields (Bloomfield, 1994; Levick, 1967; Murphy-Baum & Rowland Taylor, 2015). Therefore, the inhibitory input along the null axis counteracts the excitatory drive along the preferred axis and renders the response-profile orientation-selective.

In recent years, studies on orientation- and direction-selectivity focused on various aspects to further dissect the underlying circuits in detail. For instance, how do SACs become tuned to direction? A multitude of mechanisms such as differential chloride homeostasis (Gavrikov et al., 2003), wiring specificity of BCs (Ding et al., 2016; Kim et al., 2014), reciprocal inhibition between neighbouring SACs (Lee et al., 2010) have been shown to contribute to this specific feature.

Moreover, with BCs providing the excitatory drive into amacrine and GCs, it has been a matter of intense debate if the outputs of BCs display orientation and direction tuning (Park et al., 2014; Yonehara et al., 2013). Indeed, electrophysiological recordings revealed that the excitatory postsynaptic currents (EPSCs) of GCs show orientation and direction tuning (Taylor et al., 2000). However, these studies were criticized since it was demonstrated that space clamp errors might have led to inaccurate measurements and conclusions (Percival et al., 2019; Poleg-Polsky & Diamond, 2011). Imaging studies further corroborated the hypothesis that the output of BCs is non-selective towards direction and motion.

This chapter describes our investigation into BCs' responses towards moving stimuli. We documented these findings in a recent publication of our research group in which we showed that the retina's orientation-selective responses are dynamically and predictively tuned (Johnston et al., 2019).

5.2 Results

5.2.1 The terminals of bipolar cells comprise the first neural compartment tuned to the orientation of a visual stimulus

Electrical recordings in the soma of BCs show no tuning to the orientation of a stimulus (Hosoya et al., 2005) but might the synaptic compartments at the output show a different response profile?

To investigate whether BCs are sensitive to the direction or orientation of a stimulus, we used zebrafish that express the calcium reporter GCaMP6f in the terminals of BCs (see methods, chapter 2, pages 30 and 31). The fish larvae were mounted under a two-photon microscope with one eye looking at a screen illuminated by a projector (see methods, chapter 2, page 22). We started surveying the responses by applying a stimulus that consisted of individual dark bars which moved across the screen in 8 different directions equalling four representations in orientation space. Each direction was presented to the retina five times at random order to avoid adaptation (Fig. 5.1A and B, next page).

We did not observe any significant direction-selective responses, which allowed us to average responses across both directions (Fig. 5.1C, left, next page) and calculated the vector sum in orientation space for each of the ten repeats of four orientations (Fig. 5.1C, right, next page). We tested the resulting distribution of orientation vectors for a significant orientation sensitivity using Moore's version of Rayleigh's test with the false positive rate set to one per cent. Interestingly, we found many BC terminals that displayed orientation sensitivity; individual examples are shown in Figure 5.1C. Out of 1053 analysed terminals, 24.4% showed orientation-selective responses (Fig. 5.2A, page 87). The analysis of the distribution of average orientation preferences across all orientation-selective BCs revealed that most orientation-selective terminals are tuned to vertical stimuli (Fig. 5.2B, page 87) with a circular mean of 4.1°.

The findings presented in Figures 5.1 (next page) and 5.2 (page 87) illustrate that fundamental computations such as the detection of oriented edges emerge early within the visual pathway, namely at the output of BCs.

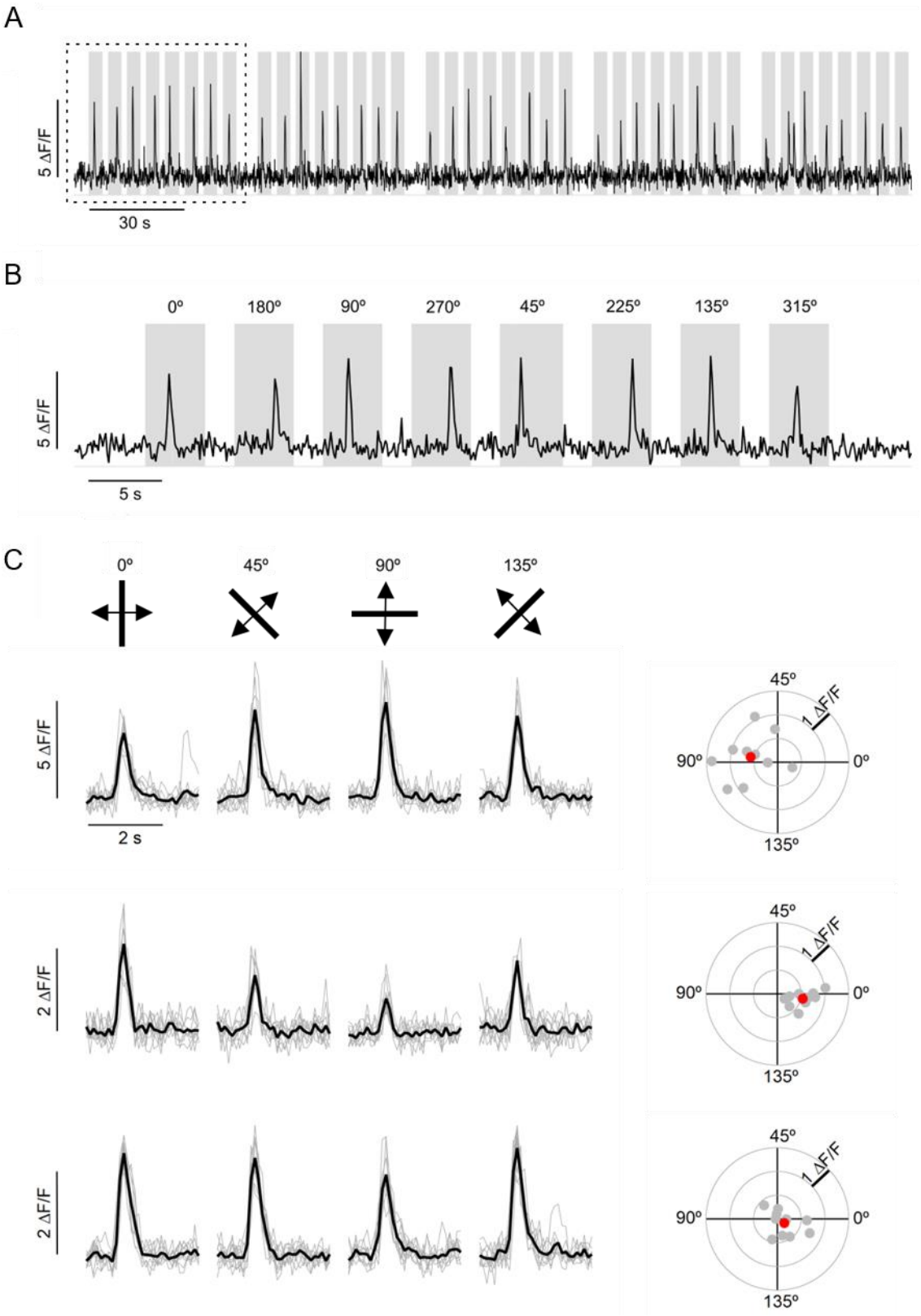

Figure 5.1: Bipolar cell terminals display orientation sensitivity

A: Responses of a BC terminal towards a bar moving in 8 directions (repeated 5 times) across the visual field. **B:** Same trace as in A but zoomed into first stimulus block (dashed line in A) showing the angles used on top. **C:** Left: Examples of 3 terminals responding to bars moving across the field of view at four → *bottom next page*

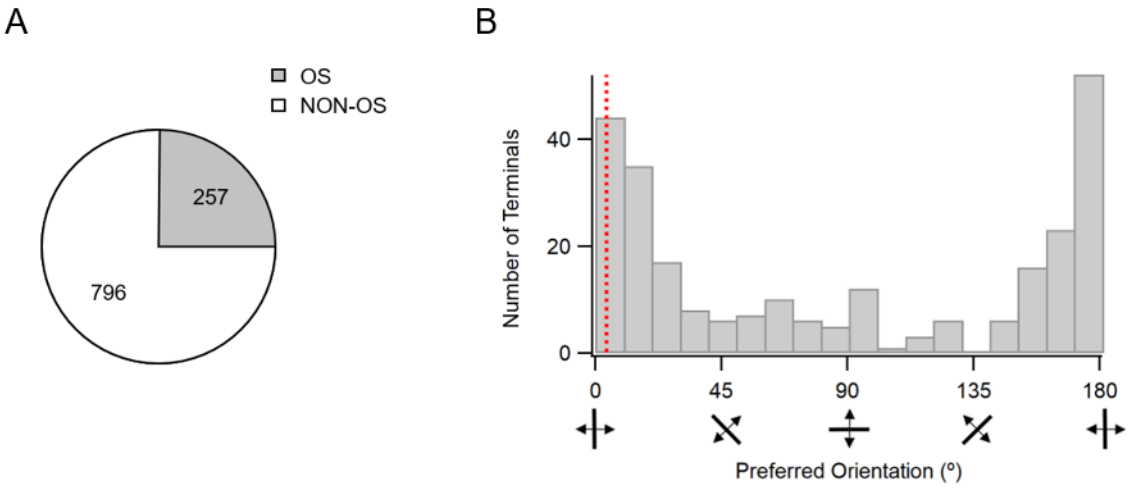

Figure 5.2: Orientation tuning of bipolar cell population

A: A total of 1053 analysed terminals were tested for orientation-selectivity; 257 (24.4%) showed preferential tuning with a false positive rate set to 1%. **B:** Histogram presenting the preferred tuning of the 257 terminals in orientation space, note the bias for vertically orientated bars (red dotted line, circular mean 4.1°).

5.2.2 Assessment of orientation preference with the orientation selectivity index

Different studies use a variety of methods to measure orientation- and direction-selectivity (Mazurek et al., 2014). One commonly used strategy to assess neurons' orientation preferences is to measure the orientation selectivity index (OSI). This method provides a mathematically quicker and straightforward analysis by which the neuron's response to the preferred orientation is compared to the response to the orthogonal orientation. Our previous study of orientation tuning in vector space revealed a strong bias for vertically oriented bars. Therefore, we used a simplified stimulus consisting of a full-field grating that switched orientation at 5 Hz from horizontal to vertical every ten seconds (Fig. 5.3A, bottom, next page). Orientation selectivity was assessed by measuring the response amplitude towards vertical (R0°) and horizontal (R90°) orientated bars and calculating the OSI defined as $(|R0° - R90°|) / (|R0°| + |R90°|)$.

---

different orientations (top, black arrows). Grey traces show single responses of 10 repetitions; black traces represent mean response. Note, first example shows plots of traces shown in A and B, last example at bottom is non-sensitive to orientation. Right: The vector sum of each of the 10 trials plotted in orientation space (grey) with the average vector sum shown in red.

Interestingly, many traces showed a hyperpolarisation below baseline upon presentation of horizontal gratings (Fig. 5.3A). Moreover, the distribution of OSI's showed a large population of cells with an OSI of 1 (Fig. 5.3B) – a maximal sensitivity towards a stimulus' orientation- as opposed to a broad population of varying OSIs.

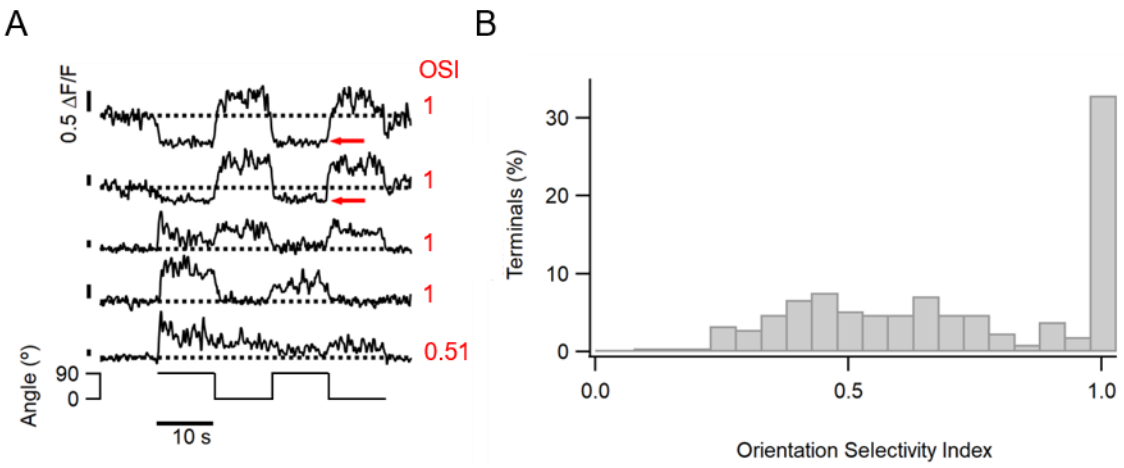

Figure 5.3: Orientation Selectivity Index of bipolar cells

A: Examples of 5 BC terminals responding to full-field grating that reverses orientation at 5 Hz from horizontal (90°) to vertical (0°) every 10 seconds. Note the hyperpolarisation below baseline (red traces) during the representation of the non-preferred orientation. **B:** Histogram presenting the OSI of 257 terminals, note the large quantity of terminals with an OSI of 1.

5.2.3 Receptive fields of bipolar cells contribute to emergence of orientation tuning

How is orientation sensitivity generated in BC terminals? One possibility is that the receptive fields of BCs are elongated and oriented along the vertical axis and generate orientation-selective responses by excitation only (Fig. 5.4A, Model 1, next page). To address if elongated receptive fields were responsible for the orientation selectivity of BC terminals, we used the filtered back projection technique to estimate the terminals receptive fields (Johnston et al., 2014). Briefly, a series of bars are presented at different locations across the retina at a given angle, the series is then repeated but with a different angle of the bar. The receptive fields are recovered by using an algorithm which is commonly used in computed tomography (CT) scans. Four examples of receptive fields from individual terminals are shown in Figure 5.4B (next page) along with the 2D

Gaussian fits used to measure the ellipticity by comparing the minor axis to the major axis. We found that the majority of receptive fields display some level of ellipticity (median 0.3) which could explain the population of varying OSIs broadly centred around the OSI of 0.5 but could not explain the large population of terminals with an OSI of 1 (Fig. 5.3B).

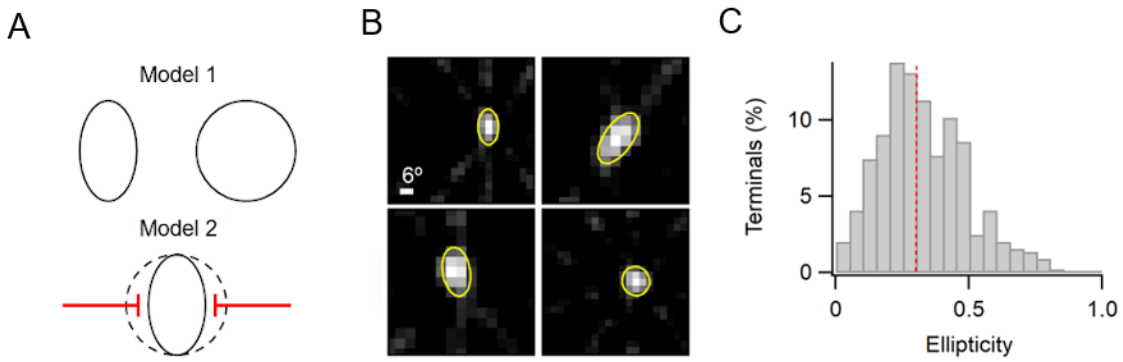

Figure 5.4: Receptive fields contribute to orientation-sensitivity

A: Modelling the emergence of orientation selectivity: Model one comprises of an elongated receptive field (left) that is generated by excitation only and oriented along the preferred axis as opposed to a receptive field that is circular (right). Model two encompasses lateral antagonism (red) along the non-preferred axis which renders the excitatory centre to the preferred axis. **B:** Example of receptive fields of four BCs. Each receptive field was fit with a 2D Gaussian, yellow contours indicate the fits at 30% of the maximum.
C: Histogram of the ellipticity (1-minor axis/major axis) of 442 measured receptive fields (median 0.3, red dashed line).

5.2.4 Lateral Antagonism shapes bipolar terminal orientation selectivity

We previously observed that many BC terminals hyperpolarised during the representation of horizontal gratings (Fig. 5.3A, page 88). Might lateral inhibition along the non-preferred axis play a role in generating orientation tuning in BC terminals (Fig. 5.4A, Model 2)?

We blocked inhibition by injecting a mix of GABAzine and strychnine into the vitreous chamber of the zebrafish eye to address this question. Interestingly, the disinhibition of BCs resulted in a drastic decrease in BC terminals that showed perfect orientation tuning (OSI = 1) in the control condition (Fig. 5.5A, next page). The analysis of the responses of BCs in vector space (Fig. 5.1 and 5.2, pages 86

and 87, respectively) showed similar changes. Whereas in the control condition, a strong bias for vertical stimuli dominated the distribution of responses in orientation space. The preference for vertically oriented stimuli disappeared under the pharmacological block (Fig. 5.5B, next page).

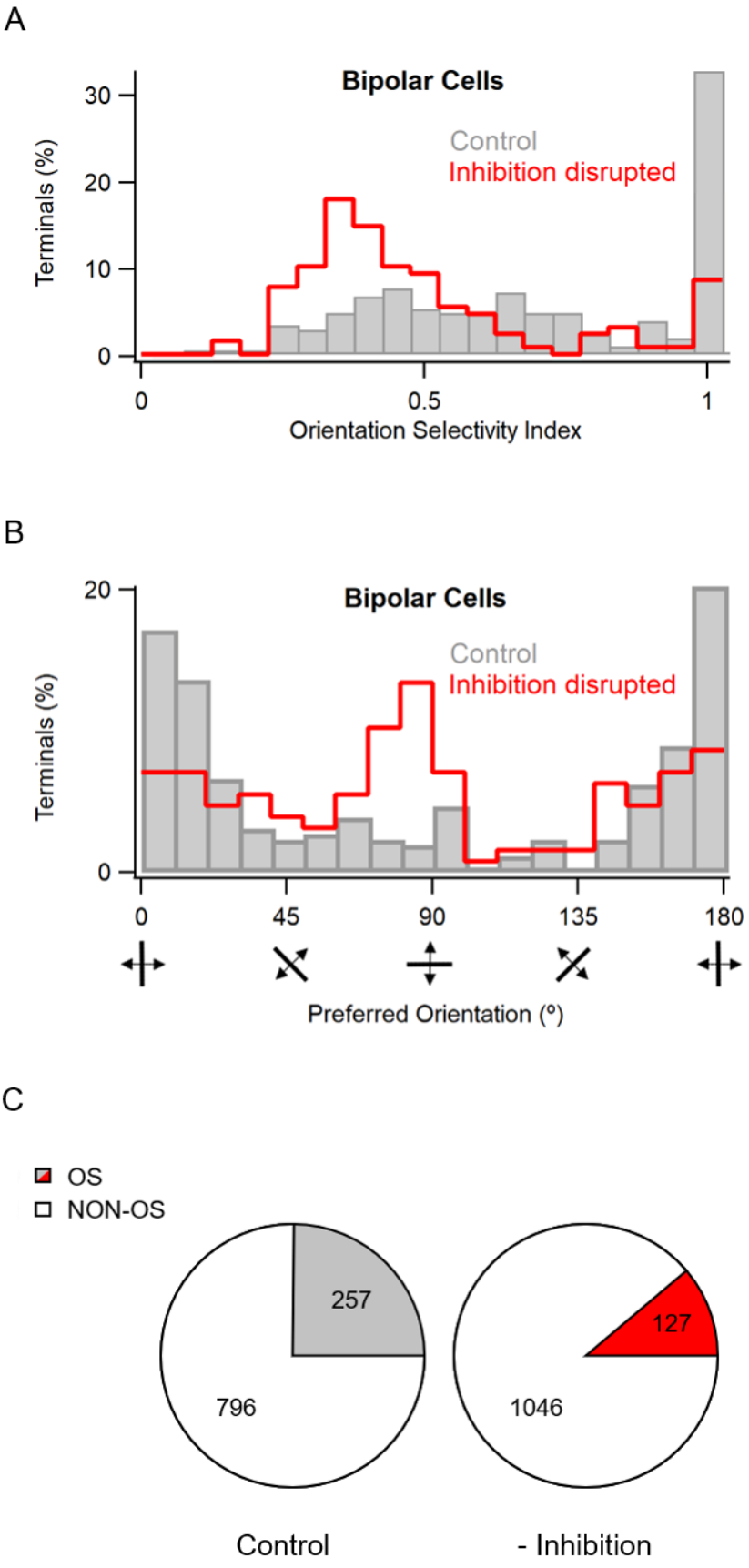

Figure 5.5: Lateral antagonism renders bipolar cell terminals orientation-selective

→ *bottom next page*

The histogram shows a flattened shape with a small increase for preferences for horizontal orientated bars. Moreover, the ratio of selective versus non-selective terminals before and after disinhibition (Fig. 5.5C, previous page) changed. Whereas 24.4% of the terminals were selective in the control condition, only 10.8% displayed significant orientation tuning post disinhibition. Therefore, the slight increase in terminals displaying a preference for horizontally oriented stimuli (Fig. 5.5B, previous page) is unlikely to be caused by a shift from vertical to horizontal tuning.

5.2.5 Amacrine cells inherit the orientation tuning from bipolar cells

BCs synapse onto ACs and are the sole source of the excitatory drive onto these inhibitory neurons of the IPL. How are ACs tuned to orientation? Might they inherit the orientation tuning of BCs or do other factors that influence these cells' response profile render their orientation tuning different? Might ACs be preferentially tuned to horizontal stimuli thus providing a simple mechanism by which BC responses are rendered selective for vertical stimuli?

To investigate ACs' orientation tuning, we used a transgenic zebrafish line (Ptf1a:Gal4) that drives expression of the calcium sensor GCaMP3.5 via the Ga4/UAS-system (see methods, chapter 2, page 32). Analysis of the AC responses in vector space (Fig. 5.6, next page) revealed that these cells show a similar distribution of orientation tuning as BCs (Fig. 5.6, next page). Vertically oriented stimuli result in larger responses. Overall, the AC tuning curve is flatter than the BCs' curve with a weak increase of represented non-vertical orientations. Lateral inhibition within the population of ACs might account for these small differences in orientation tuning.

A: Histogram displaying the distribution of orientation selectivity indices measured in BCs before (n=210) and after disinhibition (n=129). **B:** Same as A but here orientation tuning was assessed by measurement of responses in vector space; control (n=257), after disinhibition (n=127). **C:** Pie charts showing the decrease in orientation-selectivity before (left) and after disinhibition (right).

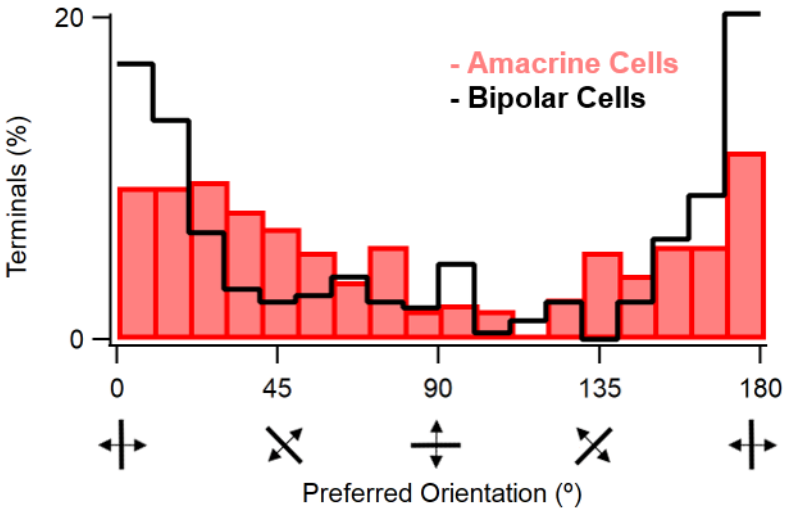

Figure 5.6: Orientation tuning in amacrine cells

Histogram displaying the distribution of orientation preferences of ACs (n=274) in comparison to BCs (n=257) measured in vector space.

5.3 Discussion

This study demonstrates that the circuits generating orientation-selective responses arise earlier within the retina than previously thought, namely at the terminals of BCs (Fig. 5.1-5.3, pages 86-88). We showed that many receptive fields of BCs are elliptical (Fig. 5.4, page 85) and suggested that this intrinsic property contributes to the emergence of orientation-selective responses at the BCs' output (Fig. 5.5A, page 91). However, we illustrated that lateral antagonism underlies strong orientation-selective responses (Fig. 5.5 A-C, page 91). Moreover, ACs inherit the orientation tuning of BCs (Fig. 5.6, page 93). Both cell types preferentially encode vertically oriented stimuli. Therefore, we suggest that laterally arranged ACs without any orientation preference render the BCs' sensitivity towards vertical orientations.

We did not find any significant levels of direction-selective responses at the outputs of BCs. This observation corroborates studies that illustrated the absence of direction-selective responses at BC terminals (Park et al., 2014; Yonehara et al., 2013). Moreover, the notion of distinct pathways encoding orientation and direction is substantiated further. However, a recent, not yet peer-reviewed publication (Matsumoto et al., 2020), showed that subtypes of BCs display direction-selective responses. These results were obtained by optical imaging of glutamate release at BC terminals in mice retinae. However, an investigation into the glutamatergic input into GCs within our group does not support these findings (Johnston et al., 2019). Species-specific properties might lie at the basis of this contradiction.

Our finding that BCs are preferentially tuned to vertically oriented stimuli agrees with the results of other studies where the output of GC terminals measured by calcium imaging of seven day old zebrafish larvae showed that the majority of outputs display a preference for the vertical orientation. (Hunter et al., 2013; Lowe et al., 2013; Nikolaou et al., 2012).

Interestingly, direction-selective inputs are developmentally invariant, whereas orientation-selective inputs change over time (Lowe et al., 2013). The first orientation-selective responses arise on the third day of development and are solely tuned to the vertical stimuli. On seven days post fertilisation four different orientations, equally covering orientation space, are encoded with a

strong preference of vertical stimuli. However, on day ten post fertilisation, the four different orientations' preferences are more levelled out with a remaining slightly larger preference for vertically oriented stimuli.

What is the function orientation sensitive BCs? A simple answer is to provide a pre-processed preference to orientation-selective GCs. Another more detailed explanation involves the phenomenon of dynamic predictive coding.

This coding strategy comprises the observation that many cells of a neuronal population quickly adapt to a persisting stimulus to signal future changes. This coding strategy is implemented in various circuits throughout the nervous system (Hosoya et al., 2005; Sohoglu & Chait, 2016; Stachenfeld et al., 2017). However, the underlying circuit mechanisms have been a matter of continuous debate.

Various models have been proposed. One of which constitutes a modifiable pattern detector that receives multiple excitatory inputs of different stimuli patterns. Synapses that signal a specific pattern strongly depress quickly so that the neuron's output signal gives more weight to the signal transmitted by other synapses (Bastos et al., 2012; Gollisch & Meister, 2010; Hosoya et al., 2005).

Indeed, in a recent publication, we substantiated the hypothesis of a pattern detector underlying dynamic predictive coding strategies (Johnston et al., 2019). We illustrated that a stimulus's orientation is dynamically and predictively encoded within some GCs by imaging glutamatergic transmission across individual cells. GCs that received mixed inputs - that is horizontally and vertically oriented static gratings– adapted their output in response to both orientations within a fraction of a second. We showed that feed-forward inhibition onto GCs through ACs signalling nulls the ongoing steady signal.

Chapter 6
General Discussion

6. General Discussion

6.1 New tools, new insights

The retina's numerous cell types perform complex computations before the signals that encode the information about a stimulus leave the retina along the optic nerve in the form of a spike code (Asari & Meister, 2012; Berens & Euler, 2017). PRs transduce the electromagnetic signal of light into an electrochemical signal propagated via the graded release of the excitatory neurotransmitter to BCs and ultimately GCs. The continuous development and optimization of genetic tools have facilitated the discovery of retinal microcircuits. Electrophysiological approaches to study the physiology of cell types like BCs and ACS has been a cumbersome task due to the difficulties in targeting their cell bodies embedded deep within the retinal layers. However, the use of genetically encoded reporters of neuronal transmission combined with optical methods has allowed for the assessments of cell populations in vivo in a non-invasive manner (Ahrens et al., 2012; Dreosti et al., 2009; Marvin et al., 2013). Manipulations of circuitries through optogenetic methods have further unravelled the underlying dynamics (Arrenberg et al., 2009; Portugues et al., 2013; Wyart et al., 2009). Moreover, genome engineering approaches by employing the CRISPR/Cas9 (Wright et al., 2016) or TALEN system (Boch, 2011) have made it possible to target sensors to cell types without the need to identify gene regulatory elements (Antinucci et al., 2016; Kölsch et al., 2021).

6.1.1 The assessment of bipolar cell physiology through genetically encoded sensors

Retinal BCs are central to the processing of visual signals within the vertebrate retina (Euler et al., 2014; Franke et al., 2017). Whereas early characterizations of BCs' physiology were traditionally assessed by measuring membrane potential or conductance changes at the soma (Euler & Masland, 2000; Werblin & Dowling, 1969), we took advantage of recent functional imaging advancements. The use of genetically encoded reporters allowed us to study neuronal transmission in different subcellular compartments of individual cells *in vivo* in zebrafish larvae under two-photon illumination.

We employed two different sensors to study different aspects of neuronal signalling. To assess the neurons' intrinsic physiology, we employed genetically encoded calcium sensors that report changes in presynaptic calcium concentration (Dreosti et al., 2009). However, presynaptic inhibition and synaptic release dynamics at the BC synapse cannot be assessed by calcium sensors. We therefore complemented our studies by expressing the glutamate sensor iGluSnFR in the neurons of the inner retina (James et al., 2019). This sensor allowed us to measure the excitatory input and output of individual neurons of the inner retina.

One part of this thesis aimed to assess if different visual stimulus properties can be segregated through individual BCs. We found that individual BCs' terminals can respond differently to increases (ON) and decreases (OFF) of light intensity. Some terminals send an excitatory signal to their postsynaptic partners in response to both polarities, whereas others signal the ON or OFF phase only. We showed that the expression of hyperpolarisation-activated and cyclic nucleotide-gated (HCN) channels and inhibition provided through glycinergic ACs endow synapses with this formerly unknown property.

This novel ON-OFF pathway through individual BCs could only be assessed with the glutamate sensor iGluSnFR. Previous investigations into the physiology of BCs by electrophysiology (Asari & Meister, 2012) or calcium imaging (chapter 3, Fig. 3.9, page 53) failed to give a direct insight into this property.

6.1.2 The potential of future investigations employing genetically encoded sensors

One route of possible future investigations could be to assess which voltage-gated calcium channels underlie the rebound polarisations. Application of T- or L-type specific calcium channel blockers not only might reveal which channel type is involved but also deliver explanations as to why calcium sensors fail in detecting the rebound excitation. For example, T-type channels activate at small membrane depolarisations and comprise a fast voltage-dependent inactivation and small single-channel conductance (Huguenard, 1996; Simms & Zamponi, 2014). If these channels are involved in promoting the rebound depolarisations, the calcium influx might be too fast or too small to be sensed by calcium reporters.

Improved versions of calcium sensors that possess faster kinetics and a higher sensitivity towards low calcium concentrations might enable us to monitor rebound depolarisations at the synaptic terminals of BCs (Dana et al., 2019; Zhang et al., 2020). The ideal system would combine red fluorescence-based calcium sensor with the green fluorescence-based glutamate sensor. There is a continuous effort of scientists to develop reporters of neuronal transmission that operate at different spectral ranges in order to be able to relate presynaptic calcium dynamics to glutamate release (Marvin et al., 2018).

Similar efforts direct at developing sensors that report changes in membrane voltage (Platisa et al., 2017; Villette et al., 2019). These sensors bear the potential to bring new insights into the physiology of neurons. We tested the voltage sensor Asap2s (Yang et al., 2016) by transiently driving expression in BCs via the Gal4/UAS system. Unfortunately, expression levels were too low in order to visualize individual neurons under two-photon excitation. Meanwhile, improved versions of this reporter have become available (Villette et al., 2019) and already proven useful in assessing voltage changes in HCs of zebrafish (Yoshimatsu et al., 2020). However, we will have to test if sufficient expression levels can be reached in BCs. Provided that this reporter can be driven strongly in BCs it would be an asset to corroborate our findings in the decomposition of ON and OFF signals through BCs by providing insights into changes of local membrane potentials of individual synapses during changes of light intensity. Hypothetically we would expect to visualize the voltage sags during prolonged phases of inhibition and the rebound depolarisation after the release from inhibition given that the reporters resolution in time is sufficient to capture these events.

6.2 The dissection of retinal circuits by pharmacological means

6.2.1 The discrepancy of used drug concentration with published data

To unravel and investigate the circuits that generate ON and OFF signals in individual BCs and turn their terminals selective for oriented stimuli, we injected drugs into the vitreous chamber of the eye as described in the methods chapter (chapter 2, page 36). We prepared a stock solution for each drug based on IC50/EC50 values described in published data whilst taking the drug’s dilution

factor of 1:10 into account. However, this approach did not change the neuron's response profile after injection compared to the control condition in all experiments. A gradual increase of the stock solution's concentration until we observed a change led us to use concentrations that showed a considerable discrepancy between our and published values. For example, 50 µM L-AP4 reversibly hyperpolarised ON BCs and blocked their response to light as assessed by intracellular recordings in an eyecup preparation of the dogfish (Shiells et al., 1981). However, we used a hundred-fold excess of L-AP4 (5 mM) to block the ON responses in BCs. To monitor the retina's health status, we simultaneously recorded OFF cells to show that the loss of ON and OFF responses in individual BCs is due to the specific effect of the drug and not due to damage of the tissue (chapter 4, Fig. 4.11, page 74). Furthermore, we occasionally observed a recovery of the cell to the control condition within a few minutes (data not shown). Similarly, the HCN-specific blocker ZD7288 blocked the hyperpolarizing current I_h of the afferent neurons of the zebrafish's lateral line when bath applied to the whole fish at a concentration of 1 mM (Trapani & Nicolson, 2011). We used a ten-fold higher concentration of ZD7288 to block OFF rebound responses in ON BCs. However, whilst the OFF responses were entirely abolished in distal and reduced in proximal terminals, the intrinsic ON responses were maintained in a similar range as in the control condition, demonstrating that the drug has a specific effect (chapter 4, Fig. 4.3 and 4.4, pages 64 and 65)

What might be the reason for the discrepancy between the concentrations in published and our data? One possibility might be that the volume of the injection bolus into the zebrafish eye might differ from the bolus we inject into the air when we assess parameters like the width of the needle opening and injection pressure before drug application. For example, the higher pressure of the vitreous chamber, as opposed to the air pressure, might reduce the volume of the injection bolus. Furthermore, the retinal layers are perfused by choroidal vessels, retinal arteries and veins, which might contribute to a dilution or clearance of the injected drug over time as described above, where the effect of L-AP4 was abolished within a time window of a few minutes.

6.2.2 GABAergic versus glycinergic inhibition

We showed that only glycinergic and not GABAergic transmission inhibits terminals of BCs that segregate ON and OFF signals (chapter 4, Fig. 4.6 and 4.7, page 68 and 69, respectively). This finding not only is of interest because the release of glycine is attributed to small- and narrow-field ACs only but also shows that glycinergic transmission can drive very distinct functions by directly modulating the output of BCs. In most studies, glycinergic inhibition has been shown to drive more broad functions by regulating the overall gain of GABAergic ACs. For instance, a study investigating the functional diversity of BCs in mice demonstrated that blocking glycinergic transmission results in a reduction of glutamate release at the output of BCs (Franke et al., 2017). Likewise, a recent study of BCs in zebrafish demonstrated the sustained OFF channel is generated through GABAergic crossover inhibition from the ON pathway, whereas the level of crossover inhibition is controlled by lateral inhibition of GABAergic ACs through glycinergic ACs (Rosa et al., 2016).

Our investigation into the emergence of orientation-selectivity within the retina revealed that ~25% of BC terminals are sensitive to the orientation of stimuli with a strong preference for vertically oriented bars (chapter 5, Fig. 5.1 - 5.3, pages 86 - 88). Moreover, we showed that lateral antagonism through ACs lies at the basis of this feature-extracting mechanism (chapter 5, Fig. 5.5, page 91). However, in contrast to our experiments in which we analyzed the decomposition of ON and OFF signals at the outputs of individual BCs, we did not distinguish between GABAergic and glycinergic ACs. We applied a mix of GABAzine and strychnine to the retina to block both modes of inhibition. However, even though GABAergic asymmetric inhibition is generally thought to establish direction- and orientation-selective responses (Antinucci & Hindges, 2018; Borst & Euler, 2011), it might be worthwhile to test the effect of glycine only.

6.3 Comparative studies of visual systems across species

An investigation into glycinergic transmission in the context of direction- and orientation selectivity as discussed above has the potential to reveal species-specific differences. Our observation that intrinsic ON cells can signal excitatory OFF responses might relate to this question because in contrast OFF BCs in mice

often send and excitatory signal in response to the onset of light, whereas only a few ON cells increase their release of glutamate to the offset (Franke et al., 2017). The zebrafish retina comprises four spectrally distinct cones. Mice possess two variants only. A comparison of BC types and their morphologies (chapter 1, Fig. 1.2, page 4) show that this increased diversity continues downstream the visual pathway. These differences in cell types and the demand to adapt neural circuits to habitats mice and fish live in - aquatic vs terrestrial- might explain the opposing response profiles of BCs within these two species.

Moreover, we showed in chapter 4 that the zebrafish genome comprises six different HCN genes (chapter 4, Table 4.1, page 66) out of which five are transcribed in the retina (chapter 4, Fig. 4.4, page 65) whereas mammals like mice only contain four variants. Two whole-genome duplication events occurred in the common ancestor of vertebrates. Teleost fish like zebrafish underwent a third teleost-specific gene duplication (Amores et al., 2011; Hoegg et al., 2004). Gene-duplication events during the evolution of species have provided genetic "raw material" to diversify functions and properties. Whether the increased variety of HCN genes in zebrafish relates to an increase of HCN channel functions in this model system will be subject to future investigations. For this purpose, we have collected cDNA from larval zebrafish and amplified sequences specific to each gene variant. We cloned these sequences into plasmids which will allow us to synthesise anti-sense probes for future expression analysis by *in situ* hybridisation. Another standard route to investigate expression patterns is the use of antibodies, but unfortunately, no zebrafish specific antibodies targeting the different variants of HCN genes are commercially available. Whether the *in situ* staining's resolution will prove sufficient to resolve gene-specific expression patterns amongst retinal cell types remains uncertain. A comparative approach of visual systems across species will give us new insights into the specialisation of neural circuits (Baden & Osorio, 2019; Baden, 2020).

6.4 Towards a refined understanding of neural circuits

The commonly lax division of ACs into GABAergic and glycinergic cells has been sufficient to unravel fundamental neural coding principles in the past. However, a more refined classification of these cells is required to discover and explore

"narrow" AC subsets' functions. For instance, a transcriptome analysis aiming to identify enriched transcripts in different cell types of the retina found an abundance of *Frmd7 (FERM domain containing 7)* transcripts in starburst ACs (Siegert et al., 2012). *Frmd7* is implicated in the eye motion disease, idiopathic congenital nystagmus (Tarpey et al., 2006). Individuals that lack a functional *FRMD7* allele perform involuntary horizontal eye movements and are deficient of the optokinetic reflex along the same axis. The eye movements and the optokinetic reflex along the vertical axis is unaffected (Thomas et al., 2008). A recent study in mice showed how *FRMD7* expression in starburst ACs is essential in establishing asymmetric inhibitory inputs into directions-selective GCs which is essential for detecting movement along the horizontal axis.

Similarly, a recent study in zebrafish demonstrated that the expression of the cell-adhesion molecule Teneurin-3 in GABAergic ACs is vital in establishing orientation-selective responses in retinal GCs (Antinucci et al., 2016). Teneurin-3 knock-out mutants show a decrease in orientation-selective responses of GCs. However, the loss of selectivity is not equally distributed as the population tuned to vertically oriented stimuli is least impaired. These two examples in the mice and zebrafish model show that even though GABAergic ACs are essential in generating orientation- and direction-selective responses in the retina more subtle functions can only be revealed by progressive profiling of AC subsets. Whether it will be possible to obtain a unique “barcode” for each cell type is unpredictable but similar efforts to identify inhibitory neurons of the cortex genetically have been successful (Ascoli et al., 2008; Tremblay et al., 2016).

However, despite all cell type profiling (Siegert et al., 2012) and mapping of the connectome (Denk & Horstmann, 2004; Helmstaedter et al., 2013; Sümbül et al., 2014), the networks' plasticity might still impede a complete comprehension of the visual systems' circuitries. For instance, we demonstrated that ON BCs' synapses can switch their excitatory response profile to the OFF polarity. This "polarity-switch" is enabled by the neuromodulator dopamine (chapter 4, Fig. 4.8, page 71).

These findings show that even with a complete understanding of a cells' synaptic connections and molecular composition, the influence of extrinsic factors might disguise a cells' or even whole networks' functional properties.

6.5 Computations in the synaptic compartment of bipolar cells

Beyond separating the visual image into parallel channels, BCs perform important modifications of signals that are relayed from the outer to the inner retina. While some fundamental feature-extracting pathways emerge at the input of the dendritic tree, transformations at the BC terminal are a vital determinant of retinal computation.

First, the synaptic ribbon endows the BC terminal with a release-machinery that allows for the translation of graded changes in membrane potential into a continuous mode of glutamate release (Lagnado & Schmitz, 2015). This facilitates the demand of encoding light intensities over a broad range (Pouli, 2010; Fred Rieke & Rudd, 2009) and also to signal fast changes such as the on- and offset of light (Neves & Lagnado, 1999; Snellman et al., 2011). Although signalling at BC terminals primarily comprises a graded mode, recent studies showed that a fast mode of transmission in the form of a spike can be observed too (Baden et al., 2013; Dreosti et al., 2011) and that this large change in voltage drives vesicle fusion at higher rates than graded signals (Baden et al., 2011; Palmer, 2006).

Second, BC synapses can show activity-dependent depression as a function of intrinsic vesicle pool depletion and inhibition through fast-acting release of neurotransmitter from ACs constituting a form of short-term plasticity (Burrone & Lagnado, 2000; Nikolaev et al., 2013; Singer & Diamond, 2006). However, the release and diffusion of neuromodulators provides a form of plasticity operational on a larger timescale and in correlation to the organisms' internal state. Our finding that ON and OFF signalling through individual BCs is modulated through dopamine emphasises this notion further (chapter 4, Fig. 4.8 and 4.9, pages 71 and 72, respectively).

Finally, important nonlinearities arise through the interaction with ACs. The transmission of visual signals from the photoreceptors' input up to the soma of BCs is roughly linear (Baccus & Meister, 2002; Schwartz & Rieke, 2011). However, the effect of inhibitory neurotransmitters and neuromodulators lead to substantial nonlinear transformations (Asari & Meister, 2012; Esposti et al., 2013; Franke et al., 2017; Rosa et al., 2016). Our findings that lateral inhibition through ACs renders the receptive field of BC terminals orientation-selective (chapter 5,

Fig. 5.5, page 91) and that the expression of HCN channels (chapter 4, Fig. 4.3 and 4.4, pages 64 and 65, respectively) combined with glycinergic inhibition (chapter 4, Fig. 4.6, page 68) enables the signalling of OFF signals in ON BCs provides further examples on the substantial transformations occurring at the BC's output.

References

Adam-Vizi, V. (1992). External Ca2+-Independent Release of Neurotransmitters. *Journal of Neurochemistry*, *58*(2), 395–405. https://doi.org/10.1111/J.1471-4159.1992.TB09736.X

Agapite, J., Albou, L. P., Aleksander, S., Argasinska, J., Arnaboldi, V., Attrill, H., Bello, S. M., Blake, J. A., Blodgett, O., Bradford, Y. M., Bult, C. J., Cain, S., Calvi, B. R., Carbon, S., Chan, J., Chen, W. J., Cherry, J. M., Cho, J., Christie, K. R., … Yook, K. (2020). Alliance of Genome Resources Portal: Unified model organism research platform. *Nucleic Acids Research*. https://doi.org/10.1093/nar/gkz813

Ahrens, M. B., Li, J. M., Orger, M. B., Robson, D. N., Schier, A. F., Engert, F., & Portugues, R. (2012). Brain-wide neuronal dynamics during motor adaptation in zebrafish. *Nature*. https://doi.org/10.1038/nature11057

Akitake, C. M., Macurak, M., Halpern, M. E., & Goll, M. G. (2011). *Transgenerational analysis of transcriptional silencing in zebrafish*. *352*(2), 191–201. https://doi.org/10.1016/j.ydbio.2011.01.002

Alviña, K., Ellis-Davies, G., & Khodakhah, K. (2009). T-type calcium channels mediate rebound firing in intact deep cerebellar neurons. *Neuroscience*, *158*(2), 635–641. https://doi.org/10.1016/j.neuroscience.2008.09.052

Amores, A., Catchen, J., Ferrara, A., Fontenot, Q., & Postlethwait, J. H. (2011). Genome evolution and meiotic maps by massively parallel DNA sequencing: Spotted gar, an outgroup for the teleost genome duplication. *Genetics*. https://doi.org/10.1534/genetics.111.127324

Antinucci, P., & Hindges, R. (2018). Orientation-selective retinal circuits in vertebrates. In *Frontiers in Neural Circuits*. https://doi.org/10.3389/fncir.2018.00011

Antinucci, P., Suleyman, O., Monfries, C., & Hindges, R. (2016). Neural Mechanisms Generating Orientation Selectivity in the Retina. *Current Biology*, *26*(14), 1802–1815. https://doi.org/10.1016/j.cub.2016.05.035

Arrenberg, A. B., Del Bene, F., & Baier, H. (2009). Optical control of zebrafish behavior with halorhodopsin. *Proceedings of the National Academy of Sciences of the United States of America*. https://doi.org/10.1073/pnas.0906252106

Asari, H., & Meister, M. (2012). Divergence of visual channels in the inner retina. *Nature Neuroscience*, *15*(11), 1581–1589. https://doi.org/10.1038/nn.3241

Ascoli, G. A., Alonso-Nanclares, L., Anderson, S. A., Barrionuevo, G., Benavides-Piccione, R., Burkhalter, A., Buzsáki, G., Cauli, B., DeFelipe, J., Fairén, A., Feldmeyer, D., Fishell, G., Fregnac, Y., Freund, T. F., Gardner, D., Gardner, E. P., Goldberg, J. H., Helmstaedter, M., Hestrin, S., … Yuste, R. (2008). Petilla terminology: Nomenclature of features of GABAergic interneurons of the cerebral cortex. In *Nature Reviews Neuroscience*. https://doi.org/10.1038/nrn2402

Ashmore, J. F., & Copenhagen, D. R. (1983). An analysis of transmission from cones to hyperpolarizing bipolar cells in the retina of the turtle. *The Journal of Physiology*. https://doi.org/10.1113/jphysiol.1983.sp014781

Attneave, F. (1954). Some informational aspects of visual perception. *Psychological Review*. https://doi.org/10.1037/h0054663

Attwell, D., Barbour, B., & Szatkowskp, M. (1993). Nonvesicular Release of

Neurotransmitter. In *Neuron* (Vol. 11).
Baccus, S. A., & Meister, M. (2002). Fast and slow contrast adaptation in retinal circuitry. *Neuron*. https://doi.org/10.1016/S0896-6273(02)01050-4
Baden, Berens, P., Franke, K., Román Rosón, M., Bethge, M., & Euler, T. (2016). The functional diversity of retinal ganglion cells in the mouse. *Nature*, *529*(7586), 345–350. https://doi.org/10.1038/nature16468
Baden, Esposti, F., Nikolaev, A., & Lagnado, L. (2011). Spikes in retinal bipolar cells phase-lock to visual stimuli with millisecond precision. *Current Biology*. https://doi.org/10.1016/j.cub.2011.09.042
Baden, Nikolaev, A., Esposti, F., Dreosti, E., Odermatt, B., & Lagnado, L. (2014). *A Synaptic Mechanism for Temporal Filtering of Visual Signals*. *12*(10), e1001972. https://doi.org/10.1371/journal.pbio.1001972
Baden, & Osorio, D. (2019). The Retinal Basis of Vertebrate Color Vision. *Annual Review of Vision Science*, *5*(1), 177–200. https://doi.org/10.1146/annurev-vision-091718-014926
Baden, T. (2020). Vertebrate vision: Lessons from non-model species. In *Seminars in Cell and Developmental Biology*. https://doi.org/10.1016/j.semcdb.2020.05.028
Baden, T., Euler, T., Weckström, M., & Lagnado, L. (2013). Spikes and ribbon synapses in early vision. *Trends in Neurosciences*, *36*(8), 480–488. https://doi.org/10.1016/j.tins.2013.04.006
Baier, H., & Wullimann, M. F. (2021). Anatomy and function of retinorecipient arborization fields in zebrafish. *Journal of Comparative Neurology*, *529*(15), 3454–3476. https://doi.org/10.1002/CNE.25204
Balasubramanian, V., & Sterling, P. (2009). Receptive fields and functional architecture in the retina. *The Journal of Physiology*, *587*(Pt 12), 2753. https://doi.org/10.1113/JPHYSIOL.2009.170704
Barlow, H. B. (1953a). Summation and inhibition in the frog's retina. *The Journal of Physiology*, *119*(1), 69–88. https://doi.org/10.1113/jphysiol.1953.sp004829
Barlow, H. B. (1953b). Summation and inhibition in the frog's retina. *The Journal of Physiology*. https://doi.org/10.1113/jphysiol.1953.sp004829
Barlow, H. B. (2013). Possible Principles Underlying the Transformations of Sensory Messages. In *Sensory Communication*. https://doi.org/10.7551/mitpress/9780262518420.003.0013
Barlow, H. B., Hill, R. M., & Levick, W. R. (1964). Retinal ganglion cells responding selectively to direction and speed of image motion in the rabbit. *The Journal of Physiology*. https://doi.org/10.1113/jphysiol.1964.sp007463
Barlow, H. B., & Levick, W. R. (1965). The mechanism of directionally selective units in rabbit's retina. *The Journal of Physiology*. https://doi.org/10.1113/jphysiol.1965.sp007638
Bastos, A. M., Usrey, W. M., Adams, R. A., Mangun, G. R., Fries, P., & Friston, K. J. (2012). Canonical Microcircuits for Predictive Coding. In *Neuron*. https://doi.org/10.1016/j.neuron.2012.10.038
Baylor, D. A., Nunn, B. J., & Schnapf, J. L. (1984). The photocurrent, noise and spectral sensitivity of rods of the monkey Macaca fascicularis. *The Journal of Physiology*. https://doi.org/10.1113/jphysiol.1984.sp015518
Bemme, S., Weick, M., & Gollisch, T. (2017). Differential Effects of HCN Channel Block on On and Off Pathways in the Retina as a Potential Cause for Medication-Induced Phosphene Perception. *Investigative Opthalmology*

& Visual Science, *58*(11), 4754. https://doi.org/10.1167/iovs.17-21572
Berens, P., & Euler, T. (2017). Neuronal Diversity In The Retina. *E-Neuroforum*, *23*(2). https://doi.org/10.1515/nf-2016-a055
Bernath, S. (1992). Calcium-independent release of amino acid neurotransmitters: Fact or artifact? *Progress in Neurobiology*, *38*(1), 57–91. https://doi.org/10.1016/0301-0082(92)90035-D
Biel, M., Wahl-Schott, C., Michalakis, S., & Zong, X. (2009). Hyperpolarization-Activated Cation Channels: From Genes to Function. *Physiological Reviews*, *89*(3), 847–885. https://doi.org/10.1152/physrev.00029.2008
Bloomfield, S. ., & Dacheux, R. F. (2001). *Rod Vision: Pathways and Processing in the Mammalian Retina*. *20*(3), 351–384. https://doi.org/10.1016/s1350-9462(00)00031-8
Bloomfield, S. A. (1994). Orientation-sensitive amacrine and ganglion cells in the rabbit retina. *Journal of Neurophysiology*. https://doi.org/10.1152/jn.1994.71.5.1672
Boch, J. (2011). TALEs of genome targeting. In *Nature Biotechnology*. https://doi.org/10.1038/nbt.1767
Borghuis, B. G., Marvin, J. S., Looger, L. L., & Demb, J. B. (2013). Two-Photon Imaging of Nonlinear Glutamate Release Dynamics at Bipolar Cell Synapses in the Mouse Retina. *Journal of Neuroscience*, *33*(27), 10972–10985. https://doi.org/10.1523/jneurosci.1241-13.2013
Borst, A., & Euler, T. (2011). Seeing Things in Motion: Models, Circuits, and Mechanisms. *Neuron*, *71*(6), 974–994. https://doi.org/10.1016/j.neuron.2011.08.031
Brainard, D. H. (1997). The Psychophysics Toolbox. *Spatial Vision*. https://doi.org/10.1163/156856897X00357
Brand, A. H., & Perrimon, N. (1993). Targeted gene expression as a means of altering cell fates and generating dominant phenotypes - PubMed. *Development*, *118*(2), 401–415. https://pubmed.ncbi.nlm.nih.gov/8223268/
Briggman, K. L., Helmstaedter, M., & Denk, W. (2011). Wiring specificity in the direction-selectivity circuit of the retina. *Nature*. https://doi.org/10.1038/nature09818
Brivanlou, I. H., Warland, D. K., & Meister, M. (1998). *Mechanisms of Concerted Firing among Retinal Ganglion Cells*. *20*(3), 527–539. https://doi.org/10.1016/s0896-6273(00)80992-7
Brown, H., Difrancesco, D., & Noble, S. (1979). How does adrenaline accelerate the heart? *Nature*. https://doi.org/10.1038/280235a0
Brown, H. F., Giles, W., & Noble, S. J. (1977). Membrane currents underlying activity in frog sinus venosus. *The Journal of Physiology*. https://doi.org/10.1113/jphysiol.1977.sp012026
Burkhardt, D. A. (2011). Contrast processing by ON and OFF bipolar cells. *Visual Neuroscience*, *28*(1), 69–75. https://doi.org/10.1017/S0952523810000313
Burkhardt, D. A., Fahey, P. K., & Sikora, M. A. (2006). Natural images and contrast encoding in bipolar cells in the retina of the land- and aquatic-phase tiger salamander. *Visual Neuroscience*, *23*(1), 35–47. https://doi.org/10.1017/S0952523806231043
Burrone, J., & Lagnado, L. (2000). Synaptic depression and the kinetics of exocytosis in retinal bipolar cells. *Journal of Neuroscience*. https://doi.org/10.1523/jneurosci.20-02-00568.2000

Calkins, D. J., Schein, S. J., Tsukamoto, Y., & Sterling, P. (1994). M and L cones in macaque fovea connect to midget ganglion cells by different numbers of excitatory synapses. *Nature*. https://doi.org/10.1038/371070a0

Chapot, C. A., Euler, T., & Schubert, T. (2017). How do horizontal cells 'talk' to cone photoreceptors? Different levels of complexity at the cone-horizontal cell synapse. *The Journal of Physiology*, *595*(16), 5495–5506. https://doi.org/10.1113/jp274177

Chen, T.-W. W., Wardill, T. J., Sun, Y., Pulver, S. R., Renninger, S. L., Baohan, A., Schreiter, E. R., Kerr, R. A., Orger, M. B., Jayaraman, V., Looger, L. L., Svoboda, K., & Kim, D. S. (2013). Ultrasensitive fluorescent proteins for imaging neuronal activity. *Nature*, *499*(7458), 295–300. https://doi.org/10.1038/nature12354

Cheong, S. K., Tailby, C., Solomon, S. G., & Martin, P. R. (2013). Cortical-like receptive fields in the lateral geniculate nucleus of marmoset monkeys. *Journal of Neuroscience*. https://doi.org/10.1523/JNEUROSCI.5208-12.2013

Connaughton, V. P. (2011). Bipolar cells in the zebrafish retina. *Visual Neuroscience*, *28*(1), 77–93. https://doi.org/10.1017/s0952523810000295

Dana, H., Sun, Y., Mohar, B., Hulse, B. K., Kerlin, A. M., Hasseman, J. P., Tsegaye, G., Tsang, A., Wong, A., Patel, R., Macklin, J. J., Chen, Y., Konnerth, A., Jayaraman, V., Looger, L. L., Schreiter, E. R., Svoboda, K., & Kim, D. S. (2019). High-performance calcium sensors for imaging activity in neuronal populations and microcompartments. *Nature Methods*. https://doi.org/10.1038/s41592-019-0435-6

Denk, Strickler, J., & Webb, W. (1990). Two-photon laser scanning fluorescence microscopy. *Science*, *248*(4951), 73–76. https://doi.org/10.1126/science.2321027

Denk, W., & Horstmann, H. (2004). Serial block-face scanning electron microscopy to reconstruct three-dimensional tissue nanostructure. *PLoS Biology*. https://doi.org/10.1371/journal.pbio.0020329

Devries, S. H. (2000). Bipolar Cells Use Kainate and AMPA Receptors to Filter Visual Information into Separate Channels. *Neuron*, *28*(3), 847–856. https://doi.org/10.1016/s0896-6273(00)00158-6

Diamond, J. S. (2017). Inhibitory Interneurons in the Retina: Types, Circuitry, and Function. *Annual Review of Vision Science*, *3*(1), 1–24. https://doi.org/10.1146/annurev-vision-102016-061345

DiFrancesco, D. (1981a). A new interpretation of the pace-maker current in calf Purkinje fibres. *The Journal of Physiology*. https://doi.org/10.1113/jphysiol.1981.sp013713

DiFrancesco, D. (1981b). A study of the ionic nature of the pace-maker current in calf Purkinje fibres. *The Journal of Physiology*. https://doi.org/10.1113/jphysiol.1981.sp013714

Ding, H., Smith, R. G., Poleg-Polsky, A., Diamond, J. S., & Briggman, K. L. (2016). Species-specific wiring for direction selectivity in the mammalian retina. *Nature*, *535*(7610), 105–110. https://doi.org/10.1038/nature18609

Distel, M., Wullimann, M. F., & Koster, R. W. (2009). Optimized Gal4 genetics for permanent gene expression mapping in zebrafish. *Proceedings of the National Academy of Sciences*, *106*(32), 13365–13370. https://doi.org/10.1073/pnas.0903060106

Dong, C. J., & Werblin, F. S. (1998). Temporal contrast enhancement via

GABAC feedback at bipolar terminals in the tiger salamander retina. *Journal of Neurophysiology*, *79*(4), 2171–2180. https://doi.org/10.1152/JN.1998.79.4.2171

Dorostkar, M. M., Dreosti, E., Odermatt, B., & Lagnado, L. (2010). Computational processing of optical measurements of neuronal and synaptic activity in networks. *Journal of Neuroscience Methods*, *188*(1), 141–150. https://doi.org/10.1016/j.jneumeth.2010.01.033

Dowling, J. E., & Boycott, B. B. (1966). Organization of the primate retina: electron microscopy. *Proceedings of the Royal Society of London. Series B. Biological Sciences*. https://doi.org/10.1098/rspb.1966.0086

Doyle, S. E., McIvor, W. E., & Menaker, M. (2002). Circadian rhythmicity in dopamine content of mammalian retina: Role of the photoreceptors. *Journal of Neurochemistry*. https://doi.org/10.1046/j.1471-4159.2002.01149.x

Dreosti, E., Esposti, F., Baden, T., & Lagnado, L. (2011). In vivo evidence that retinal bipolar cells generate spikes modulated by light. *Nature Neuroscience*, *14*(8), 951–952. https://doi.org/10.1038/nn.2841

Dreosti, E., Odermatt, B., Dorostkar, M. M., & Lagnado, L. (2009). A genetically encoded reporter of synaptic activity in vivo. *Nature Methods*, *6*(12), 883–889. https://doi.org/10.1038/nmeth.1399

Eggers, E. D., & Lukasiewicz, P. D. (2006). GABAA, GABAC and glycine receptor-mediated inhibition differentially affects light-evoked signalling from mouse retinal rod bipolar cells. *Journal of Physiology*. https://doi.org/10.1113/jphysiol.2005.103648

Erickson, T., & Nicolson, T. (2015). Identification of sensory hair-cell transcripts by thiouracil-tagging in zebrafish. *BMC Genomics*. https://doi.org/10.1186/s12864-015-2072-5

Esposti, F., Johnston, J., Rosa, J. M., Leung, K.-M., Lagnado, L., Juliana, Leung, K.-M., & Lagnado, L. (2013). Olfactory Stimulation Selectively Modulates the OFF Pathway in the Retina of Zebrafish. *Neuron*, *79*(1), 97–110. https://doi.org/10.1016/j.neuron.2013.05.001

Euler, T., Detwiler, P. B., & Denk, W. (2002). Directionally selective calcium signals in dendrites of starburst amacrine cells. *Nature*, *418*(6900), 845–852. https://doi.org/10.1038/nature00931

Euler, T., Haverkamp, S., Schubert, T., & Baden, T. (2014). Retinal bipolar cells: elementary building blocks of vision. *Nature Reviews Neuroscience*, *15*(8), 507–519. https://doi.org/10.1038/nrn3783

Euler, T., & Masland, R. H. (2000). Light-Evoked Responses of Bipolar Cells in a Mammalian Retina. *Journal of Neurophysiology*, *83*(4), 1817–1829. https://doi.org/10.1152/jn.2000.83.4.1817

Fain, G. L., Quandt, F. N., Bastian, B. L., & Gerschenfeld, H. M. (1978). Contribution of a caesium-sensitive conductance increase to the rod photoresponse. *Nature*. https://doi.org/10.1038/272467a0

Franke, K., Berens, P., Schubert, T., Bethge, M., Euler, T., & Baden, T. (2017). Inhibition decorrelates visual feature representations in the inner retina. *Nature*, *542*(7642), 439–444. https://doi.org/10.1038/nature21394

Freed, M. A., & Sterling, P. (1988). The ON-alpha ganglion cell of the cat retina and its presynaptic cell types. *Journal of Neuroscience*. https://doi.org/10.1523/jneurosci.08-07-02303.1988

Gaudry, Q., Hong, E. J., Kain, J., De Bivort, B. L., & Wilson, R. I. (2013).

Asymmetric neurotransmitter release enables rapid odour lateralization in Drosophila. *Nature*. https://doi.org/10.1038/nature11747

Gavrikov, K. E., Dmitriev, A. V., Keyser, K. T., & Mangel, S. C. (2003). Cation-chloride cotransporters mediate neural computation in the retina. *Proceedings of the National Academy of Sciences of the United States of America*. https://doi.org/10.1073/pnas.2637041100

Gavrikov, Nilson, J. E., Dmitriev, A. V, Zucker, C. L., & Mangel, S. C. (2006). *Dendritic compartmentalization of chloride cotransporters underlies directional responses of starburst amacrine cells in retina*. *103*(49), 18793–18798. https://doi.org/10.1073/pnas.0604551103

Gibson, D. G., Young, L., Chuang, R.-Y., Venter, J. C., Hutchison, C. A., & Smith, H. O. (2009). Enzymatic assembly of DNA molecules up to several hundred kilobases. *Nature Methods*, *6*(5), 343–345. https://doi.org/10.1038/nmeth.1318

Girman, S. V., Sauvé, Y., & Lund, R. D. (1999). Receptive field properties of single neurons in rat primary visual cortex. *Journal of Neurophysiology*. https://doi.org/10.1152/jn.1999.82.1.301

Gjorgjieva, J., Sompolinsky, H., & Meister, M. (2014). Benefits of Pathway Splitting in Sensory Coding. *Journal of Neuroscience*, *34*(36), 12127–12144. https://doi.org/10.1523/jneurosci.1032-14.2014

Gollisch, T., & Meister, M. (2010). Eye Smarter than Scientists Believed: Neural Computations in Circuits of the Retina. *Neuron*, *65*(2), 150–164. https://doi.org/10.1016/j.neuron.2009.12.009

Göppert-Mayer, M. (1931). Über Elementarakte mit zwei Quantensprüngen. *Annalen Der Physik*, *401*(3), 273–294. https://doi.org/10.1002/andp.19314010303

Guerrero, G., Reiff, D. F., Agarwal, G., Ball, R. W., Borst, A., Goodman, C. S., & Isacoff, E. Y. (2005). Heterogeneity in synaptic transmission along a Drosophila larval motor axon. *Nature Neuroscience*, *8*(9), 1188–1196. https://doi.org/10.1038/nn1526

Halliwell, J. V., & Adams, P. R. (1982). Voltage-clamp analysis of muscarinic excitation in hippocampal neurons. *Brain Research*. https://doi.org/10.1016/0006-8993(82)90954-4

Hartline, H. K. (1935). THE DISCHARGE OF NERVE IMPULSES FROM THE SINGLE VISUAL SENSE CELL. *Cold Spring Harbor Symposia on Quantitative Biology*. https://doi.org/10.1101/sqb.1935.003.01.028

Hartline, H. K. (1938). The response of single optic nerve fibers of the vertebrate eye to illumination of the retina. *Am. J. Physiol.* , *121*, 400–415.

Hartline, H. K. (1940). The receptive fields of optic nerve fibers. *American Journal of Physiology*, *130*, 690–699.

Heidelberger, R., Heinemann, C., Neher, E., & Matthews, G. (1994). Calcium dependence of the rate of exocytosis in a synaptic terminal. *Nature*. https://doi.org/10.1038/371513a0

Hellmer, C. B., Zhou, Y., Fyk-Kolodziej, B., Hu, Z., & Ichinose, T. (2016). Morphological and physiological analysis of type-5 and other bipolar cells in the Mouse Retina. *Neuroscience*, *315*, 246. https://doi.org/10.1016/J.NEUROSCIENCE.2015.12.016

Helmstaedter, M., Briggman, K. L., Turaga, S. C., Jain, V., Seung, H. S., & Denk, W. (2013). Connectomic reconstruction of the inner plexiform layer in the mouse retina. *Nature*, *500*(7461), 168–174.

https://doi.org/10.1038/nature12346
Hestrin, S., & Korenbrot, J. I. (1987). Effects of cyclic GMP on the kinetics of the photocurrent in rods and in detached rod outer segments. *Journal of General Physiology*. https://doi.org/10.1085/jgp.90.4.527
Hoegg, S., Brinkmann, H., Taylor, J. S., & Meyer, A. (2004). Phylogenetic timing of the fish-specific genome duplication correlates with the diversification of teleost fish. *Journal of Molecular Evolution*. https://doi.org/10.1007/s00239-004-2613-z
Hosoya, T., Baccus, S. A., & Meister, M. (2005). Dynamic predictive coding by the retina. *Nature*. https://doi.org/10.1038/nature03689
Hu, H.-J., & Pan, Z.-H. (2002). *Differential expression of K+ currents in mammalian retinal bipolar cells*. *19*(02). https://doi.org/10.1017/s0952523802191140
Hubel, D. H., & Wiesel, T. N. (1959). Receptive fields of single neurones in the cat's striate cortex. *The Journal of Physiology*. https://doi.org/10.1113/jphysiol.1959.sp006308
Hubel, D. H., & Wiesel, T. N. (1961). Integrative action in the cat's lateral geniculate body. *The Journal of Physiology*. https://doi.org/10.1113/jphysiol.1961.sp006635
Hubel, D. H., & Wiesel, T. N. (1962). Receptive fields, binocular interaction and functional architecture in the cat's visual cortex. *The Journal of Physiology*. https://doi.org/10.1113/jphysiol.1962.sp006837
Hubel, D. H., & Wiesel, T. N. (1968). Receptive fields and functional architecture of monkey striate cortex. *The Journal of Physiology*. https://doi.org/10.1113/jphysiol.1968.sp008455
Huguenard, J. R. (1996). Low-threshold calcium currents in central nervous system neurons. In *Annual Review of Physiology*. https://doi.org/10.1146/annurev.ph.58.030196.001553
Humphrey, A. L., Skeen, L. C., & Norton, T. T. (1980). Topographic organization of the orientation column system in the striate cortex of the tree shrew (Tupaia glis). II. Deoxyglucose mapping. *Journal of Comparative Neurology*. https://doi.org/10.1002/cne.901920312
Hunter, P. R., Lowe, A. S., Thompson, I. D., & Meyer, M. P. (2013). Emergent Properties of the Optic Tectum Revealed by Population Analysis of Direction and Orientation Selectivity. *Journal of Neuroscience*, *33*(35), 13940–13945. https://doi.org/10.1523/jneurosci.1493-13.2013
Iuvone, P. M., Galli, C. L., Garrison-Gund, C. K., & Neff, N. H. (1978). Light stimulates tyrosine hydroxylase activity and dopamine synthesis in retinal amacrine neurons. *Science*. https://doi.org/10.1126/science.30997
Jackson, C. R., Ruan, G. X., Aseem, F., Abey, J., Gamble, K., Stanwood, G., Palmiter, R. D., Iuvone, P. M., & McMahon, D. G. (2012). Retinal Dopamine Mediates Multiple Dimensions of Light-Adapted Vision. *Journal of Neuroscience*, *32*(27), 9359–9368. https://doi.org/10.1523/jneurosci.0711-12.2012
James, B., Darnet, L., Moya-Díaz, J., Seibel, S.-H., & Lagnado, L. (2019). An amplitude code transmits information at a visual synapse. *Nature Neuroscience*, *22*(7), 1140–1147. https://doi.org/10.1038/s41593-019-0403-6
Johnston, J., Ding, H., Seibel, S. H., Esposti, F., & Lagnado, L. (2014). Rapid mapping of visual receptive fields by filtered back projection: application to

multi-neuronal electrophysiology and imaging. *The Journal of Physiology*, *592*(22), 4839–4854. https://doi.org/10.1113/jphysiol.2014.276642

Johnston, J., Seibel, S.-H., Darnet, L. S. A., Renninger, S., Orger, M., & Lagnado, L. (2019). A Retinal Circuit Generating a Dynamic Predictive Code for Oriented Features. *Neuron*, *102*(6), 1211-1222.e3. https://doi.org/10.1016/j.neuron.2019.04.002

Jusuf, P. R., & Harris, W. A. (2009). Ptf1a is expressed transiently in all types of amacrine cells in the embryonic zebrafish retina. *Neural Development*, *4*(1), 34. https://doi.org/10.1186/1749-8104-4-34

Juusola, M., French, A. S., Uusitalo, R. O., & Weckström, M. (1996). Information processing by graded-potential transmission through tonically active synapses. *Trends in Neurosciences*, *19*(7), 292–297. https://doi.org/10.1016/s0166-2236(96)10028-x

Kaneko, A. (1970). Physiological and morphological identification of horizontal, bipolar and amacrine cells in goldfish retina. *The Journal of Physiology*, *207*(3), 623–633. https://doi.org/10.1113/JPHYSIOL.1970.SP009084

Kastner, D. B., & Baccus, S. A. (2013). Insights from the retina into the diverse and general computations of adaptation, detection, and prediction. In *Current Opinion in Neurobiology*. https://doi.org/10.1016/j.conb.2013.11.012

Kim, J. S., Greene, M. J., Zlateski, A., Lee, K., Richardson, M., Turaga, S. C., Purcaro, M., Balkam, M., Robinson, A., Behabadi, B. F., Campos, M., Denk, W., & Seung, H. S. (2014). Space-time wiring specificity supports direction selectivity in the retina. *Nature*. https://doi.org/10.1038/nature13240

Knop, G. C., Seeliger, M. W., Thiel, F., Mataruga, A., Kaupp, U. B., Friedburg, C., Tanimoto, N., & Müller, F. (2008). Light responses in the mouse retina are prolonged upon targeted deletion of the HCN1 channel gene. *European Journal of Neuroscience*. https://doi.org/10.1111/j.1460-9568.2008.06512.x

Koike, C., Numata, T., Ueda, H., Mori, Y., & Furukawa, T. (2010). TRPM1: A vertebrate TRP channel responsible for retinal ON bipolar function. *Cell Calcium*, *48*(2–3), 95–101. https://doi.org/10.1016/j.ceca.2010.08.004

Kolb, H. (1995). Roles of Amacrine Cells. In *Webvision: The Organization of the Retina and Visual System*.

Kolb, H., Nelson, R., & Mariani, A. (1981). Amacrine cells, bipolar cells and ganglion cells of the cat retina: A Golgi study. *Vision Research*. https://doi.org/10.1016/0042-6989(81)90013-4

Kölsch, Y., Hahn, J., Sappington, A., Stemmer, M., Fernandes, A. M., Helmbrecht, T. O., Lele, S., Butrus, S., Laurell, E., Arnold-Ammer, I., Shekhar, K., Sanes, J. R., & Baier, H. (2021). Molecular classification of zebrafish retinal ganglion cells links genes to cell types to behavior. *Neuron*. https://doi.org/10.1016/j.neuron.2020.12.003

Kuffler, S. W. (1953). Discharge patterns and functional organization of mammalian retina. *Journal of Neurophysiology*. https://doi.org/10.1152/jn.1953.16.1.37

Lagnado, L., Gomis, A., & Job, C. (1996). Continuous Vesicle Cycling in the Synaptic Terminal of Retinal Bipolar Cells. *Neuron*, *17*(5), 957–967. https://doi.org/10.1016/S0896-6273(00)80226-3

Lagnado, L., & Schmitz, F. (2015). Ribbon Synapses and Visual Processing in the Retina. *Annual Review of Vision Science*, *1*(1), 235–262.

https://doi.org/10.1146/annurev-vision-082114-035709
Lee, S., Kim, K., & Zhou, Z. J. (2010). Role of ACh-GABA Cotransmission in Detecting Image Motion and Motion Direction. *Neuron*. https://doi.org/10.1016/j.neuron.2010.11.031
Levick, W. R. (1967). Receptive fields and trigger features of ganglion cells in the visual streak of the rabbit's retina. *The Journal of Physiology*. https://doi.org/10.1113/jphysiol.1967.sp008140
Li, L., & Dowling, J. E. (2000). Effects of Dopamine Depletion on Visual Sensitivity of Zebrafish. *The Journal of Neuroscience*, *20*(5), 1893–1903. https://doi.org/10.1523/jneurosci.20-05-01893.2000
Li, M., Liu, F., Jiang, H., Lee, T. S., & Tang, S. (2017). Long-Term Two-Photon Imaging in Awake Macaque Monkey. *Neuron*, *93*(5), 1049-1057.e3. https://doi.org/10.1016/j.neuron.2017.01.027
Lowe, A. S., Nikolaou, N., Hunter, P. R., Thompson, I. D., & Meyer, M. P. (2013). A Systems-Based Dissection of Retinal Inputs to the Zebrafish Tectum Reveals Different Rules for Different Functional Classes during Development. *Journal of Neuroscience*, *33*(35), 13946–13956. https://doi.org/10.1523/jneurosci.1866-13.2013
Ludwig, A., Zong, X., Jeglitsch, M., Hofmann, F., & Biel, M. (1998). A family of hyperpolarization-activated mammalian cation channels. *Nature*. https://doi.org/10.1038/31255
Ludwig, A., Zong, X., Stieber, J., Hullin, R., Hofmann, F., & Biel, M. (1999). Two pacemaker channels from human heart with profoundly different activation kinetics. *EMBO Journal*. https://doi.org/10.1093/emboj/18.9.2323
Maccaferri, G., Mangoni, M., Lazzari, A., & DiFrancesco, D. (1993). Properties of the hyperpolarization-activated current in rat hippocampal CA1 pyramidal cells. *Journal of Neurophysiology*. https://doi.org/10.1152/jn.1993.69.6.2129
Macneil, M. A., & Masland, R. H. (1998). Extreme Diversity among Amacrine Cells: Implications for Function. *Neuron*, *20*(5), 971–982. https://doi.org/10.1016/s0896-6273(00)80478-x
Manookin, M. B., Beaudoin, D. L., Ernst, Z. R., Flagel, L. J., & Demb, J. B. (2008). Disinhibition Combines with Excitation to Extend the Operating Range of the OFF Visual Pathway in Daylight. *Journal of Neuroscience*, *28*(16), 4136–4150. https://doi.org/10.1523/jneurosci.4274-07.2008
Marshel, J. H., Kaye, A. P., Nauhaus, I., & Callaway, E. M. (2012). Anterior-Posterior Direction Opponency in the Superficial Mouse Lateral Geniculate Nucleus. *Neuron*. https://doi.org/10.1016/j.neuron.2012.09.021
Marvin, J. S., Borghuis, B. G., Tian, L., Cichon, J., Harnett, M. T., Akerboom, J., Gordus, A., Renninger, S. L., Chen, T.-W. W., Bargmann, C. I., Orger, M. B., Schreiter, E. R., Demb, J. B., Gan, W.-B. B., Hires, S. A., & Looger, L. L. (2013). An optimized fluorescent probe for visualizing glutamate neurotransmission. *Nature Methods*, *10*(2), 162–170. https://doi.org/10.1038/nmeth.2333
Marvin, J. S., Scholl, B., Wilson, D. E., Podgorski, K., Kazemipour, A., Müller, J. A., Schoch, S., Quiroz, F. J. U., Rebola, N., Bao, H., Little, J. P., Tkachuk, A. N., Cai, E., Hantman, A. W., Wang, S. S. H., Depiero, V. J., Borghuis, B. G., Chapman, E. R., Dietrich, D., … Looger, L. L. (2018). Stability, affinity, and chromatic variants of the glutamate sensor iGluSnFR. *Nature Methods*, *15*(11), 936–939. https://doi.org/10.1038/s41592-018-0171-3

Masland, R. H. (2001). The fundamental plan of the retina. *Nature Neuroscience*, *4*(9), 877–886. https://doi.org/10.1038/nn0901-877

Masland, R. H. (2012a). The Neuronal Organization of the Retina. *Neuron*, *76*(2), 266–280. https://doi.org/10.1016/j.neuron.2012.10.002

Masland, R. H. (2012b). The tasks of amacrine cells. *Visual Neuroscience*, *29*(1), 3–9. https://doi.org/10.1017/s0952523811000344

Matsumoto, A., Agbariah, W., Solveig Nolte, S., Andrawos, R., Levi, H., Sabbah, S., & Yonehara, K. (2020). Synapse-specific direction selectivity in retinal bipolar cell axon terminals. *BioRxiv*.

Mazurek, M., Kager, M., & Van Hooser, S. D. (2014). Robust quantification of orientation selectivity and direction selectivity. *Frontiers in Neural Circuits*, *8*. https://doi.org/10.3389/fncir.2014.00092

McCormack, C. A., & Burnside, B. (1993). Light and circadian modulation of teleost retinal tyrosine hydroxylase activity. *Investigative Ophthalmology and Visual Science*.

Molnar, A., Hsueh, H.-A., Roska, B., & Werblin, F. S. (2009). *Crossover inhibition in the retina: circuitry that compensates for nonlinear rectifying synaptic transmission*. *27*(3), 569–590. https://doi.org/10.1007/s10827-009-0170-6

Morin, L. P., & Studholme, K. M. (2014). Retinofugal projections in the mouse. *Journal of Comparative Neurology*, *522*(16), 3733–3753. https://doi.org/10.1002/cne.23635

Müller, F., Scholten, A., Ivanova, E., Haverkamp, S., Kremmer, E., & Kaupp, U. B. (2003). HCN channels are expressed differentially in retinal bipolar cells and concentrated at synaptic terminals. *European Journal of Neuroscience*, *17*(10), 2084–2096. https://doi.org/10.1046/j.1460-9568.2003.02634.x

Murphy-Baum, B. L., & Rowland Taylor, W. (2015). The synaptic and morphological basis of orientation selectivity in a polyaxonal amacrine cell of the rabbit retina. *Journal of Neuroscience*. https://doi.org/10.1523/JNEUROSCI.1712-15.2015

Nakai, J., Ohkura, M., & Imoto, K. (2001). A high signal-to-noise Ca2+ probe composed of a single green fluorescent protein. *Nature Biotechnology*, *19*(2), 137–141. https://doi.org/10.1038/84397

Neves, G., & Lagnado, L. (1999). The kinetics of exocytosis and endocytosis in the synaptic terminal of goldfish retinal bipolar cells. *Journal of Physiology*. https://doi.org/10.1111/j.1469-7793.1999.181ad.x

Nikolaev, A., Leung, K.-M., Odermatt, B., & Lagnado, L. (2013). Synaptic mechanisms of adaptation and sensitization in the retina. *Nature Neuroscience*, *16*(7), 934–941. https://doi.org/10.1038/nn.3408

Nikolaou, N., Andrew, Alison, Abbas, F., Paul, Ian, & Martin. (2012). Parametric Functional Maps of Visual Inputs to the Tectum. *Neuron*, *76*(2), 317–324. https://doi.org/10.1016/j.neuron.2012.08.040

Niven, J. E., Anderson, J. C., & Laughlin, S. B. (2007). Fly Photoreceptors Demonstrate Energy-Information Trade-Offs in Neural Coding. *PLOS Biology*, *5*(4), e116. https://doi.org/10.1371/JOURNAL.PBIO.0050116

Nomura, A., Shigemoto, R., Nakamura, Y., Okamoto, N., Mizuno, N., & Nakanishi, S. (1994). Developmentally regulated postsynaptic localization of a metabotropic glutamate receptor in rat rod bipolar cells. *Cell*. https://doi.org/10.1016/0092-8674(94)90151-1

Odermatt, B., Nikolaev, A., & Lagnado, L. (2012). Encoding of Luminance and

Contrast by Linear and Nonlinear Synapses in the Retina. *Neuron*, *73*(4), 758–773. https://doi.org/10.1016/j.neuron.2011.12.023

Ohki, K., Chung, S., Ch'ng, Y. H., Kara, P., & Reid, R. C. (2005). Functional imaging with cellular resolution reveals precise microarchitecture in visual cortex. In *Nature*. https://doi.org/10.1038/nature03274

Okada, T., Horiguchi, H., & Tachibana, M. (1995). *Ca2+-dependent C− current at the presynaptic terminals of goldfish retinal bipolar cells*. *23*(3), 297–303. https://doi.org/10.1016/0168-0102(95)00955-8

Palmer, M. J. (2006). Modulation of Ca2+-activated K+ currents and Ca2+-dependent action potentials by exocytosis in goldfish bipolar cell terminals. *Journal of Physiology*. https://doi.org/10.1113/jphysiol.2006.105205

Pan, Z.-H., Hu, H.-J., Perring, P., & Andrade, R. (2001). T-Type Ca2+ Channels Mediate Neurotransmitter Release in Retinal Bipolar Cells. *Neuron*, *32*(1), 89–98. https://doi.org/10.1016/s0896-6273(01)00454-8

Park, S. J. H., Kim, I. J., Looger, L. L., Demb, J. B., & Borghuis, B. G. (2014). Excitatory synaptic inputs to mouse on-off direction- selective retinal ganglion cells lack direction tuning. *Journal of Neuroscience*. https://doi.org/10.1523/JNEUROSCI.5017-13.2014

Parsons, M. J., Pisharath, H., Yusuff, S., Moore, J. C., Siekmann, A. F., Lawson, N., & Leach, S. D. (2009). Notch-responsive cells initiate the secondary transition in larval zebrafish pancreas. *Mechanisms of Development*, *126*(10), 898–912. https://doi.org/10.1016/j.mod.2009.07.002

Pédelacq, J. D., Cabantous, S., Tran, T., Terwilliger, T. C., & Waldo, G. S. (2006). Engineering and characterization of a superfolder green fluorescent protein. *Nature Biotechnology*. https://doi.org/10.1038/nbt1172

Percival, K. A., Venkataramani, S., Smith, R. G., & Taylor, W. R. (2019). Directional excitatory input to direction-selective ganglion cells in the rabbit retina. *Journal of Comparative Neurology*. https://doi.org/10.1002/cne.24207

Platisa, J., Vasan, G., Yang, A., & Pieribone, V. A. (2017). Directed Evolution of Key Residues in Fluorescent Protein Inverses the Polarity of Voltage Sensitivity in the Genetically Encoded Indicator ArcLight. *ACS Chemical Neuroscience*. https://doi.org/10.1021/acschemneuro.6b00234

Poleg-Polsky, A., & Diamond, J. S. (2011). Imperfect space clamp permits electrotonic interactions between inhibitory and excitatory synaptic conductances, distorting voltage clamp recordings. *PLoS ONE*. https://doi.org/10.1371/journal.pone.0019463

Pologruto, T. A., Sabatini, B. L., & Svoboda, K. (2003). ScanImage: Flexible software for operating laser scanning microscopes. *BioMedical Engineering Online*. https://doi.org/10.1186/1475-925X-2-13

Popova, E. (2014). Role of dopamine in distal retina. *Journal of Comparative Physiology A*, *200*(5), 333–358. https://doi.org/10.1007/s00359-014-0906-2

Popova, Elka. (2015). ON-OFF Interactions in the Retina: Role of Glycine and GABA. *Current Neuropharmacology*, *12*(6), 509–526. https://doi.org/10.2174/1570159x13999150122165018

Portugues, R., Claudia, Engert, F., & Michael. (2014). Whole-Brain Activity Maps Reveal Stereotyped, Distributed Networks for Visuomotor Behavior. *Neuron*, *81*(6), 1328–1343. https://doi.org/10.1016/j.neuron.2014.01.019

Portugues, R., Severi, K. E., Wyart, C., & Ahrens, M. B. (2013). Optogenetics in a transparent animal: Circuit function in the larval zebrafish. In *Current*

Opinion in Neurobiology. https://doi.org/10.1016/j.conb.2012.11.001

Pouli, T. (2010). Statistical Regularities in Low and High Dynamic Range Images. *Proceedings of the 7th Symposium on Applied Perception in Graphics and Visualization*. https://doi.org/10.1145/1836248.1836250

Ribelayga, C., Cao, Y., & Mangel, S. C. (2008). The Circadian Clock in the Retina Controls Rod-Cone Coupling. *Neuron*. https://doi.org/10.1016/j.neuron.2008.07.017

Ribelayga, C., Wang, Y., & Mangel, S. C. (2004). A circadian clock in the fish retina regulates dopamine release via activation of melatonin receptors. In *Journal of Physiology*. https://doi.org/10.1113/jphysiol.2003.053710

Rieke, F., & Baylor, D. A. (1996). Molecular origin of continuous dark noise in rod photoreceptors. *Biophysical Journal*. https://doi.org/10.1016/S0006-3495(96)79448-1

Rieke, Fred, & Rudd, M. E. (2009). *The Challenges Natural Images Pose for Visual Adaptation*. *64*(5), 605–616. https://doi.org/10.1016/j.neuron.2009.11.028

Robles, E., Filosa, A., & Baier, H. (2013). Precise Lamination of Retinal Axons Generates Multiple Parallel Input Pathways in the Tectum. *Journal of Neuroscience*, *33*(11), 5027–5039. https://doi.org/10.1523/JNEUROSCI.4990-12.2013

Robles, E., Laurell, E., & Baier, H. (2014). The Retinal Projectome Reveals Brain-Area-Specific Visual Representations Generated by Ganglion Cell Diversity. *Current Biology*, *24*(18), 2085–2096. https://doi.org/10.1016/j.cub.2014.07.080

Rosa, J. M., Ruehle, S., Ding, H., & Lagnado, L. (2016). Crossover Inhibition Generates Sustained Visual Responses in the Inner Retina. *Neuron*, *90*(2), 308–319. https://doi.org/10.1016/j.neuron.2016.03.015

Rose, T., Goltstein, P. M., Portugues, R., & Griesbeck, O. (2014). Putting a finishing touch on GECIs. *Frontiers in Molecular Neuroscience*, *7*. https://doi.org/10.3389/fnmol.2014.00088

Rudolph, S., Tsai, M. C., von Gersdorff, H., & Wadiche, J. I. (2015). The ubiquitous nature of multivesicular release. In *Trends in Neurosciences*. https://doi.org/10.1016/j.tins.2015.05.008

Ruzicka, L., Howe, D. G., Ramachandran, S., Toro, S., Van Slyke, C. E., Bradford, Y. M., Eagle, A., Fashena, D., Frazer, K., Kalita, P., Mani, P., Martin, R., Moxon, S. T., Paddock, H., Pich, C., Schaper, K., Shao, X., Singer, A., & Westerfield, M. (2019). The Zebrafish Information Network: New support for non-coding genes, richer Gene Ontology annotations and the Alliance of Genome Resources. *Nucleic Acids Research*. https://doi.org/10.1093/nar/gky1090

Sagdullaev, B. T., McCall, M. A., & Lukasiewicz, P. D. (2006). Presynaptic inhibition modulates spillover, creating distinct dynamic response ranges of sensory output. *Neuron*, *50*(6), 923–935. https://doi.org/10.1016/J.NEURON.2006.05.015

Saito, T., & Kaneko, A. (1983). Ionic mechanisms underlying the responses of off-center bipolar cells in the carp retina: I. Studies on responses evoked by light. *Journal of General Physiology*. https://doi.org/10.1085/jgp.81.4.589

Sakai, H. M., & Naka, K. I. (1987). Signal transmission in the catfish retina. V. Sensitivity and circuit. *Https://Doi.Org/10.1152/Jn.1987.58.6.1329*, *58*(6), 1329–1350. https://doi.org/10.1152/JN.1987.58.6.1329

Santoro, B., Liu, D. T., Yao, H., Bartsch, D., Kandel, E. R., Siegelbaum, S. A., & Tibbs, G. R. (1998). Identification of a gene encoding a hyperpolarization-activated pacemaker channel of brain. *Cell*. https://doi.org/10.1016/S0092-8674(00)81434-8

Schiller, P. H., Sandell, J. H., & Maunsell, J. H. R. (1986). *Functions of the ON and OFF channels of the visual system*. *322*(6082), 824–825. https://doi.org/10.1038/322824a0

Schmitt, E. A., & Dowling, J. E. (1999). Early retinal development in the Zebrafish, Danio rerio: Light and electron microscopic analyses. *Journal of Comparative Neurology*. https://doi.org/10.1002/(SICI)1096-9861(19990222)404:4<515::AID-CNE8>3.0.CO;2-A

Schnapf, J. L., Nunn, B. J., Meister, M., & Baylor, D. A. (1990). Visual transduction in cones of the monkey Macaca fascicularis. *The Journal of Physiology*, *427*(1), 681–713. https://doi.org/10.1113/JPHYSIOL.1990.SP018193

Schwartz, G., & Rieke, F. (2011). Nonlinear spatial encoding by retinal ganglion cells: When 1 + 1 ≠ 2. In *Journal of General Physiology*. https://doi.org/10.1085/jgp.201110629

Seifert, R., Scholten, A., Gauss, R., Mincheva, A., Lichter, P., & Kaupp, U. B. (1999). Molecular characterization of a slowly gating human hyperpolarization-activated channel predominantly expressed in thalamus, heart, and testis. *Proceedings of the National Academy of Sciences of the United States of America*. https://doi.org/10.1073/pnas.96.16.9391

Semmelhack, J. L., Donovan, J. C., Thiele, T. R., Kuehn, E., Laurell, E., & Baier, H. (2014). A dedicated visual pathway for prey detection in larval zebrafish. *ELife*, *3*. https://doi.org/10.7554/ELIFE.04878

Shiells, R. A., Falk, G., & Naghshineh, S. (1981). Action of glutamate and aspartate analogues on rod horizontal and bipolar cells. *Nature*, *294*(5841), 592–594. https://doi.org/10.1038/294592a0

Siegert, S., Cabuy, E., Scherf, B. G., Kohler, H., Panda, S., Le, Y. Z., Fehling, H. J., Gaidatzis, D., Stadler, M. B., & Roska, B. (2012). Transcriptional code and disease map for adult retinal cell types. *Nature Neuroscience*. https://doi.org/10.1038/nn.3032

Simms, B. A., & Zamponi, G. W. (2014). Neuronal voltage-gated calcium channels: Structure, function, and dysfunction. In *Neuron*. https://doi.org/10.1016/j.neuron.2014.03.016

Simon, E. J., Lamb, T. D., & Hodgkin, A. L. (1975). Spontaneous voltage fluctuations in retinal cones and bipolar cells. *Nature*. https://doi.org/10.1038/256661a0

Singer, J. H., & Diamond, J. S. (2006). Vesicle depletion and synaptic depression at a mammalian ribbon synapse. *Journal of Neurophysiology*. https://doi.org/10.1152/jn.01309.2005

Singer, J. H., Lassova, L., Vardi, N., & Diamond, J. S. (2004). Coordinated multivesicular release at a mammalian ribbon synapse. *Nature Neuroscience*. https://doi.org/10.1038/nn1280

Snellman, J., Mehta, B., Babai, N., Bartoletti, T. M., Akmentin, W., Francis, A., Matthews, G., Thoreson, W., & Zenisek, D. (2011). Acute destruction of the synaptic ribbon reveals a role for the ribbon in vesicle priming. *Nature Neuroscience*. https://doi.org/10.1038/nn.2870

Sohoglu, E., & Chait, M. (2016). Detecting and representing predictable

structure during auditory scene analysis. *ELife*. https://doi.org/10.7554/eLife.19113

Stachenfeld, K. L., Botvinick, M. M., & Gershman, S. J. (2017). The hippocampus as a predictive map. *Nature Neuroscience*. https://doi.org/10.1038/nn.4650

Sterling, P., & Laughlin, S. (2015). Principles of neural design. In *Principles of Neural Design*. https://doi.org/10.7551/mitpress/9780262028707.001.0001

Sümbül, U., Song, S., McCulloch, K., Becker, M., Lin, B., Sanes, J. R., Masland, R. H., & Seung, H. S. (2014). A genetic and computational approach to structurally classify neuronal types. *Nature Communications*, *5*(1). https://doi.org/10.1038/ncomms4512

Suster, M. L., Kikuta, H., Urasaki, A., Asakawa, K., & Kawakami, K. (2009). Transgenesis in Zebrafish with the Tol2 Transposon System. In *Methods in molecular biology (Clifton, N.J.)* (Vol. 561, pp. 41–63). https://doi.org/10.1007/978-1-60327-019-9_3

Tachibana, M., Okada, T., Arimura, T., Kobayashi, K., & Piccolino, M. (1993). Dihydropyridine-sensitve calcium current mediates neurotransmitter release from bipolar cells of the goldfish retina. *Journal of Neuroscience*. https://doi.org/10.1523/jneurosci.13-07-02898.1993

Tarpey, P., Thomas, S., Sarvananthan, N., Mallya, U., Lisgo, S., Talbot, C. J., Roberts, E. O., Awan, M., Surendran, M., McLean, R. J., Reinecke, R. D., Langmann, A., Lindner, S., Koch, M., Jain, S., Woodruff, G., Gale, R. P., Degg, C., Droutsas, K., … Gottlob, I. (2006). Mutations in FRMD7, a newly identified member of the FERM family, cause X-linked idiopathic congenital nystagmus. *Nature Genetics*. https://doi.org/10.1038/ng1893

Taylor, W. R., He, S., Levick, W. R., & Vaney, D. I. (2000). Dendritic computation of direction selectivity by retinal ganglion cells. *Science*. https://doi.org/10.1126/science.289.5488.2347

Thermes, V., Grabher, C., Ristoratore, F., Bourrat, F., Choulika, A., Wittbrodt, J., & Joly, J.-S. (2002). I-SceI meganuclease mediates highly efficient transgenesis in fish. *Mechanisms of Development*, *118*(1–2), 91–98. http://www.ncbi.nlm.nih.gov/pubmed/12351173

Thomas, S., Proudlock, F. A., Sarvananthan, N., Roberts, E. O., Awan, M., McLean, R., Surendran, M., Anil Kumar, A. S., Farooq, S. J., Degg, C., Gale, R. P., Reinecke, R. D., Woodruff, G., Langmann, A., Lindner, S., Jain, S., Tarpey, P., Raymond, F. L., & Gottlob, I. (2008). Phenotypical characteristics of idiopathic infantile nystagmus with and without mutations in FRMD7. *Brain*. https://doi.org/10.1093/brain/awn046

Thoreson, W. B., & Stella, S. L. (2000). Anion modulation of calcium current voltage dependence and amplitude in salamander rods. *Biochimica et Biophysica Acta - Biomembranes*. https://doi.org/10.1016/S0005-2736(99)00257-6

Tian, L., Hires, S. A., Mao, T., Huber, D., Chiappe, M. E., Chalasani, S. H., Petreanu, L., Akerboom, J., McKinney, S. A., Schreiter, E. R., Bargmann, C. I., Jayaraman, V., Svoboda, K., & Looger, L. L. (2009). Imaging neural activity in worms, flies and mice with improved GCaMP calcium indicators. *Nature Methods*, *6*(12), 875–881. https://doi.org/10.1038/nmeth.1398

Tikidji-Hamburyan, A., Reinhard, K., Seitter, H., Hovhannisyan, A., Procyk, C. A., Allen, A. E., Schenk, M., Lucas, R. J., & Münch, T. A. (2015). Retinal output changes qualitatively with every change in ambient illuminance.

Nature Neuroscience, *18*(1), 66–74. https://doi.org/10.1038/nn.3891

Trapani, J. G., & Nicolson, T. (2011). Mechanism of spontaneous activity in afferent neurons of the zebrafish lateral-line organ. *Journal of Neuroscience*. https://doi.org/10.1523/JNEUROSCI.3369-10.2011

Tremblay, R., Lee, S., & Rudy, B. (2016). GABAergic Interneurons in the Neocortex: From Cellular Properties to Circuits. In *Neuron*. https://doi.org/10.1016/j.neuron.2016.06.033

Van Hook, M. J., & Berson, D. M. (2010). *Hyperpolarization-Activated Current (Ih) in Ganglion-Cell Photoreceptors*. *5*(12), e15344. https://doi.org/10.1371/journal.pone.0015344

Van Hooser, S. D., Heimel, J. A. F., Chung, S., Nelson, S. B., & Toth, L. J. (2005). Orientation selectivity without orientation maps in visual cortex of a highly visual mammal. *Journal of Neuroscience*. https://doi.org/10.1523/JNEUROSCI.4042-04.2005

Vardi, N., Duvoisin, R., Wu, G., & Sterling, P. (2000). Localization of mGluR6 to dendrites of ON bipolar cells in primate retina. *Journal of Comparative Neurology*. https://doi.org/10.1002/1096-9861(20000731)423:3<402::AID-CNE4>3.0.CO;2-E

Venkataramani, S., & Taylor, W. R. (2010). Orientation selectivity in rabbit retinal ganglion cells is mediated by presynaptic inhibition. *Journal of Neuroscience*. https://doi.org/10.1523/JNEUROSCI.2081-10.2010

Vielma, A. H., Retamal, M. A., & Schmachtenberg, O. (2012). Nitric oxide signaling in the retina: What have we learned in two decades? *Brain Research*, *1430*, 112–125. https://doi.org/10.1016/J.BRAINRES.2011.10.045

Villette, V., Chavarha, M., Dimov, I. K., Bradley, J., Pradhan, L., Mathieu, B., Evans, S. W., Chamberland, S., Shi, D., Yang, R., Kim, B. B., Ayon, A., Jalil, A., St-Pierre, F., Schnitzer, M. J., Bi, G., Toth, K., Ding, J., Dieudonné, S., & Lin, M. Z. (2019). Ultrafast Two-Photon Imaging of a High-Gain Voltage Indicator in Awake Behaving Mice. *Cell*. https://doi.org/10.1016/j.cell.2019.11.004

Vlasits, A. L., Bos, R., Morrie, R. D., Fortuny, C., Flannery, J. G., Feller, M. B., & Rivlin-Etzion, M. (2014). Visual Stimulation Switches the Polarity of Excitatory Input to Starburst Amacrine Cells. *Neuron*. https://doi.org/10.1016/j.neuron.2014.07.037

Von Gersdorff, H., & Matthews, G. (1994). Dynamics of synaptic vesicle fusion and membrane retrieval in synaptic terminals. *Nature*. https://doi.org/10.1038/367735a0

Wahl-Schott, C., & Biel, M. (2009). HCN channels: Structure, cellular regulation and physiological function. *Cellular and Molecular Life Sciences*, *66*(3), 470–494. https://doi.org/10.1007/s00018-008-8525-0

Wei, W. (2018). Neural mechanisms of motion processing in the mammalian retina. In *Annual Review of Vision Science*. https://doi.org/10.1146/annurev-vision-091517-034048

Weliky, M., Bosking, W. H., & Fitzpatrick, D. (1996). A systematic map of direction preference in primary visual cortex. *Nature*. https://doi.org/10.1038/379725a0

Werblin, F. S., & Dowling, J. E. (1969). Organization of the retina of the mudpuppy, Necturus maculosus. II. Intracellular recording. *Journal of Neurophysiology*, *32*(3), 339–355. https://doi.org/10.1152/jn.1969.32.3.339

Westerfield, M. (2000). *The zebrafish book. A guide for the laboratory use of zebrafish (Danio rerio).* (4th ed.). University of Oregon Press.

Westheimer, G. (2007). The ON–OFF dichotomy in visual processing: From receptors to perception. *Progress in Retinal and Eye Research*, *26*(6), 636–648. https://doi.org/10.1016/j.preteyeres.2007.07.003

White, R. M., Sessa, A., Burke, C., Bowman, T., Leblanc, J., Ceol, C., Bourque, C., Dovey, M., Goessling, W., Burns, C. E., & Zon, L. I. (2008). Transparent Adult Zebrafish as a Tool for In Vivo Transplantation Analysis. *Cell Stem Cell*, *2*(2), 183–189. https://doi.org/10.1016/j.stem.2007.11.002

Wright, A. V., Nuñez, J. K., & Doudna, J. A. (2016). Biology and Applications of CRISPR Systems: Harnessing Nature's Toolbox for Genome Engineering. In *Cell*. https://doi.org/10.1016/j.cell.2015.12.035

Wyart, C., Bene, F. Del, Warp, E., Scott, E. K., Trauner, D., Baier, H., & Isacoff, E. Y. (2009). Optogenetic dissection of a behavioural module in the vertebrate spinal cord. *Nature*. https://doi.org/10.1038/nature08323

Yang, H. H. H., St-Pierre, F., Sun, X., Ding, X., Lin, M. Z. Z., & Clandinin, T. R. R. (2016). Subcellular Imaging of Voltage and Calcium Signals Reveals Neural Processing In Vivo. *Cell*. https://doi.org/10.1016/j.cell.2016.05.031

Yates, A. D., Achuthan, P., Akanni, W., Allen, J., Allen, J., Alvarez-Jarreta, J., Amode, M. R., Armean, I. M., Azov, A. G., Bennett, R., Bhai, J., Billis, K., Boddu, S., Marugán, J. C., Cummins, C., Davidson, C., Dodiya, K., Fatima, R., Gall, A., … Flicek, P. (2020). Ensembl 2020. *Nucleic Acids Research*. https://doi.org/10.1093/nar/gkz966

Yazulla, S., & Studholme, K. M. (2001). Neurochemical anatomy of the zebrafish retina as determined by immunocytochemistry. *Journal of Neurocytology*, *30*(7), 551–592. https://doi.org/10.1023/A:1016512617484

Yonehara, K., Farrow, K., Ghanem, A., Hillier, D., Balint, K., Teixeira, M., Jüttner, J., Noda, M., Neve, R. L., Conzelmann, K. K., & Roska, B. (2013). The first stage of cardinal direction selectivity is localized to the dendrites of retinal ganglion cells. *Neuron*. https://doi.org/10.1016/j.neuron.2013.08.005

Yoshimatsu, T., Bartel, P., Schröder, C., Janiak, F. K., St-Pierre, F., Berens, P., & Baden, T. (2020). Near-optimal rotation of colour space by zebrafish cones in vivo. *BioRxiv*.

Zenisek, D., Davila, V., Wan, L., & Almers, W. (2003). Imaging Calcium Entry Sites and Ribbon Structures in Two Presynaptic Cells. *The Journal of Neuroscience*, *23*(7), 2538–2548. https://doi.org/10.1523/jneurosci.23-07-02538.2003

Zhang, Y., Rózsa, M., Bushey, D., Zheng, J., Reep, D., Broussard, Gerard Joey; Tsang, A., Tsegaye, G., Patel, R., Narayan, S., Li, J. X., Zhang, R., Ahrens, M. B. ., Turner, G. C. ., & Wang, Samuel S.-H.; Svoboda, L. L. (2020). *jGCaMP8 Fast Genetically Encoded Calcium Indicators*. Janelia Research Campus. Online Resource. 2020 10.25378/Janelia.13148243.V1.

Zheng, N., & Raman, I. M. (2009). Ca Currents Activated by Spontaneous Firing and Synaptic Disinhibition in Neurons of the Cerebellar Nuclei. *Journal of Neuroscience*, *29*(31), 9826–9838. https://doi.org/10.1523/jneurosci.2069-09.2009

Zhou, M., Bear, J., Roberts, P., Janiak, F., Semmelhack, J., Yoshimatsu, T., & Baden, T. (2020). *What the Zebrafish's Eye Tells the Zebrafish's Brain: Retinal Ganglion Cells for Prey Capture and Colour Vision*. Cold Spring

Harbor Laboratory. https://doi.org/10.1101/2020.01.31.927087

Zimmermann, M. J. Y., Nevala, N. E., Yoshimatsu, T., Osorio, D., Nilsson, D.-E., Berens, P., & Baden, T. (2018). Zebrafish Differentially Process Color across Visual Space to Match Natural Scenes. *Current Biology*, *28*(13), 2018-2032.e5. https://doi.org/10.1016/j.cub.2018.04.075